

**Genetic and Biochemical Analyses of the *Arabidopsis*
atToc90 Protein**

**Thesis submitted for the degree of
Doctor of Philosophy
at the University of Leicester**

by

**Panagiotis Lympereopoulos (BSc Iasi)
Department of Biology
University of Leicester**

2011

Declaration

I hereby declare that no part of this thesis has been previously submitted to this or any other University as part of the requirements for a higher degree. The content of this thesis is the result of my own work unless otherwise acknowledged in the text or by reference.

The work was conducted in the Department of Biology, University of Leicester during the period 1st of October 2007 to 10th of August 2011.

Signed.....Panagiotis Lympelopoulos.....

Panagiotis Lympelopoulos, April 2012

Abstract

Genetic and Biochemical Analyses of the *Arabidopsis* atToc90 Protein

Panagiotis Lympopoulos

Chloroplasts are photosynthetic organelles in plant and algal cells that capture sunlight energy to form energy-rich molecules that are the basis for almost all life. Chloroplast development requires more than 3000 different proteins, most of which are encoded by nuclear DNA. Thus, chloroplasts must import most of their proteins from the cytosol. They are surrounded by a double membrane called the envelope. Embedded in the envelope are the TOC and TIC complexes (translocon at the outer and innner envelope membrane of the chloroplast, respectively), which mediate protein import into the organelle. Several components of the TOC and TIC complexes have been identified. One example is the receptor Toc159, which in the model plant *Arabidopsis thaliana* has four isoforms: atToc159, atToc132, atToc120 and atToc90. It is known that atToc159 supports accumulation of photosynthetic proteins, while atToc132 and atToc120 support the import of non-photosynthetic, housekeeping proteins. However, the role of atToc90 remains uncertain. I investigated the function of atToc90 genetically by studying a series of *Arabidopsis toc90* double and triple mutants, and by overexpressing atToc90 in mutants lacking other receptor isoforms. This work suggested limited functional redundancy between atToc90 and other TOC receptors (most notably, atToc159). By tagging TOC receptors known to act in each of the photosynthetic and non-photosynthetic import pathways, I was able to purify different TOC complexes from transgenic plants using tandem affinity purification (TAP). This indicated that atToc90 is present promiscuously in both atToc159- and atToc132/120-containing TOC complexes. Publicly available Affymetrix microarray data suggested a role for atToc90 during senescence. Thus, I investigated whether *toc90* knockout mutants display any differences from wild type regarding leaf senescence. Indeed, some defects were observed, suggesting a role for atToc90 in the biochemical changes that occur in chloroplasts during leaf senescence.

ACKNOWLEDGEMENTS

I would like to start by thanking my supervisor Professor Paul R. Jarvis. During these four years, he has consistently shown me not only how to find the way to the answers, but more importantly, to ask the right questions and then seek the answers. He has directed me in understanding how to look to a problem and devise the methods and different ways to go about finding the solution. He always made himself available to my questions, and was ready to balance the stress of the daily laboratory work with his patience. It was a life's opportunity and privilege to do my Ph.D in Professor's Jarvis laboratory.

I am also very thankful to Dr Jocelyn Bedard for his guidance during my first 2 years, his friendship and his advices regarding the TAP experiments even when he was far away to Japan. I would like to thank Dr Sybille Kubis for her data regarding the TAP-tagging experiments, her patience showing me how to perform chloroplast isolation in the "Siberia" room, and her friendship which was developed all these years, sharing frustrations and happiness.

I have also to express my profound gratitude for my parents, Anna and Thodoros, my two brothers, Kostas and Giorgos, and my two sisters, Chara and Olga for their unconditional support throughout the years. Without their constant support and confidence, I would not have got this far. Thanks for all the love.

I must thank from the bottom of my heart my grandparents, Fani and Panagiotis. Their unconditional love, support, affection and kindness since I was a little boy, have contributed to be the person I am. Unfortunately, they both have passed away when I was in my 3rd year of my Ph.D and I did not have the chance to return back to Greece on time and say to them goodbye, a big thank you for the amazing years I had the chance to spent with them, and most to say that I will always remember and love them. For this reason, as a minimum gratitude to them, I would like to dedicate my thesis in their memory.

None of this could ever be done without the unconditional love and support of my fiancée Anca. She accepted the challenge of coming to a foreign country and dealing with all the difficulties that would arise to be my very pillar of support. She has shown

extreme devotion and love, being by my side on the most difficult moments (when chloroplasts started invading my brain) as well as the most pleasant ones. When I finally managed to TAP tag my nerves, she was there to make me see the bright side of things. Whenever any challenge seemed overwhelming, her smile and her good words gave me the strength I needed to go on.

I must also thank my friends who are living back to Greece and the friends I made here and who also left their country and became a big family here. Special thanks to my flatmate Alberto Hidalgo Bravo and his wife Lupita Perez Garcia for their friendship, help and the time shared together in the flat. I would like to thank Lupita for her spicy inspirations and influence in my Greek-Romanian cuisine and Alberto for his unstoppable laugh and smile...even if we were watching horror movies.

Thanks to all my colleagues, current and former members of the Jarvis laboratory. Special thanks to Ramesh Patel for his detailed repeated discussions. His truly support during my work when I needed him.

I would like also to thank my internal and external examiners, regardless the result.... for their patience to read this thesis.

Finally, but not less important, I would like to express my gratitude to BBSRC for funding this project and to Leicester University to offers me this great opportunity.

Contents

Chapter One	Page
1 Introduction	
1.1 The Chloroplast	19
1.1.1 Origin and evolution of the chloroplasts	19
1.1.2 Division of chloroplasts	20
1.2 The Chloroplast Protein Import Machinery	
1.2.1 Targeting of preproteins from the cytosol to the chloroplast	21
1.2.2 Important cytosolic components	21
1.3 The receptors Toc34 and Toc159	22
1.3.1 The two models of the protein import machinery	23
1.3.1.1 The motor model	24
1.3.1.2 The targeting model	25
1.4 The chloroplast translocation machinery of the outer envelope membrane	27
1.5 The TOC complex and its components	27
1.5.1 Function of Toc159 and Toc34 isoforms in different import pathways	28
1.5.2 TOC isoforms of <i>Arabidopsis thaliana</i>	28
1.5.2.1 Toc34 and its homologues in <i>Arabidopsis thaliana</i>	29
1.5.2.2 Toc159 and its homologues in <i>Arabidopsis thaliana</i>	31
1.5.2.3 Toc75	33
1.5.2.4 Toc12	35
1.5.2.5 Toc64	36
1.6 The chloroplast translocation machinery of the inner envelope membrane	37
1.7 The TIC machinery and its components	39
1.7.1 Tic110	39
1.7.2 Tic20 and Tic22	39
1.7.3 Tic40	41
1.7.4 Tic55, Tic32, and Tic62	41

1.8	Chaperones: Hsp93 and Hsp70	42
1.9	Transport from the outer envelope membrane into the inner envelope membrane	43
1.10	Senescence	44
1.10.1	Leaf Senescence	44
1.10.2	Structural and biochemical changes in leaf senescence	45
1.10.3	The vacuole and its role during senescence	46
1.10.4	Molecular approaches during senescence and regulation of leaf senescence	47
1.10.5	The role of plant hormones in the onset of leaf senescence	47
1.10.6	Induction of leaf senescence through the sugar signalling	50
1.10.7	Role of signalling cascades in the initiation of senescence	50
1.11	Aims of this thesis	51

Chapter Two

Genetic studies revealing new insight into the function of atToc90, a chloroplast outer envelope protein

2.1	Introduction	59
2.2	Results	60
2.2.1	Identification of atToc90 knockout mutants	60
2.2.2	Double mutant studies	61
2.2.2.1	The <i>toc90-1 toc159</i> double mutant displays a more severe phenotype than <i>toc159</i>	61
2.2.3	<i>Arabidopsis thaliana</i> Toc90 triple mutants reveal significant functional redundancy	62
2.2.3.1	Analysis of a <i>toc90-1 toc132 toc120</i> triple homozygous mutant	62
2.2.3.2	Analysis of a <i>toc90-1 toc132 toc120</i> triple heterozygous mutant	63
2.2.3.3	Analysis of a <i>toc90-1 toc159 toc120</i> triple homozygous mutant	63
2.2.3.4	Analysis of a <i>toc90-1 toc33 toc34</i> triple mutant	63
2.2.4	Analysis of atToc90 function by overexpression	64
2.2.4.1	Generating new atToc90 overexpression lines	64
2.2.4.2	Identification and genotyping analysis of transformants	65

2.2.4.3	Phenotypic analysis of the transformants	66
2.2.4.4	Protein expression analysis	67
2.3	Discussion	68

Chapter 3

Purification and characterization of TOC complexes containing atToc33 and atToc34 from *Arabidopsis* chloroplasts

3.1	Introduction	83
3.1.1	Multiple isoforms of the TOC receptors in <i>Arabidopsis thaliana</i>	83
3.1.2	TAP (tandem affinity purification)-tagging	84
3.2	Results	85
3.2.1	Generation of transgenic plants expressing TAP tagged atToc33 and atToc34	85
3.2.1.1	Characteristics of plants expressing Toc33-NTAPi and Toc34-NTAPi	85
3.2.2	Small scale TAP-tagging	86
3.2.3	Large scale TAP-tagging	87
3.2.4	Silver staining and colloidal coomassie blue	89
3.2.5	Mass spectrometric protein identification	89
3.3	Discussion	91

Chapter 4

Possible involvement of the *Arabidopsis* atToc90 protein in leaf senescence

4.1	Introduction	103
4.2	Results	
4.2.1	Analysis of the atToc90 knockout mutants and an overexpression line	105
4.2.2	Jasmonic acid treatment	106
4.2.3	Induction of leaf senescence in attached darkened leaves	107
4.2.4	Light stress treatment	109
4.2.5	Osmotic stress treatment	110

4.3	Discussion	111
-----	------------	-----

Chapter 5

Materials and Methods

5.1	<i>Arabidopsis thaliana</i> plants growth conditions and manipulation	122
	5.1.1 <i>In vitro</i> culture	122
	5.1.2 Soil culture	122
	5.1.3 Cross-pollination of <i>Arabidopsis</i> plants	123
	5.1.4 Chlorophyll measurements	123
5.2	Molecular biology techniques	124
	5.2.1 Bacterial work	124
	5.2.1.1 Growing bacteria	124
	5.2.1.2 <i>Escherichia coli</i> transformation	124
	5.2.1.3 <i>Agrobacterium</i> transformation	124
	5.2.1.4 Transformation of <i>Arabidopsis thaliana</i> using the floral dip method	125
	5.2.1.5 Plasmid preparation from bacterial growth overnight cultures	125
	5.2.1.6 Preparation of high quality plasmid DNA	126
	5.2.1.7 Quantification of DNA and RNA	126
	5.2.2 Nucleic acid and protein preparation	126
	5.2.2.1 Plant DNA extraction	126
	5.2.2.2 Plant RNA extraction	126
	5.2.3 Polymerase chain reaction	127
	5.2.4 Reverse transcriptase-PCR	128
	5.2.5 Total protein extraction from <i>Arabidopsis thaliana</i> plants	127
	5.2.6 Quantification of protein	127
	5.2.7 TAP tagging purification	129
5.3	Electrophoresis technique	
	5.3.1 Agarose gels	132
	5.3.2 SDS-PAGE and Western blotting	132
	5.3.3 Coomassie stained gels	133
	5.3.4 Silver stained gels	133

5.4	Chloroplast isolation	134
5.5	Establishing the yield of the intact chloroplast	135

Chapter 6

General Discussion	137
---------------------------	-----

References	145
-------------------	-----

Appendix	160
-----------------	-----

List of figure

1.1	Description of the process of protein import via TOC/TIC import machinery	53
1.2	Two different schematic models for preprotein recognition by the TOC GTPases Toc34 and Toc159	54
1.3	Structure of the TOC/TIC chloroplast import apparatus	55
1.4	Model of substrate specific protein import pathways	56
2.1	Schematic diagram showing the structure of the <i>Arabidopsis</i> Toc90 gene and the location of each T-DNA	70
2.2	PCR gel analyses of the <i>toc90-1 toc120-2</i> double mutant	71
2.3	The <i>toc90</i> knockout mutant does not interact genetically with many other TOC component mutations	72
2.4	Characterization of the <i>toc90-1 toc159</i> double knockout mutant	73
2.5	Characterization of the <i>toc90-1 toc132 toc120</i> triple homozygous mutant	74
2.6	Characterization of the <i>toc90-1 toc132 toc120</i>	75
2.7	Characterization of the <i>toc90-1 toc159 toc120</i>	76
2.8	Characterization of the <i>toc90-1 toc33 toc34</i>	77
2.9	RNA levels for the 35S- <i>atTOC90</i> full length in the background of <i>toc159</i>	78
2.10	RNA levels for the 35S- <i>atTOC90</i> full length in the background of <i>toc132 toc120</i>	79
2.11	Phenotypic and mRNA analysis together with protein levels	80
2.12	Phenotypic and mRNA analysis together of the 35S- <i>atTOC90</i> lines in the background of <i>toc159</i> and <i>toc132-3 toc132-3; +/-toc120-2</i>	81
3.1	PCR gel analysis for the T-DNA insertion of <i>atToc34-NTAPi G7</i>	93

3.2	PCR gel analysis to confirm the function of atToc34-NTAPi G7 transgenic line	94
3.3	Structure of TAP tag cassette and expression analysis of atToc33-NTAPi and atToc34-NTAPi	95
3.4	Schematic overview of the TAP tagging method	96
3.5	Small scale TAP tagging experiment using the atToc33-NTAPi (33N) G2 transgenic line	97
3.6	Large scale TAP tagging experiment using the atToc33-NTAPi (33N) G2 transgenic line	98
3.7	Large scale TAP tagging experiment using the atToc34-NTAPi (34N) G7 transgenic line	99
3.8	Silver and coomassie staining of the TAP tagged atToc33 and atToc34 complexes	100
4.1	Analysis of the expression of major TOC and TIC genes using Genevestigator	113
4.2	Visible phenotypes and molecular characterization of the three atToc90 knockout and a 35S- <i>atTOC90</i> transgenic line	114
4.3	Analysis of photosynthetic parameters in the atToc90	115
4.4	Treatment of the atToc90 knockout and overexpressor lines with jasmonic acid	116
4.5	Induction of senescence in individual attached leaves of the atToc90 knockout and overexpressor line	117
4.6	Analysis of mRNA from senescenced individual attached leaves of the atToc90 knockout and overexpressor line after dark treatment	118
4.7	Treatment of the atToc90 knockout and overexpressor lines with high light stress	119
4.8	Treatment of the atToc90 knockout and overexpressor lines under osmotic stress conditions	120

List of tables in APPENDIX

- 1 Genetic analysis of Arabidopsis Toc90 double homozygous knockout mutants. All the double mutants have been PCR tested and comprehensive phenotypic analysis was carried out with the appropriate controls
- 2 Genetic analysis of Arabidopsis Toc90 triple mutants. All the triple mutants have been PCR tested and comprehensive phenotypic analysis was carried out with the appropriate controls
- 3 The T-DNA and gene specific primers used for genotyping
- 4 atToc90 gene specific primers used to make the overexpressor for the construct complementation studies
- 5 atToc90 and translation initiation factor *eIF4E1* gene specific primers used for RT-PCR
- 6 Table of TOC/TIC components

Abbreviations

aa	amino acid
A-domain	acidic domain
ADP	adenosine diphosphate
ATP	adenosine triphosphate
APS	ammonium persulfate
BSA	bovine serum albumin
CaMV	cauliflower mosaic virus
Col	Columbia
CDS	coding sequence
CIB	chloroplast isolation buffer
DNA	deoxyribonucleic acid
cDNA	complementary DNA
dNTP	deoxynucleotide triphosphate
DDM	dodecyl- β -D-maltoside
DTT	dithiothreitol
DMF	dimethylformamide
<i>E. coli</i>	<i>Escherichia coli</i>
EDTA	ethylenediaminetetraaceticacid
EGTA	ethyleneglycoltetraaceticacid
FNR	ferredoxin NAD(P) reductase
G-domain	GTP-binding domain
Gent	gentamycin
GFP	green fluorescent protein
GDP	guanosine diphosphate
GTP	guanosine triphosphate
HMS	HEPES-MgSO ₄ -Sorbitol buffer

IgG	immunoglobulin G
IPA	isopropanol
IMS	intermembrane space
Kan	kanamycin
kb	kilo base pairs
kDa	kilo Dalton
LB-agar	Luria-Bertani broth agar
M-domain	membrane domain
MS	Murashige and Skoog
NAD(P) ⁺	nicotinamide adenine dinucleotide (phosphate), oxidized
NADPH	nicotinamide adenine dinucleotide phosphate hydrolyzed
PBS	phosphate buffered saline
PCR	polymerase chain reaction
PEB	protein extraction buffer
ppi	plastid protein import
PPT	phosphinothricin
protA	protein A
RNA	ribonucleic acid
RT	room temperature
rpm	revolution per minute
RT-PCR	reverse transcriptase PCR
RubisCO	ribulose-1,5-bisphosphate carboxylase oxygenase
SDS	sodium dodecyl sulfate
SDS-PAGE	SDS-polyacrylamide gel electrophoresis
SRP	signal recognition particle
TAP tag	tandem affinity purification tag
TBS	Tris buffered saline
TBS-tween	Tris buffer saline with Tween
T-DNA	transfer DNA

TEV	tobacco etch virus
TEMED	<i>N,N,N,N'</i> - tetramethylethylenediamine
TIC	translocon at the inner chloroplast envelope membrane
TOC	translocon at the outer chloroplast envelope membrane
TPR	tetratrico peptide repeat
Tris	tris (hydroxymethyl) aminomethane
T ₁	transformant generation 1
UTR	untranslated region
wt	wild type
w/v	weight per volume

To my grandparents; Fani and Panagiotis.

You are always in my mind and heart.

Chapter 1

Introduction

1. INTRODUCTION

1.1 The Chloroplast

By definition the name chloroplast derives from the Greek words “chloros” (meaning green) and “plast” (meaning unit). Chloroplasts are well known members of a class of plant cell organelles called plastids and all originate from protoplastids. During plant development the protoplastids differentiate to form three major groups of plastids, the chloroplasts, the chromoplasts and the leucoplasts. Among them the most abundant and important plastids are the chloroplasts. Chloroplasts are located in plant’s green tissues as they contain chlorophyll pigments and are the site of photosynthesis. Their ability to harvest energy from sunlight to split water and fix carbon dioxide to produce sugars involves the production of ATP and NADPH through a complex set of processes (Pyke, 1999). Chloroplasts are about 5-10 μm in diameter and 3-4 μm in thickness and they are bounded by two envelope membranes (López-Juez and Pyke, 2005) (Fig. 1). The photosynthetic apparatus is localised in an internal system, the thylakoids, which each enclose a central space called the lumen. At various places within the chloroplast these are stacked in arrays called grana (Fig. 1). The thylakoids carry numerous molecules of chlorophyll which are responsible for light harvesting. The stroma surrounds the thylakoid membranes (Fig. 1), and is an area inside of the chloroplast where numerous enzymatic reactions occur, and where starch, and sugars are formed.

1.1.1 Origin and evolution of the chloroplasts

Chloroplasts originated from an endosymbiotic event, in which an ancestral photosynthetic cyanobacterium was taken up by a heterotrophic host cell that already contained mitochondria. Genes encoding the vast majority of the protein components of plastids were transferred to the nuclear genome as a result of subsequent evolution. In response to this dislocation of genetic material, plastids have evolved a system to post-translationally import nuclear encoded preproteins from their site of synthesis on cytosolic ribosomes (Keegstra and Cline, 1999; Jarvis, 2003). Chloroplasts like mitochondria contain their own genome and divide independently from the cell. Another characteristic of this organelle is the similarity in the transcriptional and translational machinery to those found in bacteria. The plastid genome encodes 80-200 plastid localized proteins that are translated on 70S ribosomes and functionally assembled within

the plastid (Jarvis and Robinson, 2004). On the other hand, several thousand different proteins must be imported from the cytosol.

1.1.2 Division of chloroplasts

The molecular nature of chloroplast division has been studied extensively (Maple et al., 2007; Yang et al., 2008). As leaf development progresses, chloroplasts become progressively larger, suggesting that division occurs early in chloroplast biogenesis (Pyke, 1999; Okazaki et al., 2009). Chloroplasts divide by binary fission, driven by two contractile protein rings that form each side of the chloroplast envelope. The inner division ring forms first and is composed of the FtsZ1 and FtsZ2 proteins, which are phylogenetically distinct homologues of the tubulin-like bacterial cell division protein FtsZ (Osteryoung and McAndrew, 2001). The constituents of the outer ring are not fully known, but the plastid division1 (PDV1) and PDV2 proteins in the outer envelope membrane recruit a cytosolic dynamin-like component, DRP5B, around the chloroplast exterior in alignment with the inner ring (Miyagishima et al., 2006). It has been shown that PDV1 and PDV2 are determinants of the rate and extent of chloroplast division. *Arabidopsis thaliana pdv1* and *pdv2* mutants had earlier been shown to contain large, deformed chloroplasts (Miyagishima et al., 2006). In contrast, when both PDV1 and PDV2 are overexpressed together, *Arabidopsis* cells contain small chloroplasts that are twice as numerous as in wild-type (Okazaki et al., 2009). Interestingly, the levels of PDV protein decrease in relation with the rates of chloroplast division as leaves age, but FtsZ2 and DRPB5 levels remain at similar levels throughout development (Okazaki et al., 2009). Constitutive expression of the cytokinin responsive transcription factor *CRF2* and the application of exogenous cytokinins increased the activity of PDV2, linking cell division and chloroplast division, implying that the PDV proteins are major mechanistic components in determining the cell's chloroplast complement (Okazaki et al., 2009).

1.2 The Chloroplast Protein Import Machinery

1.2.1 Targeting of preproteins from the cytosol to the chloroplast

The majority of the proteins required for plastid functions are encoded in the nucleus and synthesized on cytoplasmic ribosomes. These nuclear encoded proteins need to be targeted to the chloroplast surface. Proteins destined to be imported have to pass through the two envelope membranes before carrying on inside the chloroplast. The majority of the imported proteins are synthesised as precursor proteins with a cleavable N-terminal transit peptide. This peptide is essential and sufficient to address the preproteins to the plastid outer membrane and to transfer them through the chloroplast translocation machinery (Becker et al., 2004a). Proteins targeted to the thylakoid lumen bear bipartite N-terminal presequences, with two domains, one for each of the two membrane systems (envelope and thylakoid) that the protein needs to be targeted across (Robinson and Bolhuis, 2001).

Once the precursor protein has been guided to the chloroplast surface, a process involving several cytosolic chaperones, the precursor interacts with receptors on the chloroplast outer membrane surface and is transported through the membranes in a GTP and ATP dependent manner (Fig. 2). Two multi-protein translocon complexes facilitate the transport across the outer (TOC: translocon at the outer envelope membrane of chloroplasts) and inner (TIC: translocon at the inner envelope membrane of chloroplasts) envelope membranes of most preproteins (Li and Chiu, 2010; Jarvis, 2008) (Fig. 2).

1.2.2 Important cytosolic components

Most precursor proteins, either chloroplast or mitochondrial targeted, have a potential to bind the cytosolic heat shock protein Hsp70, which is a highly conserved chaperone, with well described ATP-dependent and co-chaperone regulated features functions in protein folding and assistance (Mayer, 2005). Binding of Hsp70 to mitochondrial and chloroplast precursor proteins has been shown in several *in vitro* experiments (Ivey et al., 2000). Since ca. 80% of the chloroplast transit peptides have an Hsp70 binding site (Zhang and Glaser, 2002; Rial et al., 2000) and Hsp70 was shown to bind to the transit peptides of the small subunit of Rubisco and ferredoxin NAD(P) reductase (FNR) (Aubry et al., 2008), it is highly possible that Hsp70 plays an important role in protein import.

Other cytosolic components were identified to associate with Hsp70s. A 14-3-3 dimer was shown to bind to the transit peptide of the small subunit of Rubisco and other precursors. Binding take place at a phosphorylated 14-3-3 binding site of the transite peptide, which was detected in these precursors (May and Soll, 2000). The kinase responsible for the phosphorylation of these precursors was identified and isolated from *Arabidopsis* cytosol preparation (Martin et al., 2006). It belongs to a family of three homologous plant specific STY-kinases, containing a serine/threonine as well as a tyrosine phosphorylation domain (Martin et al., 2006). The formation of this so called guidance complex might well have a regulatory function, in relation to specificity, since plant mitochondrial precursors do not form such complexes.

Another major heat shock protein chaperone is involved in guiding precursors to the chloroplast. Hsp90 is a well described chaperone in prokaryotic and eukaryotic organisms, where its function is mainly to assist the folding of transcription factors and protein kinases with the assistance of several co-chaperones (Wandinger et al., 2008). The *Arabidopsis* genome encodes seven isoforms of Hsp90, four of which are localized in the cytosol (Krishna and Gloor, 2001). Down regulation of all cytosolic Hsp90 forms in *Arabidopsis* indicates significant and diverse roles of these proteins in plant development (Sangster et al., 2007). Binding of Hsp90 to precursor proteins in the plant cytosol not only prevents those proteins from aggregation, but also mediates docking of the bound precursors to an outer envelope membrane protein, Toc64 via its cytosolically exposed tetratricopeptide repeats (TPR) domains (Qbadou et al., 2006; Qbadou et al., 2007).

1.3 The receptors Toc34 and Toc159

GTP is necessary during the early steps of protein translocation (Kessler and Blobel, 1996; Olsen and Keegstra, 1992). Toc34 and Toc159 were originally proposed to regulate the initial steps of protein import through a GTP binding and hydrolysis cycle because of their homology to GTP-binding proteins and their capacity to bind GTP *in vitro* (Kessler and Blobel, 1996). Toc34 was also shown to display essential GTPase activity, further supporting the function in GTP-dependent regulation of protein import (Seedorf et al., 1995). Based on sequence analysis it was proposed that the Toc34 and Toc159 G-domains form a novel class of GTPases proteins (Seedorf et al., 1995) because the members of each of the two families share a common domain organisation. The Toc159

homologues have a C-terminal domain anchoring the proteins in the outer membrane (M-domain), while the central GTP binding domain (G-domain) and a highly acidic domain (A-domain) at the N-terminus face the cytosol. Toc34 is a 34 kDa protein that resembles other tail anchored proteins and has an N-terminal region exposed to the cytoplasm (Borgese et al., 2003; Seedorf et al., 1995). The M-domain of Toc159 is rather hydrophilic and does not exhibit typical hydrophobic transmembrane helices (Kessler et al., 1994; Bauer et al., 2000). The insensitivity to protease treatment in isolated chloroplasts is evidence to the membrane protected nature of the M-domains (Kessler et al., 1994; Bauer et al., 2000).

GTP binding proteins are known to act as molecular switches by alternating between active GTP-bound and inactive GDP-bound states (Vernoud et al., 2003). Interestingly, the G-domains of Toc34 and Toc159 interact and this is believed to be important insight of the import mechanism. Both homodimerization and heterodimerization of the G-domains have been observed using biochemical methods (Yeh et al., 2007; Bauer et al., 2002). Dimerization was suggested to stimulate the GTPase activity of Toc34 but this is conflicting with the finding that substitution of a putative arginine finger (Arg130) for an alanine residue (R130A) in an *Arabidopsis* homologue called atToc33 does not affect its GTPase activity, but instead greatly inhibits dimerization (Weibel et al., 2003; Lee et al., 2009). Many GTPases also associate with a second protein, a guanine nucleotide exchange factor (GEF), that promotes the exchange of GDP for GTP at the binding pocket of the GTPase (Bourne et al., 1991).

1.3.1 The two models of the protein import machinery

Recent efforts to define the roles of Toc34 and Toc159 receptors in preproteins recognition led to the emergence of two models (Fig. 3): the targeting model, and the motor model (Kessler and Schnell, 2004). The targeting model proposes that Toc159 is the primary receptor, and that it also plays a role in preprotein targeting from the cytosol to the chloroplast surface. In contrast, the motor model suggests that Toc34 carries out the role of primary receptor, whereas Toc159 acts as a molecular motor to drive preprotein translocation across the outer envelope (Kessler and Schnell, 2004).

1.3.1.1 The motor model

In the motor model, Toc159 functions as a GTP-dependent motor that pushes preproteins through the TOC channel via multiple rounds of GTP hydrolysis (Fig 3b). The proposed central function of Toc159 as a motor and the close 1:1 stoichiometric association of the Toc34 with the Toc75 channel in the core complex (Schleiff et al., 2003a), led to the suggestion that Toc34 is likely to function as the preliminary receptor (Becker et al., 2004a). This proposed motor model was further supported by the fact that Toc34 is crosslinking to precursors only at the initial energy-independent binding stage of import; by contrast, Toc159 appears to remain in close proximity with precursors throughout their translocation through the OEM (Kouranov and Schnell, 1997). Becker et al., (2004a), presented strong evidence in favour of the motor model. First, detailed subcellular fractionation studies suggested that the previously-observed soluble form of Toc159 (Hiltbrunner et al., 2001a) (see Section 1.3.2.2 below) is an artefact produced by the fractionation method used. It was concluded that Toc159 is only present as an integral protein of the chloroplast outer envelope membrane. In contrast with Toc34, which binds phosphorylated transit peptides with high affinity (Sveshnikova et al., 2000a), Toc159 only recognizes the non-phosphorylated form of the transit peptide. Furthermore, by using peptides spanning either the C- or N- terminal regions of a transit peptide, they revealed that a Toc159 fragment spanning the G- and M- domains (Toc86) displays high affinity (Becker et al., 2004a; Sveshnikova et al., 2000b).

The differential peptide-binding properties of Toc34 and Toc159 were used to show that Toc34 functions before Toc159 in the binding and translocation of precursor proteins. This was demonstrated by using the different peptides to inhibit binding and import into proteoliposomes containing the reconstituted core TOC complex (TOC proteoliposomes) (Becker et al., 2004a). Only the phosphorylated C-terminal peptide was able to significantly inhibit binding of preproteins into TOC proteoliposomes, whereas both the phosphorylated C-terminal peptide and the N-proximal peptide inhibited import of the precursor. This clearly indicates that in order to bind to the chloroplasts, precursors need to interact with Toc159 to be imported.

Furthermore, Becker et al., (2004a) have investigated how GTP and GDP affect the stability of the TOC complex. Immunoprecipitation experiments from outer envelope vesicles OEVs with antibodies against both receptors showed that the association of

Toc34 with the TOC is destabilized by GDP. In contrast, in presence of a non-hydrolysable form of GTP (GMP-PNP) the association of Toc34 with the TOC was favoured. Also, the association of Toc159 with Toc75 was nucleotide insensitive. When (OEVs) were solubilised in the presence of GDP, the core TOC components were enriched in low-density fractions as compared with in the absence of nucleotides (Sveshnikova et al., 2000a).

In conclusion, from the results described above the motor model proposes that Toc34-GTP initially recognizes and binds to the phosphorylated C-terminal region of an arriving transit peptide. Hydrolysis of GTP by Toc34 causes the release of the C-terminal region of the transit peptide, allowing an unidentified phosphatase to dephosphorylate the Toc159-bound peptide. After dephosphorylation, the C-terminal part of the transit peptide also binds to Toc159, promoting its GTPase activity. GTP hydrolysis by Toc159 induces a change in conformation of the protein, which in turn promotes dissociation of Toc34-GDP from the TOC complex and the insertion of the preproteins into the Toc75 channel (Becker et al., 2004a).

1.3.1.2 The targeting model

In the targeting model, after preprotein recognition, Toc159 associates with the secondary receptor, Toc34, to promote the transfer of the precursor to the Toc75 channel (Fig. 4a). This model is based on the early findings of (Kouranov and Schnell, 1997) and on the work of (Hiltbrunner et al., 2001a). The latter study found an abundant cytosolic form of Toc159 that exists in addition to its integral membrane form. This was supported by subcellular fractionation experiments in *Arabidopsis* and pea, which revealed that Toc159 exists in a soluble cytosolic form, whereas Toc34 and Toc75 could not. However, recent studies revealed that the cytosolic form was probably not the full length Toc159 protein (Agne et al., 2009; Agne et al., 2010).

In vitro targeting studies revealed that Toc159 binding and insertion are regulated by the protein's GTPase activity. GTP binding by Toc159 promotes binding of the receptor to the chloroplast outer membrane, and GTP hydrolysis is required for efficient insertion of the M-domain into the membrane (Smith et al., 2002; Bauer et al., 2002). *In vivo* studies have shown that a functional GTPase domain is required for Toc159 transgenes to fully complement an *Arabidopsis* atToc159 null mutant called protein plastid import2 (*ppi2*) (Lee et al., 2003; Bauer et al., 2002). However, the G-domain of Toc159 is not essential

for targeting *in vivo*, since a truncated form of Toc159 composed exclusively of the M-domain was found to accumulate at the OEM, and to mediate partial complementation of *ppi2* (Lee et al., 2003). Toc159 was found to insert equally in presence of either GTP or GDP.

Studies by both Hiltbrunner et al., (2001b) and Smith et al., (2002) suggested that Toc159 targeting to the chloroplast is mediated by an interaction with Toc34 (Smith et al., 2002). They further showed that this specific interaction corresponds to a homotypic interaction between the G-domains of both proteins. In another study it was revealed that binding and insertion of Toc159 into the OEM is also dependent upon Toc34 GTPase activity (Wallas et al., 2003), confirming the importance of a GTP regulated interaction between the homologous G-domains of Toc34 and Toc159. It is possible that initial binding occurs between Toc159-GTP and Toc34-GTP, and that induces GTP hydrolysis by both GTPases. In addition (Wallas et al., 2003) revealed that the presence of Toc75 is essential for the membrane insertion of the M-domain of Toc159. It is possible that due to its overall hydrophilic nature, the insertion of the Toc159 M-domain involves the formation of β -strands (Schleiff et al., 2003a), and that these are stabilized through interactions with Toc75.

1.4 The chloroplast translocation machinery of the outer envelope membrane

The translocation through the TOC complex was at one point thought to be driven solely by the activities at the TIC complex. However more evidence has accumulated that point toward some kind of motor activity in of the outer envelope membrane aiding transfer through the Toc75 channel (Kovacheva et al., 2007) (Fig. 4). Experimental evidence for the GTP motor hypothesis above (Schleiff et al., 2003a), implied that Toc159 is a GTP-driven motor that pushes the preprotein through the TOC channel. This study used purified and reconstituted core TOC complexes and individual TOC components to determine the minimal requirements for translocation. They showed that proteoliposomes loaded with both Toc86 (a proteolytic fragment of Toc159) and Toc75 were able to import preproteins in a GTP-dependent manner. Since proteoliposomes loaded with Toc34 and Toc75 in combination, or Toc75 alone, were not able to support translocation, it was concluded that Toc159 and Toc75 make up the minimal translocase. To explain the GTP dependence of this minimal translocase, it was proposed that GTP hydrolysis by

Toc159 induces a change in conformation that would lead to the insertion of the preprotein into the TOC channel. However, the demonstration that the M-domain of Toc159 is sufficient to partially complement the *ppi2* mutant argues strongly against an essential role for the G-domain of Toc159 in driving translocation (Lee et al., 2003).

The involvement of chaperones offers an alternative possibility. It is well known that the formation of the early import complex requires ATP, which may imply the involvement of molecular chaperones in this process (Olsen and Keegstra, 1992). Between the TOC and TIC complexes in a hypothetical intermembrane space, Hsp70 chaperone may act as a molecular “magnet” by binding on to proteins as they exit the TOC complex and making sure that translocation occurs in just one direction, in a manner similar to mitochondria (Neupert and Brunner, 2002). Hsp70 was found in close proximity to the TOC complex when other components were isolated (Schnell and Hebert, 2003). Even more intriguing, is that Toc12 was proposed to act as a co-chaperone modulating the action of Hsp70 (Becker et al., 2004b). Toc12 is a DnaJ-like protein that was reported to be anchored in the outer envelope membrane exposing its C-terminal J-domain in the intermembrane space (Figure 4). The J domain was proposed to stimulate the activity of the Hsp70 to promote transport. It is also thought to function in redox-sensing through the action of a disulphine bond (Becker et al., 2004b). However, recent evidence revealed that Toc12 is actually located in the stroma (Chiu, 2011), while attempts to identify a gene encoding the intermembrane space Hsp70 have been unsuccessful (Ratnayake, 2008; Su, 2008).

1.5 The TOC complex and its components

As was described earlier (see Section 1.3), preproteins targeting to the TOC complex has been shown to involve cytosolic factors, such as a heat shock or regulatory proteins. These factors are implicated in the guiding of cytosolic preproteins to the chloroplast envelope and different pathways have been described. Thereafter, it is well known that the initial targeting of preproteins through the outer membrane is mediated by the interaction of their transit peptides with two GTPase receptors, Toc34 and Toc159 (Agne and Kessler, 2009). The receptor proteins have been shown by co-immunoprecipitation studies to form a stable trimeric complex together with the Toc75 channel protein. These three proteins form the TOC core complex and appear to be sufficient for *in vitro* translocation of a precursor protein in lipid vesicles (Schleiff et al., 2003b). The mass of

this core complex is estimated to be around 1 MDa in *Arabidopsis* (Kikuchi et al., 2009). In pea, stoichiometries of 4-5:4:1 or 3:3:1 between Toc34, Toc75, and Toc159 have been determined (Kikuchi et al., 2006; Schleiff et al., 2003b).

1.5.1 Function of Toc159 and Toc34 isoforms in different import pathways

Analysis of *Arabidopsis* TOC complexes indicated that the Toc132 and Toc120 proteins are present in complexes that excluded Toc159 protein (Ivanova et al., 2004), and are present in the protein import complex of proplastids (Brautigam and Weber, 2009). Moreover, Toc34 was present in Toc132/120 comprising complexes, whereas there is a preferential association of atToc159 and atToc33 (Ivanova et al., 2004). These two components are strongly expressed in young green tissues, and together are associating to form TOC complexes specialized for the import of highly expressed photosynthetic preproteins during chloroplast biogenesis (Fig. 6). Moreover, since atToc132, atToc120 and atToc34 share similar expression patterns (Kubis et al., 2003; Kubis et al., 2004; Ivanova et al., 2004), they are likely to associate together to form TOC complexes specific for the import of non-photosynthetic proteins. Furthermore, the only growth defect exhibited by atToc34 knockout mutants, called *ppi3*, is in the roots, which are non-photosynthetic organs (Constan et al., 2004). The existence of distinct translocon complexes with different preprotein binding preferences might be essential to prevent the bulk flow of abundant precursors from competing with the import of less abundant proteins (Fig. 6). However, genetic data indicate that neither pathway exhibits absolute substrate specificity. Components of the TIC complex such as Tic40, Tic110, and Hsp93 seem to be involved in the import of both photosynthetic and non-photosynthetic preproteins (Kovacheva et al., 2005).

1.5.2 TOC isoforms of *Arabidopsis thaliana*

The existence of several isoforms of the import components in *Arabidopsis* and other organisms seems to enable the plants to regulate protein import. In *Arabidopsis* small gene families encode homologues of originally identified pea Toc34 and Toc159 proteins (called psToc34 and psToc159). Two *Arabidopsis* genes, *atTOC33* and *atTOC34*, encode homologues of psToc34, whereas four genes, *atTOC159*, *atTOC132*, *atTOC120* and *atTOC90*, encode homologues of psToc159 (Bauer et al., 2000; Hiltbrunner et al., 2001a; Jarvis et al., 1998) (Table 1). The Toc159 homologues show more variation, especially across the A- domain, which varies in length and sequence between the different

isoforms. However, the G- and M- domains of each homologue display significant levels of homology with psToc159. The G- and M- domains of atToc132 and atToc120 are very similar. These two receptors show greater homology to each other than to atToc159, and thus appear to form a subgroup within the Toc159 family (Ivanova et al., 2004; Kubis et al., 2004). Lastly, atToc90 is the only Toc159 homologue that lacks the A-domain; instead it has a short, non acidic N-terminal extension. Based on its G- and M- domains, atToc90 may be slightly more closely related to atToc159 than to atToc132 and atToc120 (Ivanova et al., 2004). However, the phylogenetic analysis conducted by (Kubis et al., 2004) suggested that atToc90 represents a unique subtype of Toc159-related proteins, distinct from the atToc159- and atToc132/atToc120- related subgroups. More recently, *in vivo* studies have shown that overexpression of atToc90 can partially complement *ppi2* (Toc159) and restore sufficient protein import for autotrophic growth (Infanger et al., 2011).

1.5.2.1 Toc34 and its homologues in *Arabidopsis thaliana*.

The first identified *Arabidopsis* plastid protein import mutant, *ppi1*, was originally identified in a screen for mutants displaying reduced expression of nucleus encoded photosynthetic genes (Jarvis et al., 1998). The *ppi1* mutant carries a T-DNA insertion that abolishes the expression of the atToc33 gene. Young plants homozygous for the insertion display a uniformly pale phenotype caused by a defect in chloroplast biogenesis. As the plant becomes older, mature leaves develop a greener phenotype similar to wild-type leaves, whereas young expanding leaves display a chlorotic phenotype. In *Arabidopsis thaliana*, two homologues of *psTOC34* are present (see Appendix); *atTOC33*, which seems to be a functional analogue of *psTOC34* and can be switched off by phosphorylation, and *atTOC34* which seems not to be phosphorylated and therefore functions as a constitutive receptor for protein import (Gutensohn et al., 2000; Yu and Li, 2001).

Analysis of the expression levels of *atTOC33* and *atTOC34* in developing seedlings revealed that both genes are developmentally regulated, showing higher levels of expression in young seedlings than in older plants. By comparing the levels of steady state mRNA found in young leaves and old leaves of older plants, both genes were found to be up-regulated in young developing leaves. In addition *atTOC33* was expressed at ~5 fold higher levels than *atTOC34*, in both young and old leaves. This led to the conclusion

that atToc33 is important to cope with the high import requirements associated with rapid chloroplast biogenesis in young, expanding tissues (Jarvis et al., 1998).

More detailed studies of *atTOC33* and *atTOC34* further established that the two genes display different patterns of expression (Kubis et al., 2003; Gutensohn et al., 2000). Quantitative and comparative analyses of the expression levels of both genes in different tissues and at different developmental stages confirmed that *atTOC33* is strongly up-regulated in young developing green tissues (Kubis et al., 2003). In contrast, *atTOC34* expression was considerably lower than that of atTOC33, and was relatively more uniform. Interestingly, in roots the two genes were found to be expressed at similar levels, indicating that *atTOC34* may play a relatively more important role in root plastid development than in chloroplast biogenesis (see Section 2.1.2).

Furthermore, the two Toc34 receptor homologues display some level of recognition specificity towards the transit peptides of different precursors, as was shown by testing the affinity of atToc33 and atToc34 for various preproteins *in vitro* (Jelic et al., 2003). The functional specificity between the two *Arabidopsis* Toc34 receptor homologues has also been addressed *in vivo* by taking advantage of the *ppi1* mutant, other similar T-DNA insertion mutants, and transgenic antisense lines (Constan et al., 2004; Gutensohn et al., 2000; Kubis et al., 2003). Because the *atTOC33* gene is strongly up-regulated in tissues where chloroplast biogenesis occurs, it was suggested that the atToc33 receptor may be involved specifically in the import of highly expressed photosynthetic proteins (Kubis et al., 2003). A role of atToc33 as a specific receptor for photosynthetic preproteins and, by extension that of atToc34 as a non-photosynthetic preprotein receptor, has been addressed by Gutensohn, (2004) who identified and characterized a new knockdown allele of atToc33. This allele carries a T-DNA insertion within the first exon of the gene, in the upstream un-translated region, resulting in near complete loss of atToc33 expression and in a phenotype similar that of *ppi1*. By taking similar immunoblotting and proteomics approaches to those taken by Kubis et al., (2003), it was shown that photosynthetic proteins are less abundant in the mutant than in the wild type, although some did appear to be unaffected. When the expression of atToc34 was also repressed, by the introduction of an antisense transgene into the atToc33 knockdown mutant, it was revealed that that the photosynthetic proteins unaffected in the atToc33 mutant were now significantly reduced. This result suggests that the proposed specificities of atToc33 and atToc34 for photosynthetic and non-photosynthetic preproteins, respectively, are not absolute.

The only phenotype reported for the atTOC34 knockout *ppi3* consists of a slight reduction in root growth; further supporting the prediction that atToc34 may be involved in root plastid development. However, a *ppi1 ppi3* double homozygous mutant, were revealed to be embryo lethal. This indicates that the two Toc34 homologues are essential for plastid biogenesis, and that atToc34 is likely responsible for the residual level of chloroplast development observed in *ppi1* (Constan et al., 2004).

1.5.2.2 Toc159 and its homologues in *Arabidopsis thaliana*

The second *Arabidopsis* plastid protein import mutant to be identified, termed *ppi2*, is a null T-DNA insertion mutant of *atTOC159* (Bauer et al., 2000). Initial RNA blot analysis of steady state mRNA levels indicated that *atTOC159* is expressed at a level approximately seven-fold higher than *atTOC132* and *atTOC120*, in green young, wild-type seedlings. In addition, the expression of all three receptors appeared to be stimulated roughly two-fold by light. These results suggested that atToc159 is likely the predominant Toc159 receptor homologue during seedling development. This is in line with the finding that *ppi2* is seedling lethal, since it develops albino cotyledons but fails to produce first true leaves when grown in soil. The albino phenotype is due to the fact that plastids do not develop and the plants cannot grow autotrophically (Bauer et al., 2000). Interestingly, growth on medium supplemented with sucrose can partially “rescue” the mutant, allowing it to develop into a small albino plant. This indicated that it can still carry out essential plastid functions other than photosynthesis. Transmission electron micrographs of the plastids in *ppi2* cotyledons indicated that these remain largely undifferentiated, lacking thylakoid membranes which are a specific characteristic of chloroplasts associated directly with photosynthesis (see Section 1.1). Further characterization of the mutant revealed that the major photosynthetic proteins, like the large rubisco subunit, the small rubisco subunit and the light harvest chlorophyll (namely RbcL, RbcS and LhcII), were present in *ppi2* plastids, but only at much lower levels than in wild-type chloroplasts. This indicated that although accumulation of photosynthetic proteins was severely reduced in plastids lacking atToc159, these organelles were still capable of importing these proteins. This led to the conclusion that atToc159 is the main receptor for the efficient import of photosynthetic chloroplast preproteins, and for chloroplast biogenesis (Bauer et al., 2000). Interestingly, the photosynthesis-related nuclear genes encoding the photosynthetic proteins are down-regulated at the transcriptional level (Bauer et al., 2000). Recently it has been proposed that, in *ppi2*, this down-regulation of photosynthesis-related nuclear

genes may be mediated by new plastid-to-nucleus retrograde signalling pathways involving the protein called GUN1 (Kakizaki et al., 2009).

In addition, it was proposed that the other Toc159 homologues, atToc132 and atToc120, (see Appendix) are responsible for the normal accumulation of non-photosynthetic plastid proteins, as well as for the limited accumulation of photosynthetic proteins observed in *ppi2* mutants. Less is known still about the function of *atTOC90*, but what is known is summarized in the next section. This thesis will try to shed light in this area. Double knockout mutants of the atToc120 and atToc132 genes display either an albino phenotype (Kubis et al., 2004) or an embryo lethal phenotype (Ivanova et al., 2004), whereas the respective single mutants had no or only a weak phenotype (Ivanova et al., 2004; Kubis et al., 2004). The overexpression of either atToc120 or Toc132 complemented the double mutant phenotype, indicating a significant functional overlap between the two proteins and a function distinct from the atToc159 (Kubis et al., 2004). While *ppi2* affected aerial tissues, the *toc132 toc120* plants exhibit structural abnormalities in the roots suggesting a role in the import of house-keeping substrates or in non-photosynthetic tissues (Kubis et al., 2004). Analysis of *Arabidopsis* TOC complexes indicated that Toc120 and Toc132 proteins are present in complexes that exclude Toc159 (Ivanova et al., 2004) and are present in protoplasts (Brautigam and Weber, 2009).

Due to its proteolytic sensitivity, Toc159 was first identified as an 86 kDa protein (Waagemann and Soll, 1991) and was then initially named Toc86 (Hirsch et al., 1994; Kessler et al., 1994). Recently, {Inoue, 2010 #651} has reported that *in vivo* function of atToc159 and atToc132 can be largely switched by swapping their A- domains in transgenic *Arabidopsis thaliana*. It was proposed that the A- domains of Toc159 receptors are major determinants of distinct pathways for protein import (Inoue et al., 2010). Complementation studies of the *Arabidopsis ppi2* mutant have revealed that the A-domain is dispensable. “Toc86” or Toc159GM consisting only of the G-and M-domains rescued the albino phenotype of the *ppi2* mutant (Lee et al., 2003; Agne and Kessler, 2009). Thus, these results indicate that the “Toc86” form of Toc159 most likely is an active protein. While clearly the A-domain is non-essential, it cannot be ruled out that it may be somehow functionally redundant with the A-domains of other Toc159 homologues (Bauer et al., 2000). The M-domain anchors the protein to the chloroplast outer membrane, and is sufficient to complement the defect in protein import in *Arabidopsis* protoplasts (Lee et al., 2003). The G-domain contains GTP binding motifs as

well as a dimerisation motif (Sun et al., 2002). The G-domain binds GTP and is involved in the targeting of Toc159 to the membrane in the presence of GTP (Smith et al., 2002; Lee et al., 2003).

Recently, it has been proposed that the TOC complex interacts with actin and the interaction is mediated by Toc159 (Jouhet and Gray, 2009). The role of this interaction remains to be investigated further, but a possible explanation is a role in gravitropism which involves actin. Gravitropism has been recently linked to the TOC complex by the observation that atToc75-III and atToc132 are responsible for enhancing root gravitropism (Stanga et al., 2009).

1.5.2.3 The Toc75 protein and channel of the outer envelope membrane

The channel in the outer membrane of chloroplast is formed by the Toc75 protein. Toc75 is the most abundant outer membrane protein (Perry and Keegstra, 1994). *In vitro* analysis has demonstrated that Toc75 interacts with preproteins during import (Ma et al., 1996; Schnell et al., 1994). Evidence that Toc75-related proteins are present in plant species other than pea was provided by Summer and Cline (1999), who used an anti-psToc75 antibody to identify a 75-kD protein in chromoplasts from red bell pepper. In addition proteolytic treatment of either chloroplasts or outer membrane vesicles does not cause degradation of Toc75, indicating that the protein is deeply embedded in the membrane (Tranel et al., 1995). Tranel et al. (1995) showed that on treating isolated chloroplasts with different proteases, Toc75 is protected from thermolysin treatment, and is producing a large 52 kDa proteolysis-protected fragment after trypsin treatment (Schnell et al., 1997; Tranel et al., 1995). These two proteases have been used to analyse the topology of chloroplast envelope membranes, since thermolysin cannot penetrate the outer membrane whereas trypsin damages the outer membrane and gains access to proteins exposed in the inter membrane space but not to the stroma (Jackson et al., 1998).

Further analysis of the amino acid sequence of Toc75 has shown that it has a two-domain structure typical of the outer membrane protein85 (Omp85) family, with an N-terminal domain containing polypeptide-transport-associated (POTRA) signatures and a C-terminal β -barrel domain formed by β -strands (Sánchez-Pulido et al., 2003). Structural analysis of Toc75 has shown that this β -barrel-type channel is lined by 16 or 18 transmembrane β -sheets (Sveshnikova et al., 2000b; Sánchez-Pulido et al., 2003; Schleiff et al., 2003b). The Omp85 family comprises proteins essential for integration of β -barrel

protein substrates in the outer membrane in Gram-negative bacteria and mitochondria (Sam50), and this may also be the case for OEP80 in the chloroplast (Gentle et al., 2005; Patel et al., 2008). Patch clamp analysis of planar lipid bilayers has shown that reconstituted pea Toc75 forms a voltage-gated ion channel interacting specifically with precursor proteins (Hinnah et al., 1997). The pore size has been estimated to be 14 Å at the narrowest part (Hinnah et al., 2002). The N-terminal part of Toc75 is characterized by the presence of three POTRA domains, thought to perform secondary functions such as TOC complex assembly, preprotein recognition or chaperone-like activity (Ertel et al., 2005).

Toc75 is the only protein of the TOC complex to process an N-terminal cleavable targeting sequence. Its N-terminal part consists of a classical transit peptide, and this part reaches the chloroplast stroma where it is cleaved by the stromal processing peptidase. The C-terminal part of the bipartite targeting sequence spans the intermembrane space and is cleaved by an envelope-bound type-I signal peptidase (Inoue and Keegstra, 2003). A polyglycine stretch in the C-terminal part appears to play an essential role in retaining Toc75 at the outer chloroplast membrane. The role of the polyglycine stretch is not clear yet, though it has been hypothesized that the stretch could prevent association with Hsp70 to the intermediate of Toc75 (after cleavage of the transit peptide) before complete insertion, thereby assuring correct folding of Toc75 at the envelope (Inoue and Keegstra, 2003; Baldwin and Inoue, 2006).

To date two Toc75 encoding genes are known to be present in the pea genome; Toc75, coding for the protein-conducting channel and Toc75-V discovered on the basis of its sequence similarity with the bacterial homologue. It has been proposed that Toc75-V could be a direct ortholog of the cyanobacterial ancestor, and Toc75 a paralog (Eckart et al., 2002). A number of Toc75 isoforms are present in *Arabidopsis thaliana* (see Appendix), and they are named according to the chromosome location of the genes (Jackson-Constan and Keegstra, 2001); atTOC75-III, atTOC75-IV, atTOC75-V and atTOC75-I.

AtTOC75-III is the closest homologue of pea Toc75, and is most likely the channel of the *Arabidopsis* TOC complex. atToc75-III was present in an immunocomplex isolated using an affinity purified antibody against atToc33 (Hiltbrunner et al., 2001a). Furthermore, the Toc75-III knockout mutant is embryo-lethal, indicating an essential role in plastid

development (Baldwin et al., 2005; Hust and Gutensohn, 2006). Recently, Huang et al. (2011), conducted detailed studies on plants silenced for atToc75-III or atOEP80 and the results showed that both proteins are important for chloroplast biogenesis at postembryonic stages of development.

A second homologue, *atTOC75-IV* having a shorter N-terminal region lacking the POTRA domain and five of the eighteen predicted β -strands, does not appear to be essential for protein import under normal growth conditions. Earlier work from Baldwin et al. (2005) showed that the *atTOC75-IV* gene is expressed at very low levels, and that knockout mutant plants do not exhibit obvious developmental defects, suggesting that the atToc75-IV protein plays a relative minor, highly specialized role (Baldwin et al., 2005). However, the ultrastructure of etioplasts from dark-grown plants is altered in *toc75-IV* mutants, suggesting a specialized role in etioplasts (Baldwin et al., 2005).

A third homologue, atTOC75-V, has a molecular weight of 80 kDa and is thought to be involved specifically in the biogenesis of outer membrane proteins (Huang et al., 2011). It has been named outer envelope protein of 80 kDa (OEP80). It does not appear to be part of the TOC complex (Eckart et al., 2002).

atTOC75-I, the fourth homolog, was shown to be a pseudogene interrupted by a gypsy transposon insertion (Baldwin et al., 2005).

In silico analysis has shown that Toc75 is the only component of the TOC complex of cyanobacterial origin, and it is perhaps derived from the secretory pathway of the original endosymbiont (Reumann et al., 1999). Toc34 and Toc159 appear to have been added to the core complex later on, but still at an early step of evolution as the components are common to all higher plants, mosses as well as green algae (Kalanon and McFadden, 2008; Reumann et al., 2005).

1.5.2.4 Toc12 and its role

Toc12, a protein containing a J-domain, was initially reported to be located at the intermembrane face of the outer envelope (Becker et al., 2004b). Toc12 has been shown to interact with Toc64 (Becker et al., 2004b). *In vitro*, Toc12 interacts with Hsp70 proteins and it enhances their ATP hydrolysis. A possible role of Toc12 is to retain Hsp70 proteins in the close vicinity of the TOC complex, in order to bind to any incoming preproteins and prevent them from slipping back into the cytosol at the early intermediate

stage. A disulfide bridge in the loop region of the J-domain was implicated in the redox regulation of the Toc12/Hsp70 interaction (Becker et al., 2004b). Translocation across the dual membrane envelope is accomplished in a synergistic way, where the TOC and TIC complexes are in close proximity at contact sites between the two membranes (Schnell et al., 1994; Nielsen et al., 1997). These contact sites may be mediated by Toc12 and Tic22, which are both largely facing the intermembrane space, and so may act by “bridging” the two translocon complexes (Kouranov and Schnell, 1997; Ma et al., 1996); Becker et al., 2004b). However, more recently it has been shown that Toc12 is actually a truncated form of a largely protein called J8, which is a stromal protein (Chiu et al., 2011). Moreover, it has not been possible to identify an *Arabidopsis* gene encoding an intermembrane space Hsp70 (Ratnayake et al., 2008; Su et al., 2008). Thus, the above mentioned hypotheses for translocation between the TOC and TIC complexes must be revised.

1.5.2.5 Toc64

The role of Toc64 is less well-defined. The C-terminal domain has three tetratricopeptide repeat motifs (TPR), which are exposed on the cytosolic face of the organelle (Sohrt and Soll, 2000). TPR motifs exhibit a large degree of sequence diversity. Individual TPR domains are composed of two anti-parallel alpha helices separated by a turn. TPR motif-containing proteins act as scaffolds for the assembly of different multiprotein complexes including the anaphase promoting, the peroxisomal import receptor and the NADPH oxidase complexes. The N-terminal region contains a transmembrane region and the central domain has homology with amidases (Sohrt and Soll, 2000). Toc64 is loosely associated with the TOC core complex (Sohrt and Soll, 2000; Qbadou et al., 2006). Toc64 has been proposed to be involved in the targeting of cytosolic preproteins to the TOC complex, with the TPR domain acting as a docking station for the Hsp90 chaperone carrying preproteins (Schlegel et al., 2007). Pea has one known gene for Toc64, whereas in *Arabidopsis* three paralogs have been found; atToc64-I, atToc64-III, and atToc64-V (Jackson-Constan and Keegstra, 2001). Toc64-III is targeted to the outer envelope membrane of chloroplasts (Lee et al., 2003), whereas the two others are not chloroplastic. Toc64-I, or AMI1, is a cytosolic protein that possesses only the amidase region and lacks the transmembrane region as well as the TPR motifs. Toc64-I is non-essential for chloroplast protein import (Aronsson et al., 2007). atToc64-V is a mitochondrial protein

and has been proposed to be the plant analogue of the animal and fungal component of the translocase of the outer membrane of mitochondria, Tom70 (Chew et al., 2004).

1.6 The chloroplast translocation machinery of the inner envelope membrane

In mitochondria, translocation of the presequence through the translocase of the inner membrane₂₃ (TIM23) complex is driven by the electrical potential across the inner membrane, which exerts an electrophoretic effect on the positively charged presequence (Geissler et al., 2000). However, chloroplast are not believed to maintain a strong electric potential across the envelope and also it has been shown that a membrane potential is not necessary for protein translocation across the envelope (Theg et al., 1989). The first of the known TIC components to be encountered by a translocating preprotein is most likely Tic22 (Kouranov and Schnell, 1997; Kouranov et al., 1998). This protein resides in the intermembrane space and more likely facilitates the passage of preproteins from the TOC to TIC complex. A domain of Toc64 was also proposed to contribute to translocation across the intermembrane space (Qbadou et al., 2007), but since the vast majority of this protein is oriented towards the cytosol it would appear to be an unlikely participant in this process (Hofmann and Theg, 2005a). The Tic22 protein might also play a role in the formation of the so called TOC-TIC supercomplexes (Akita et al., 1997; Kouranov et al., 1998), which presumably serve to facilitate simultaneous transport across both envelope membranes (Fig. 4).

The most basic function of the TIC apparatus is the formation of an aqueous pore for preprotein conductance. A role of Tic110 was supported by electrophysiological studies done on protein reconstituted into artificial membranes (Heins et al., 2002), whereas as the candidacy of Tic20 is based on its predicted topology and similarity with bacterial branched-chain amino acid transporters and channel components of the mitochondrial TIM machinery (Reumann and Keegstra, 1999). Though, recent results from Kasmati et al. (2011) shown that analysis of Tic20 sequences from many species indicated that they are phylogenetically unrelated to mitochondrial Tim17-22-23. Antisense downregulation of the major *Arabidopsis* isoform of Tic20 caused defects in chloroplast biogenesis associated with inefficient transport across the inner membrane (Chen et al., 2002). More recently, Tic21, a protein with topological similarity to Tic20, was identified as a third

putative channel component (Teng et al., 2006), although the role of this component in chloroplast protein import has been disputed (Duy et al., 2007).

A binding chain pathway that would expose the transit peptide at the exit of the translocation channel would allow stromal factors involved in protein translocation to gain access to the translocating preprotein. A high level of energy (ATP) is required in the stroma to complete preprotein translocation across the envelope (Theg et al., 1989). Three stromal molecular chaperones have been reported to associate specifically with the TIC complex: Cpn60 (Kessler and Blobel, 1996) and Hsp93 (Akita et al., 1997; Nielsen et al., 1997) (Fig. 4). Cpn60 was initially identified as the predominant protein co-immunoprecipitating with Tic110 from solubilised chloroplasts (Kessler and Blobel, 1996) and later was shown to associate with the TOC-TIC complexes (Kouranov et al., 1998). The absence of other significantly co-immunoprecipitated proteins under the experimental conditions suggested that Cpn60 may interact directly with the stromal domain of Tic110.

The Tic110 stromal domain can bind transit peptides, and probably functions to recruit molecular chaperones to protein import sites (Akita et al., 1997; Inaba et al., 2003). It is thought that chaperones held at Tic110 bind to emerging preproteins, ensuring unidirectional movement into the stroma through a ratchet-type mechanism (Kessler and Blobel, 1996; Nielsen et al., 1997). Hsp93 the second stromal molecular chaperone found to interact with the TIC complex and was identified in cross-linking experiments with early import intermediates (Akita et al., 1997). Recently the human muscle protein titin (Ruprecht et al., 2010), has been used as a model cargo to understand the molecular mechanisms of unfolding. Titin has been used before to analyze the unfolding properties of the mitochondrial translocon (Oguro et al., 2009; Sato et al., 2005). Using the same set of titin and titin mutants (Ruprecht et al., 2010) have shown that energy for initial unfolding of the chloroplast precursors provided by the chloroplast translocon is higher than that provided by the mitochondrial one. Furthermore, the initial unfolding of the precursor is driven by an independent chaperone system interconnecting the two translocons of the chloroplast envelope, and final translocation is achieved in chloroplasts by Hsp93 (Ruprecht et al., 2010).

1.7 The TIC machinery and its components

The composition and stoichiometry of the machinery involved in the import of preproteins into chloroplasts at the inner envelope membrane is less known than that of the TOC machinery. Seven or eight proteins have been proposed to form the TIC apparatus in higher plants: Tic110, Tic20 and Tic21 as putative constituents of a translocon channel; the co-chaperone Tic40 and the translocon associated Tic55, Tic32 and Tic62 subunits (Stengel et al., 2008) (Fig. 4). Tic21 is the most recently added putative component of the TIC translocon (Teng et al., 2006).

1.7.1 Tic110

Tic110 is one of the most abundant protein of the inner envelope membrane and plays an essential role in plastid biogenesis, since knockout mutants of the single *atTIC110* gene in *Arabidopsis* are not viable (Inaba et al., 2005) and even the heterozygous knockout plants display a mild phenotype (Kovacheva et al., 2005). It comprises two membrane spanning α -helices in the extreme N-terminus, which are necessary for targeting to and insertion into the inner envelope (Lübeck et al., 1997; Kessler and Blobel, 1996). The carboxy-terminus is largely hydrophilic and according to one hypothesis, it forms a large globular domain on the stromal side where it recruits chaperones (Inaba et al., 2003; Jackson et al., 1998). Other recent results demonstrated that the largely α -helical C-terminus features four additional transmembrane domains, consisting of amphipathic α -helices (Balsera et al., 2009a). This was corroborated by protease treatment of inner envelope vesicles, which resulted in proteolytic degradation of Tic110 from the intermembrane space side. Electrophysiological measurements of the heterologously expressed C-terminus showed that this part of Tic110 alone, without the two hydrophobic α -helices, is able to form a cation-selective calcium sensitive channel (Heins et al., 2002). Interestingly, Tic110 seems to be in a reduced state in the dark and to get oxidized in the light, which might indicate that disulfide bridge formation is stress related phenomenon in Tic110 (Balsera et al., 2009b).

1.7.2 Tic20 and Tic22

The second component with a proposed channel function is Tic20 (Kouranov et al., 1998). Tic20 is an integral protein in the inner envelope membrane. The function of Tic20 in protein import has been supported by its direct interaction with preproteins in

crosslinking experiments, its association with other TIC components and specific defects of *Arabidopsis* antisense mutants in protein translocation at the level of inner membrane (Kouranov et al., 1998; Chen et al., 2002). The predicted topology of Tic20 involves four α -helical membrane spans, much like the pore-forming Tim23 and Tim22 proteins from mitochondria. In addition because some preproteins were imported at a decreased rate, a channel function for Tic20 was postulated. A study applying blue native polyacrylamide gel electrophoresis (BN-PAGE) with pea chloroplasts revealed the existence of 1 MDa complex consisting mainly of Tic20 (Kikuchi et al., 2009). This was interpreted as an indication for Tic20 functioning as an import channel. Support for this notion comes from a study in the complex plastid of *Toxoplasma gondii*, where Tic20 proved to be essential for protein import (van Dooren et al., 2008). Importantly, according to these findings Tic20 was eliminated as a candidate for the general import pore and assigned an alternative import channel for specific subsets of proteins, but biochemical evidence for channel function of Tic20 is still lacking.

In the *Arabidopsis* genome two close homologues to the pea Tic20 are found as well as two more distantly related genes. The observed low-expression of *Arabidopsis* tic20-I and tic20-IV isoforms at both the level of RNA (Teng et al., 2006) and protein (Vojta et al., 2004; Kleffmann et al., 2004) suggests that Tic20 is sub-stoichiometric to other Tic components and Toc75 (Chen and Li, 2007; Vojta et al., 2004). Recently, it was shown by Kasmati et al. (2011) that after complementation studies it was confirmed a redundancy between atTic20-I and atTic20-IV. It was also shown that the double mutants *tic20-I tic20-II* and *tic20-I tic20-V* have a severe phenotype and are albino plants.

However, it has been proposed that during plant development, *Arabidopsis* Tic21 might have a pattern of expression complementary to Tic20 and might also form a channel for the TIC complex that compensates for the low accumulation of Tic20 (Teng et al., 2006).

As was discussed earlier, Tic22 is a soluble protein in the intermembrane space, peripherally associated to the TIC complex. It interacts with the TOC complex through Toc12 and Toc64 and might participate in TIC-TOC supercomplex formation (Becker et al., 2004a). Tic22 has been found intimately associated with Tic20. Its accumulation and probably its function seem to be controlled by the redox status of photosynthetic electron flow (Fulda et al., 2002).

1.7.3 Tic40

Tic40 were detected by immunoblotting in pea, and both forms were found to be in a close proximity with translocating preproteins, predominantly at the inner membrane but also at the outer membrane. Tic40 was shown to behave as an integral membrane protein, and is anchored by a single, transmembrane α -helix at the N-terminus. The C-terminal part of Tic40 is largely hydrophilic, and was shown to be protected from trypsin proteolysis in isolated chloroplasts, suggesting that it protrudes into the stroma (Chou et al., 2003). Tic110 and Tic40 are therefore likely to have a similar topology. This, in addition to the finding that the two proteins were found to be cross-linked together by a disulfide bond under oxidative conditions (Stahl et al., 1999), leads to the suggestion that they work together as a complex facilitating protein translocation. This was also supported by genetic analysis (Kovacheva et al., 2005).

Interestingly, Tic40 possesses conserved domains placing it in the family of Hip/Hop co-chaperones (Hsp70-interacting protein/Hsp90-organizing protein) (Bédard et al., 2007; Chou et al., 2003; Stahl et al., 1999). The soluble C-terminal domain contains motifs similar to Sti1, the Hip co-chaperone interacting with Hsp70 yeast. Notably, the Tic40 Sti1 domain is functionally equivalent to that of the Hip co-chaperone. This was demonstrated by complementation of *tic40* plants with Tic40 containing the human Hip Sti1 domain (Bédard et al., 2007). The presence of a degenerated TPR domain was also discussed (Chou et al., 2003), though recent database alignments argue against this notion. It rather seems that two Sti1 domains in tandem are located at the C-terminus (Balsera et al., 2009b). *In vitro* analysis revealed that the so-called TPR domain interacts with Tic110 (Majeran et al., 2008), while the Sti1 motif is responsible for binding Hsp93 as well as stimulating its ATPase activity (Chou et al., 2006). These findings indicate that Tic40 rather regulates import efficiency than fulfils an essential function.

1.7.4 Tic55, Tic32 and Tic62

Tic55 is anchored to the inner envelope by two transmembrane helices at the C-terminus and it exposes a large soluble domain in the stroma which contains a Rieske-type iron sulphur centre and a mononuclear iron-binding site (Caliebe et al., 1997). It was originally found in a complex with precursor proteins, Tic110 and Tic62. Import experiments in the presence of the Rieske-inhibitor diethylpyrocarbonate (DEPC) suggested an important role in the import process. However, a recent study presented

evidence that Tic55 is not the target of DEPC, since Tic55 knockout mutants show the same import block after DEPC treatment (Boij et al., 2009). Tic55 was recently identified as a potential thioredoxin target by affinity chromatography on a thioredoxin-column (Bartsch et al., 2008).

Tic62 and Tic32 are extrinsic proteins of the inner surface of the inner envelope membrane, and belong to the extended and classical family of short chain dehydrogenases, respectively, and both bind NADP(H) (Küchler et al., 2002; Chigri et al., 2006). For both proteins an electron transfer activity was demonstrated *in vitro*, though no endogenous substrates have been identified so far. A dynamic association of Tic32 and Tic62 with the “core” translocon represented by Tic110 was observed, which was dependent on the metabolic redox state in the stroma, reflected by the NADP⁺/NADPH ratio (Chigri et al., 2006). Tic62 has a bimodular architecture: the N-terminus is involved in NADP(H)-binding; the C-terminus specifically interacts with ferredoxin-NADP-oxidoreductase (FNR) (Küchler et al., 2002; Stengel et al., 2008); Chigri et al., 2006). The C-terminus domain consists of a repetitive Pro/Ser-rich motif, which occurs exclusively in vascular plants (Küchler et al., 2002). In addition, Tic62 was shown to have a triple localization in chloroplasts; it is not only found at the inner envelope membrane where it was originally detected, but depending on the redox state, also in the stroma as well as at the thylakoid membrane (Benz et al., 2009; Stengel et al., 2008). Tic32 also has a bimodular functional organization with an N-terminal NADP(H) binding region and a C-terminal calmodulin binding domain (Hörmann et al., 2004).

1.8 Chaperones: Hsp93 and Hsp70

In *Arabidopsis* two isoforms of Hsp93 are encoded: atHsp93-V and atHsp93-III, the one on chromosome five being the dominant form (Constan et al., 2004; Kovacheva et al., 2007). Knockout mutants of Hsp93-V are pale and small, whereas single knockout plants of Hsp93-III have the same appearance as wild type plants (Constan et al., 2004). Double mutants are not viable, indicating that at least a certain level of Hsp93 is absolutely required. In general, members of this superfamily of molecular chaperones use ATP to mediate protein folding/unfolding (Doyle and Wickner, 2009). They function either independently as chaperones or act as regulatory associates of the Clp protease complex.

In *Arabidopsis* and pea, Hsp93 has a dimeric form which has been found in the stroma (Peltier et al., 2004), although the likelihood is that it functions as a hexamer.

Apart from Hsp93, there is evidence of two stromal Hsp70 isoforms (Shi et al., 2010; Su et al., 2010; Su et al., 2008). Recent experimental studies have shown that one of two Hsp70 isoforms in *Physcomitrella* chloroplasts is essential for viability. By utilizing a conditional Hsp70 knockdown mutant for *in vitro*, experiments after heat shock it was shown that plastids containing the temperature-sensitive Hsp70 mutant protein have a reduced import capacity (Shi et al., 2010). *Arabidopsis* co-immunoprecipitation experiments found incoming precursor proteins bound to Hsp70 as well as to Hsp93, implying a coordinated action of both chaperones in translocation (Su and Li, 2010). Moreover, double mutants of atTic40 and atHsp70-1 proved to be lethal, which indicates that these proteins have an overlapping, essential function (Su and Li, 2010).

1.9 Transport from the outer membrane into the inner envelope membrane

All proteins destined for the inner envelope membrane engage the TOC complex for the initial import step. At the level of the inner envelope, proteins follow one of two possible pathways: conservative sorting or stop transfer, depending on targeting information contained within their mature parts (Firlej-Kwoka et al., 2008; Tripp et al., 2007). The conservative sorting was first described for Tic40 and Tic110, which prior to inner envelope membrane insertion reach the stroma. The second route, the stop transfer, was proposed for ARC6, which is arrested at the level of the inner envelope membrane and laterally inserted into the lipid bilayer (Firlej-Kwoka et al., 2008; Tripp et al., 2007). Recently, a study on targeting and insertion of a protein called albino or pale green mutant1 (APG1), identical to IEP37, revealed that the single transmembrane domain represents the stop-transfer signal and likewise determines membrane topology (Viana et al., 2010). The post import route includes a complete translocation into the stroma and re-targeting to the inner envelope. Examples for proteins travelling via this pathway are Tic110 and Tic40 (Lübeck et al., 1997). It is not clear how the soluble intermediates are recognised in the stroma and re-inserted into the membrane, though some evidence was provided that Hsp93 and Tic40 are involved in these processes (Li and Schnell, 2006; Vojta et al., 2007).

1.10 Senescence

Senescence is a process that occurs naturally simultaneous with age or is prematurely induced by a variety of biotic and abiotic factors (Nooden and Penney, 2001). The natural age-related senescent processes are regulated by internal genetic, hormonal, and metabolic factors. In contrast, induced senescence occurs independent of age and has vital roles in plant defence against viral, bacterial, and fungal pathogens, controlling high levels of oxidative stress (Lim et al., 2007). Like autophagy, senescence is responsible for the degradation and remobilization of macromolecules, including lipids, amino acids and nucleic acids (Lim et al., 2007). Senescence degradation is achieved through the coordination of at least two intracellular degradation pathways: the ubiquitin/proteasome pathway and the vacuolar degradation pathway. However, in contrast to the autophagy pathway, senescence predominantly leads to death of the organism, organ or tissue (Liu et al., 2005).

1.10.1 Leaf senescence

The most well studied form of senescence is the organ-specific degradation of leaves, termed leaf senescence. The most striking example occurs in the trees in autumn (Hortensteiner, 2006), during which the high nitrogen composition in the chloroplasts is remobilized prior to leaf abscission. In contrast, for many short lived plant species, leaf senescence is correlated with completion of the entire life cycle. Nutrients are continually mobilized from old to young leaves and ultimately to the upper leaf (Gregersen et al., 2008). In the case of *Arabidopsis*, each leaf reaches maturity following a period of rapid expansion approximately twelve days after its emergence from the vegetative meristem as a leaf primordium (Zentgraf et al., 2004). After a period, leaves begin to senesce ~28-34 days after post emergence (Lim et al., 2007). This is due, to the addition of new rosette leaves, which shade the older leaves, and the accumulation of oxidative damage as a result of photosynthesis (Zentgraf et al., 2004). Upon flowering, the formation of leaves stops and nutrients are assimilated and relocated to the reproductive structures.

1.10.2 Structural and biochemical changes in leaf senescence

Leaf cells at the senescence stage show some distinctive structural and biochemical changes. A notable feature of cellular structural change during leaf senescence is the order of disintegration of intracellular organelles (Kato et al., 2002). The earliest structural changes occur in the chloroplast. In contrast, the nucleus and mitochondria that are essential for gene expression and energy production, respectively, remain intact until the last stages of senescence. This reflects that the leaf cells need to remain in function for progression of senescence until a late stage, possibly for effective mobilization of the cellular material.

Chloroplasts are the main source of reactive oxygen species (ROS) in plants. During photosynthesis, light energy is absorbed by a series of redox reactions and transferred to the reaction centres of the photosystems. During senescence, chloroplasts are converted into “gerontoplasts”. Electron microscopy revealed that the chloroplasts of senescing leaves show an increased number of enlarged plastoglobuli, a disorientation of the grana stacks, and an enlargement of the thylakoids (Gan and Amasino, 1995). This loss of chloroplast integrity can be observed in the very early stages of senescence; it is associated with the breakdown of the chlorophylls, and the degradation products are transported into the vacuole (Gan and Amasino, 1995). Interestingly, the composition of the thylakoid membrane appears unchanged. The conversion of chloroplasts to gerontoplasts in leaves is mostly reversible in all higher plants (Thomas et al., 2003). The chloroplasts may play a regulatory role during leaf senescence same importance as of that of mitochondria during animal programmed cell death (PCD). There, mitochondria integrate signals of proapoptotic and antiapoptotic proteins regulating the release of cytochrome *c* and the production of ROS that direct subsequent apoptotic processes (Green and Reed, 1998; Dufour and Larsson, 2004). Cytochrome *c* release from mitochondria and the decrease of Calvin cycle activity in chloroplasts both lead to an increased generation of ROS in the respective organelle (Jimenez et al., 1998).

These observations imply that leaf senescence involves cellular events that finally lead to PCD. The loss of integrity of the plasma membrane leads to disruption of cellular homeostasis, ending the life of a cell in senescing leaves. The cellular biochemical changes in senescing leaves are first accompanied by reduced anabolism (Bleecker and Patterson, 1997). The overall cellular content of polysomes and ribosomes decreases

fairly early, reflecting a decrease in protein synthesis. This occurs concomitantly with reduced synthesis of rRNAs and tRNAs. Further cellular biochemical changes like hydrolysis of macromolecules and subsequent remobilization, which require the operation of a complex array of metabolic pathways. Chloroplast degeneration is accompanied by chlorophyll degradation and the progressive loss of proteins in the chloroplast, such as a ribulose biphosphate carboxylase (Rubisco) and chlorophyll *a/b* binding protein (CAB). Hydrolysis of proteins to free amino acids depends on the actions of several endo- and exopeptidases (Hortensteiner and Feller, 2002; Otegui et al., 2005). Senescence-associated cysteine proteases, which are accumulated in the vacuole, also play a role in protein degradation. Lipid degrading enzymes, such as phospholipase D, phosphatic acid phosphatase, lytic acyl hydrolase, and lipoxygenase appear to be involved in the hydrolysis and metabolism of the membrane lipids in senescing leaves (Thompson et al., 1998; Thompson et al., 2000).

1.10.3 The vacuole and its role during senescence

In higher plant cells, most hydrolytic activities reside in the central vacuole, which typically contains 50-100% of acid nuclease and 80-100% of acid protease activity of the cell. Various lines of evidence point to an important role of the central vacuole in the execution of programmed cell death in certain developmental scenarios, such as differentiation/death of immature tracheary elements (Kuriyama and Fukuda, 2002). However, while rupture of the central vacuole and release of hydrolytic enzymes into the cytosol precedes terminal differentiation (death) of immature tracheary elements, the central vacuole remains intact and compartmentation is maintained during senescence of leaves (Nooden and Penney, 2001).

The central vacuole is involved in recycling cytosolic proteins (Canut et al., 1985), and in degradation of unexpectedly proteins (Canut et al., 1986) and endoplasmic reticulum resident proteins (Tamura et al., 2004). Sugar starvation triggers vacuolar autophagy of cytoplasm and some organelles in suspension cell cultures (Yu, 1999). In wheat, the activity of four cysteine proteases increases during senescence induced by protracted incubation in darkness, water deficit or during normal monocarpic senescence associated with reproduction, and these senescence-associated proteases localize to the central vacuole (Martinez et al., 2007). Thus, the central vacuole might contain a significant part of the proteases whose expression is associated with leaf senescence. However, since

most proteins degraded during senescence come from the chloroplast, the involvement of the central vacuole requires the operation of some sort of hitherto unknown specific traffic pathway from the chloroplast. Several possible routes for internalisation of chloroplast components by the central vacuole are outlined already (Weber et al., 2006).

1.10.4 Molecular approaches during senescence and regulation of leaf senescence

The understanding of the molecular and hormonal regulation of senescence has come from two main areas of investigation: the identification of senescence associated genes (SAGs) using genomic techniques and the analysis of mutant plants with altered senescence responses. Extensive work in multiple plant species, including maize, barley, potato and *Arabidopsis* has led to the identification of a large number of SAGs. In *Arabidopsis*, affymetrix GeneChip arrays representing 24,000 genes were utilized for analyzing changes in global expression pattern during leaf senescence. This analysis had identified more than 800 SAGs (van der Graaff et al., 2006; Buchanan-Wollaston et al., 2005). Initial cDNA profiling experiments in *Arabidopsis* identified 12 genes that were induced or repressed during senescence. In addition, analysis of 1,300 *Arabidopsis* enhancer trap lines led to the identification of 147 genes with senescence specific activation of the GUS reporter gene (He et al., 2001). Approximately 300 transcription factors were up-regulated in the genomic analysis (van der Graaff et al., 2006). They represent many families including NAC, and WRKY family members (Lin and Wu, 2001; Yang et al., 2001). NTL9 is a NAC protein induced during oxidative stress. Like all NAC proteins, NTL9 is dormant in its native membrane bound form and becomes active following condition dependent proteolytic cleavage and nuclear localization (Yoon et al., 2008). Consistent with its designation as a senescence associated transcription factor, NTL9 overexpression leads to premature activation of many SAGs (Yoon et al., 2008).

1.10.5 The role of plant hormones in the onset of leaf senescence

Plant hormones attenuate plant growth and development with environmental conditions and also mediate defence responses. All of the abiotic and biotic factors that induce hormone production, including drought, pathogen attack, osmotic stresses, and oxidative stresses, can also induce senescence. Not surprisingly therefore, hormones implicated in the response to these stimuli have either positive or negative roles in the regulation of induced senescence. Analysis of microarray data and enhancer trap lines revealed that many SAGs are induced by exogenous application of several key plant hormones,

including abscisic acid (ABA), cytokinin, SA, ethylene and jasmonic acid (JA) (Weaver et al., 1998; He et al., 2001). Each plant hormone affects various developmental and environmental events in a complex manner; this causes difficulties in assaying the roles of the hormonal pathways in leaf senescence.

Cytokinins, which function during cell division, chloroplast maturation, and shoot morphogenesis, have also been found to be senescence delaying hormones. Endogenous cytokinin levels drop during leaf senescence and exogenous application or endogenous enhancement of cytokinin content using the senescence specific *SAG12* promoter delays senescence (McCabe et al., 2001; Ori et al., 1999). Consistent with the physiological finding that the cytokinin level decreases during leaf senescence, genomic scale molecular analysis revealed that genes involved in cytokinin synthesis, a cytokinin synthase and adenosine phosphate isopentenyl-transferase (IPT), genes are downregulated and a gene for cytokinin degradation, cytokinin oxidase, is up-regulated in senescing leaves (Buchanan-Wollaston et al., 2005). Cytokinin functions by delaying chloroplast degradation and increasing the activities of photosynthesis related genes, including Rubisco, and NADH-dependent hydroxypyruvate reductase (HPR) (Gan and Amasimo, 1995). This activity is mediated by histidine kinase 3 (AHK3), a cytokinin receptor. An AHK3 gain of function mutant (*ore2*) displays increased leaf longevity through the phosphorylation of the *Arabidopsis* response regulator 2 (ARR2), which may directly regulate transcription suppressing senescence (Kim et al., 2006).

Abscisic acid (ABA) is a key plant hormone mediating plant responses to environmental stresses. It also functions in plant development such as seed germination and plant growth. It can also mediate responses to drought (stomata regulation) (Lopez et al., 2008), and high salt concentrations (Hirayama and Shinozaki, 2007). All the above mentioned factors can contribute to induce senescence. The ABA level increases in senescing leaves and exogenously applied ABA induces expression of several *SAGs* (Woo et al., 2001), which is consistent with the effect on leaf senescence. In rice leaves, ABA stimulates the production of hydrogen peroxide, resulting in increased oxidative stress and the promotion of senescence (Hirayama and Shinozaki, 2007).

In contrast to ABA, microarray data suggest that SA functions predominantly during natural rather induced senescence (Buchanan-Wollaston et al., 2005). Salicylic acid is known to function in the systemic acquired resistance pathway in response to pathogen

infection. The concentration of endogenous SA is four times higher in senescing leaves of *Arabidopsis*. A transcriptome analysis of transgenic SA-deficient *NahG* plants indicates SA is required for the up-regulation of several SAGs during leaf senescence (Morris et al., 2000; Buchanan-Wollaston et al., 2005). This includes the cysteine protease SAG12, which is undetectable in SA signalling, and biosynthesis mutants *pad4* and *npr1* (Morris et al., 2000).

Methyl jasmonate (MeJA) and its precursor form jasmonic acid (JA) promote senescence in detached oat (*Avena sativa*) leaves (Ueda and Kato, 1980). Exogenously applied MeJA in detached *Arabidopsis* leaves has shown to lead to a rapid loss of chlorophyll content and to photochemical efficiency of photosystem II (PSII) and increased expression of SAGs such as *SEN4* and *SEN5*. A more convincing support of the role of JA in leaf senescence comes from the observation that JA-dependent senescence is defective in the JA-insensitive mutant *coronatine insensitive 1 (coi1)*, implying that the JA signalling pathway is required for JA to promote leaf senescence (He et al., 2002).

Ethylene has a clearly established role in the induction and promotion of dark-induced senescence. Ethylene has long been associated with the ripening of fruit, maturation of reproductive organs and induction of senescence (Yen et al., 1995). Analysis of the “onset of leaf death” mutants demonstrates ethylene’s involvement in the regulation of senescence (Jing et al., 2005). Three classes of mutants were described: those with ethylene-enhanced premature senescence phenotypes, those with ethylene dependent senescence phenotypes, and those with phenotypes so severe that ethylene treatment had no effect (Jing et al., 2005). In all cases, the effect of ethylene appears to be age-dependent since senescence could not be in cotyledons or young leaves. In addition, while increased duration of ethylene treatment causes leaf yellowing, variation is observed in the attenuation of the mutants to the ethylene signal. This suggests several of the genes may encode signalling components. In addition, ethylene insensitive mutants such as *ethylene insensitive (ein2)* display a delayed senescence phenotype (Oh et al., 1997) and three ethylene biosynthesis genes, including *1-aminocyclopropane-1-carboxylate (ACC)* synthases, are up regulated during senescence (van der Graaff et al., 2006).

1.10.6 Induction of leaf senescence through the sugar signalling

The main role of sugars in metabolism is as carriers of energy and carbon. However, sugars have several additional roles, such as the maintenance of osmotic potential and signalling the energy status of plant parts. Microarray analysis indicates that the senescence specific gene *SAG12* is induced more than 900 fold by glucose, and several enzymes involved in nitrogen assimilation, including the nitrate transporter AtNRT2 and glutamine synthetase GLN1, are also up-regulated (Pourtau et al., 2006). In castor bean leaf blades, accumulation of callose deposition in the sieve plates prevents the flow of phloem. This leads to “back up” of excess sugars into the leaf tissues. Since this occurs just prior to the senescent breakdown of chlorophyll, it reinforces the connection between high sugar concentration and the onset of senescence (Jongebloed et al., 2004).

Detached leaves of tobacco and barley incubated under strong light, showed accelerated yellowing, associated with sugar accumulation suggesting that high sugar levels can induce early yellowing in these species. *Arabidopsis* plants showed earlier leaf senescence when grown at long days (16 h light) rather than short days (12 h light), both at relatively low light levels ($100 \mu\text{mol m}^{-2}\text{s}^{-1}$). Leaf senescence was even more advanced when plants were held at long days at relatively high light levels ($200 \mu\text{mol m}^{-2}\text{s}^{-1}$). No positive correlation was found between leaf senescence and the glucose and fructose concentrations in the leaves of plants grown at low light levels, but the concentrations in these hexoses were higher in leaves of plants grown at relatively high light levels (Wingler et al., 2006). When *Arabidopsis* plants were grown on agar at high and low N levels, the presence of 1-2% glucose or sucrose in the agar induced earlier leaf yellowing in the plants grown at low N levels. Addition of sorbitol or mannitol had no effect, indicating that the response was not due to an osmotic effect in the root zone (Pourtau et al., 2004; Pourtau et al., 2006). The sugar treatment resulted in an early decrease of a chlorophyll fluorescence parameter (F_v/F_m), which also decreased prior to normal developmental leaf yellowing (Wingler et al., 2004). These data led to the hypothesis that high sugar levels in the leaf cells are the cause of early leaf senescence.

1.10.7 Role of signalling cascades in the initiation of senescence

Senescence is often described as the terminal phase of plant development. However, it is important to understand the meaning of the terminal nature of senescence with the realization that senescence of one part of a plant is often essential for the ongoing

development of other organs and tissues. Perhaps the clearest example of this is leaf senescence and the attendant translocation of nutrients from the dying leaf tissue to developing seeds (Kaup et al., 2002). Senescence is induced by endogenous signals including age, developmental cues and plant growth regulators (Gan and Amasino, 1995); (Nooden and Penney, 2001; Riefler et al., 2006). However, it can also be engendered prematurely by a number of exogenous environmental stresses, including light and temperature stress, dehydration, nutrient stress and pathogen ingression (Beers and McDowell, 2001; Pic et al., 2002; Xiong et al., 2005). Moreover, these endogenous and exogenous signals inducing senescence appear to be coordinated through a common signalling network (Fig. 8) designed to engage the transcriptional activity underlying senescence (Buchanan-Wollaston et al., 2003a; Lim et al., 2003).

Recent analysis of gene expression in mutant *Arabidopsis* plant lines has indicated that signalling pathways involving ethylene, jasmonic acid and salicylic acid regulate the expression of genes required for developmental senescence (Buchanan-Wollaston et al., 2005). Studies of age related changes required for leaf senescence in *Arabidopsis* have resulted in characterization of a number of *old* (onset of leaf death) mutants (Jing et al., 2002). The ability of ethylene to induce leaf senescence under normal conditions is limited to a precise stage of age, and some of these *old* mutants, for example *old1*, display an early senescence response to ethylene (Jing et al., 2005). Premature senescence is also induced by exogenous factors, including treatment with jasmonic acid, and in such instances there is an accompanying up-regulation of many of these genes known to be involved in developmentally induced senescence (He et al., 2002).

1.11 Aims of this thesis

This thesis is specifically focused on the study of atToc90, its role, and its interaction with the TOC machinery. The TOC machinery performs two essential functions: firstly, it recognizes those proteins that need to be imported as they arrive at the chloroplast surface; and secondly, it forms a channel through the outer membrane so that the proteins can pass across, once recognized. As atToc90 is a receptor, my focus was on the first of these functions: recognition.

Quite recently it was found that there are actually several different types (or isoforms) of the TOC receptors. For example in *Arabidopsis* there are two different Toc34 isoforms, called atToc33 and atToc34. The different isoforms probably have different client-

recognition preferences (i.e for photosynthetic and non-photosynthetic preproteins), and exist so that chloroplasts can efficiently recognize all of the many different proteins they need to import. Different *Arabidopsis* TOC complexes were purified using the tandem affinity purification (TAP) method. By purifying atToc34- and atToc33-containing TOC complexes, I aimed to elucidate the association preferences (and functions) of atToc90. A secondary goal was to identify novel components of the outer membrane import machinery. Proteins in the purified TOC complexes were studied by SDS-PAGE, immunoblotting and mass spectrometry (see Chapter 3).

Another important aim was to elucidate the role of atToc90 using genetics. Taking into consideration the findings of Kubis et al. (2004) and Hiltbrunner et al. (2004), a large group of double and triple mutants was identified and studied. All of the mutant combinations studied involved *toc90* (the atToc90 knockout mutation) in combination with various other mutations affecting the TOC complexes for photosynthetic and non-photosynthetic preproteins. The aim of this part of the study was to look for genetic interactions between *toc90* and mutations affecting other TOC components (see Chapter 2).

The final aim of my thesis was to investigate whether atToc90 plays a role in leaf senescence. This hypothesis emerged following a careful analysis of *atTOC90* gene expression (together with other TOC component genes) using Genevestigator, a software tool for the analysis of publicly-available data from Affymetrix microarray experiments. This work involved the analysis of multiple *toc90* mutant alleles under various stress conditions and treatments (particularly those related to senescence). In each experiment, *toc90* was compared to the wild type (see Chapter 4). For these physiological experiments, a new atToc90 overexpression transgenic line was generated (using the full-length *atTOC90* cDNA sequence) and analysed at each step.

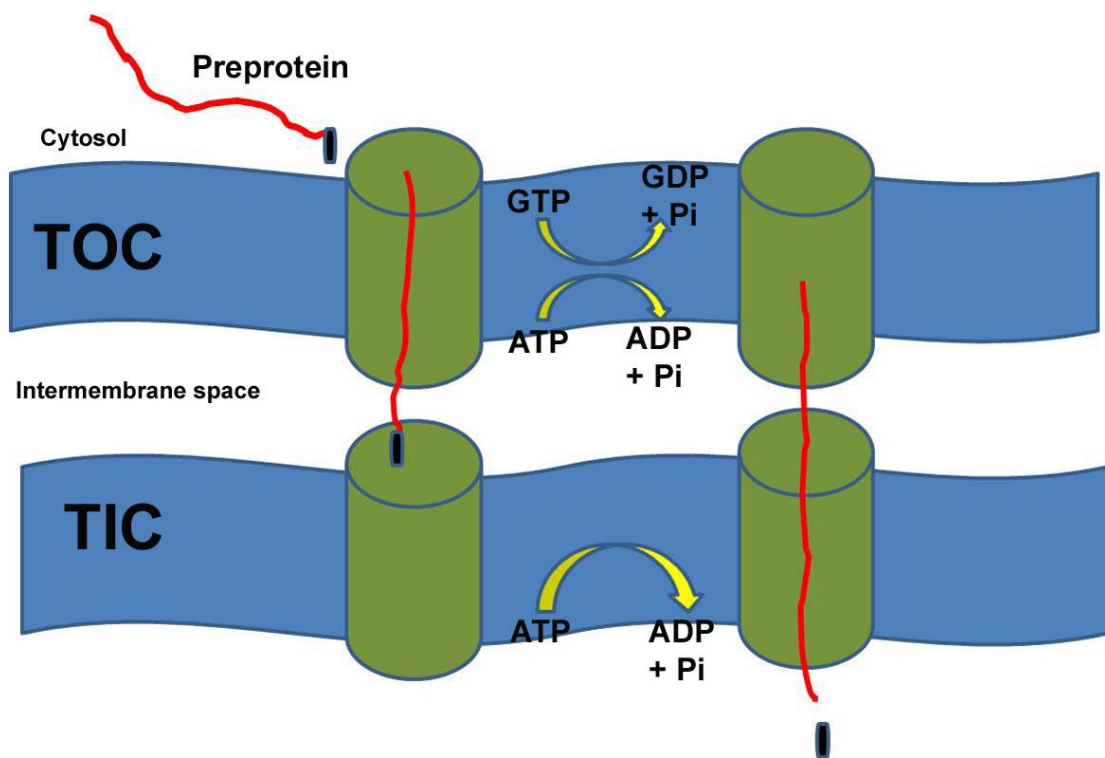


Figure 1.1: Description of the process of protein import via the TOC/TIC import machinery.

The first stage is called “energy-independent binding”, where the transit peptide makes reversible contacts with receptor components of the TOC complex. In the second stage GTP and a low concentration of ATP in the intermembrane space are needed. The preprotein is inserted across the outer envelope membrane (OM) and it is coming in contact with the TIC complex in the inner membrane (IM). The third and final stage requires high concentrations of ATP in the stroma so the preprotein can translocate across both envelope membranes. The transit peptide will be removed by stromal processing peptidase (SPP), and the mature protein will take its final conformation. Adapted from Jarvis (2008).

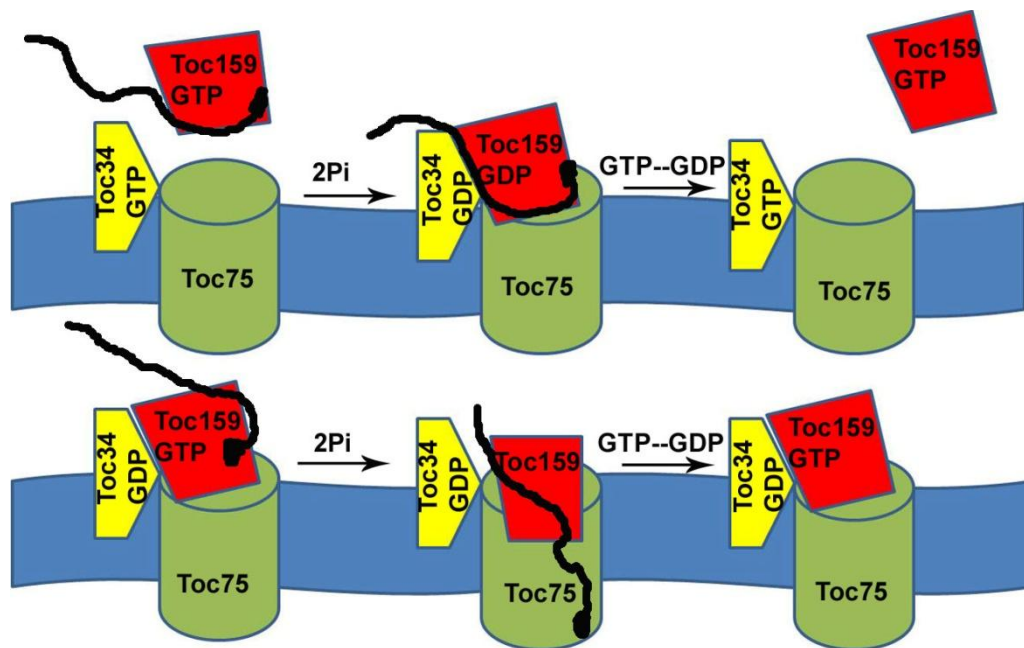


Figure 1.2: Two different schematic models for preprotein recognition by the TOC GTPases, Toc34 and Toc159.

(a) The targeting model, where a newly synthesized preprotein is bound by the central GTPase domain of the cytosolic Toc159; electrostatic interactions between the positively charged transit peptide and the amino-terminal acidic domain of Toc159 might facilitate this interaction. Toc159-GTP and Toc34-GTP associate in a low affinity interaction through a homotypic association between their GTP domains. This interaction between the two GTPase domains and the transit peptide stimulates GTP hydrolysis by both proteins, leading to the integration of Toc159 into the TOC complex and the insertion of the preprotein across the OEM. Preprotein translocation is then completed by an Hsp70 protein of the intermembrane space. Once translocation is complete, the two GTPases undergo GDP-GTP exchange, which leads to the dissociation of Toc159 to the cytoplasm for subsequent cycles of targeting. (b) The second model is called the motor model. In the “motor” hypothesis the transit peptide is first phosphorylated near its carboxyl end. Preprotein recognition occurs by binding of Toc34-GTP at the outer membrane to the C-terminus of the phosphorylated transit peptide. The transit peptide stimulates GTP hydrolysis by Toc34 and after dephosphorylation of the transit peptide, leads to transfer of the preprotein to Toc159. The C-terminal region of the transit peptide stimulates Toc159 GTPase activity, and Toc34-GDP dissociates from the TOC complex, which enables Toc159 to thread the preprotein through the channel via repeated cycles of GTP hydrolysis. After multiple rounds of GTP hydrolysis the complex is able to accept a new precursor substrate. Adapted from Jarvis (2008).

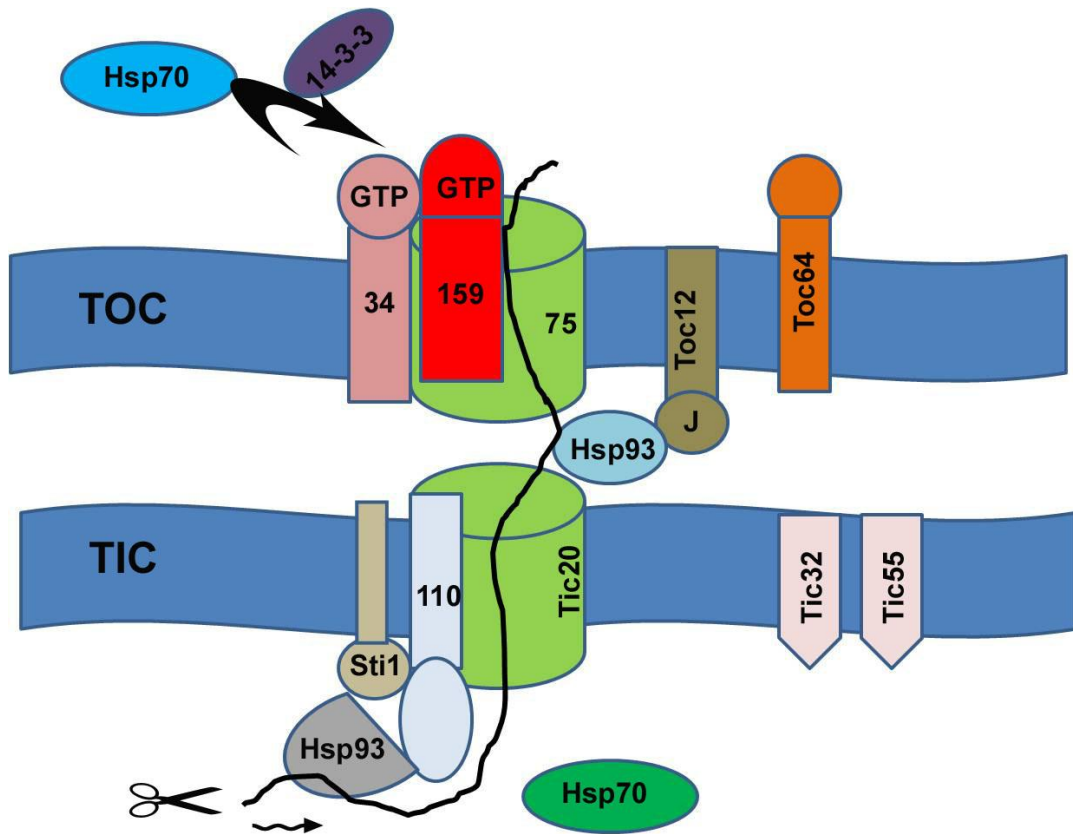


Figure 1.3: Structure of the TOC/TIC chloroplast protein import apparatus.

The core TOC translocon resides in the outer membrane (OM), and is composed of three major proteins: Toc34, Toc159 and Toc75. Toc75 forms the outer envelope channel, whereas Toc34 and Toc159 function as receptors for the transit peptides of incoming proteins. Cytosolic proteins 14-3-3, Hsp90 and Hsp70 direct nuclear encoded plastid proteins to the distinct TOC receptors as illustrated. Toc12, Toc64 and Hsp70 along with Tic22 have been proposed that act as transporters of the preproteins across the intermembrane space and deliver them in the TIC complex. It has been suggested that the TIC complex is formed by Tic110, although Tic20 and Tic21 also could be channel components. Tic40 is associated with the stroma exposed domain of Tic110 and with the stromal chaperone Hsp93 in the formation of a stromal import motor complex. After reaching the interior, the transit peptide is cleaved by stromal processing peptidase (SPP) and the mature protein is folded with the help of Cpn60 and stromal Hsp70. The stromal ATP protein was also shown to play a role in driving preprotein import, perhaps working in parallel with Hsp93Tic55, Tic62, and Tic32 are proposed to be involved in redox regulation with FNR or calmodulin (CaM). Adapted from Jarvis (2008).

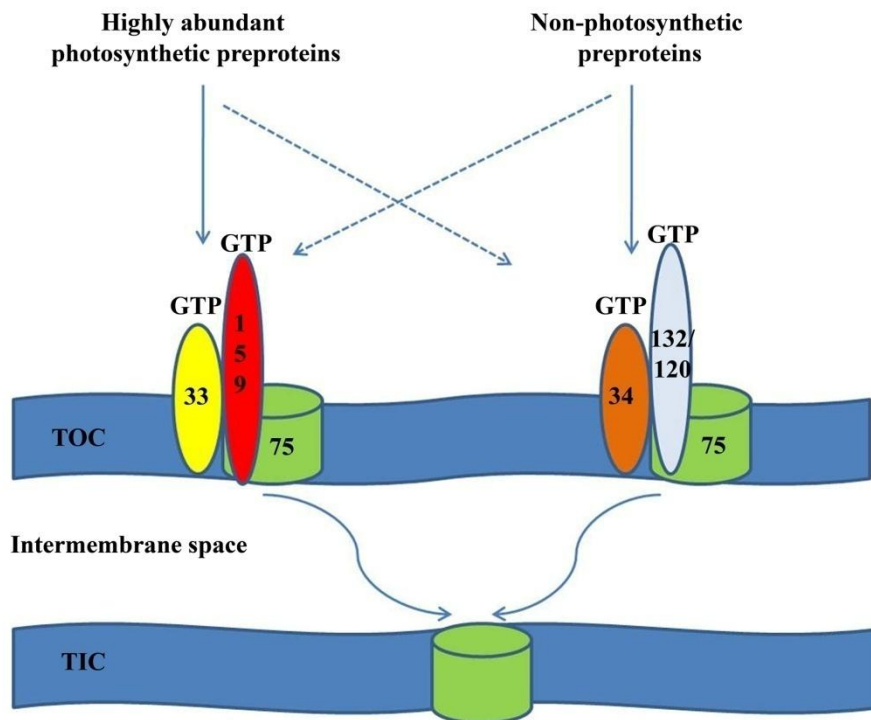


Figure 1.4: Model for substrate-specific protein import pathways.

The TOC GTPases are encoded by small gene families in *Arabidopsis* and other species. Evidence from genetic and biochemical studies suggests that the different isoforms encoded by these genes exhibit a substantial degree of functional specialization, and that they associate preferentially to form different TOC complexes with substrate specificity. Specifically, it is proposed that atToc159 associates with atToc33 and together these two mediate import of the most highly-abundant photosynthetic preproteins (Class 1 substrates). It is also suggested that atToc34 and atToc132 and/or atToc120 form a complex with specificity mostly for low abundance preproteins. However, genetic data indicate that neither pathway exhibits absolute substrate specificity and this is indicated by the crossing dotted arrows. It is even possible that a third putative class of preproteins follows either pathway with equal efficiency. Nonetheless, following OEM translocation, the import pathways converge at the TIC complex. Putative redox-sensing components of the TIC machinery (Tic62, Tic55 and Tic32 alongside with CaM and FNR) may be recruited to the complex specifically during the import of photosynthetic preproteins. Adapted from Jarvis (2008).

Table 6: Major components of the TOC chloroplast protein import machinery with their distinguished phenotype and homologous in *Arabidopsis thaliana*. (Adapted from Jarvis, 2008)

	Component	Arabidopsis thaliana TOC proteins	Distinguish mutant phenotype	Reference
1	Toc34	atToc33	pale	Jarvis <i>et al.</i> (1998); Kubis <i>et al.</i> (2003)
2		atToc34	green	Constan <i>et al.</i> (2004a)
3	Toc159	atToc159	Major isoform in photosynthetic preproteins albino	Bauer <i>et al.</i> (2000); Kubis <i>et al.</i> (2004)
4		atToc132	Minor isoform in non-photosynthetic preproteins yellow-green	Ivanova <i>et al.</i> (2004); Kubis <i>et al.</i> (2004)
5		atToc120	green	Ivanova <i>et al.</i> (2004); Kubis <i>et al.</i> (2004)
6		atToc90	Minor isoform green	Kubis <i>et al.</i> (2004); Hiltbrunner <i>et al.</i> (2004)
7	Toc75	atToc75-III	Major isoform pale/homozygous;embryo lethal	Baldwin <i>et al.</i> (2005); Hust <i>et al.</i> (2006)
8		atToc75-IV	green	Baldwin <i>et al.</i> (2005)
9		atToc75-V / OEP80	no data	no data
10		atToc12	no data	no data
11		atToc64-III		Qbadou <i>et al.</i> (2006); Aronsson <i>et al.</i> (2007)

Chapter 2

**Genetic studies revealing new insight into the function of
atToc90, an chloroplast outer envelope protein**

2.1 Introduction

The chloroplast, like the mitochondrion, has its own genome and therefore has the ability to synthesize some of the envelope proteins necessary for the processes of photosynthesis and biogenesis. Embedded in the envelope membranes are multiprotein complexes called TOC and TIC, standing for translocon at the outer and inner envelope membrane of the chloroplast, respectively. The TOC complex initiates the import of nuclear-encoded proteins from the cytosol into the organelle (Chen and Schnell, 1999; Keegstra and Cline, 1999). The core of the TOC complex is composed of two GTPase receptors, Toc159 (Kessler et al., 1994; Perry and Keegstra, 1994) and Toc34 (Gutensohn et al., 2000; Jelic et al., 2002), and a β -barrel membrane channel, Toc75, through which precursors are translocated across the outer membrane (Schnell et al., 1994; Hinnah et al., 1997). The Toc34 and Toc159 GTP binding domains are exposed at the surface of the chloroplast. Toc159 has a large cytosolic N-terminal acidic domain (A-domain), a C-terminal membrane anchoring domain (M-domain), and a cytosolic GTPase domain (G-domain).

For some components of the import complexes in *Arabidopsis* there are multiple homologues. *Arabidopsis* has two homologues of Toc34: atToc34 and atToc33. Evidence for the existence of an import pathway with preference for photosynthetic precursors was gained by detailed studies on the atToc33 knockout mutant *ppi1* (Jarvis et al., 1998; Kubis et al., 2003). Recent complementation studies of atToc33 knockout plants with several mutated forms of the atToc33 protein have shown that neither dimerization nor GTP binding is essential for chloroplast development *in vivo*, although, import efficiency was reduced in the complemented plants (Aronson et al., 2010; Lee et al., 2009).

The Toc159 family of GTPases has been proposed to mediate the initial recognition of preproteins by plastids. It is well known that Toc159 has four homologues: atToc159, atToc132, atToc120 and atToc90 (Hiltbrunner et al., 2001). Complementation studies of the Toc159 knockout mutant *ppi2* (see Section 1.5.2.2) in *Arabidopsis* have revealed that the A-domain is dispensable. Toc159GM, consisting only of the G- and M-domains only, rescued the albino phenotype of the *ppi2* mutant (Agne et al., 2009).

Previous studies suggested that atToc90 supports accumulation of photosynthetic proteins in plastids, although it is not strictly required for the import of proteins. The atToc90 protein associates with the chloroplast surface *in vivo* and with the TOC complex *in vitro*, similar to atToc159, suggesting that it has a function in chloroplast protein import similar to that of

atToc159 (Hiltbrunner et al., 2004). To determine the subcellular location of atToc90, Hiltbrunner et al. (2004) had expressed the protein as a GFP-fusion in isolated *Arabidopsis* protoplasts, and what they found was that GFP-Toc90 was present at the chloroplast periphery suggesting a chloroplast outer membrane location. To determine whether atToc90 functions in chloroplast protein import, the proteins ability to associate with isolated chloroplasts and the TOC complex was analysed (Hiltbrunner et al., 2004)

In this part of the thesis the phenotypes of a group of double and triple atToc90 mutants were studied, to try to get an insight into possible functions of atToc90. The vast majority of these mutants were made by Ramesh Patel in 2004 and all of them were confirmed to contain the respective T-DNA insertion and to be homozygous by PCR test. The below described studies have been carried out with seeds of the same harvesting time and PCR tested again. An example of the PCR results is given below (Fig. 2.2). The aim of this study was to look for genetic interactions (which might suggest functional redundancy or overlap) between atToc90 knockout mutations and mutations affecting other TOC components.

2.2 Results

2.2.1 Identification of atToc90 knockout mutants

To genetically assess functional relationships between atToc90 and other major TOC proteins, I crossed the corresponding knockout mutants (Tables 1 and 2) and then identified all the double and triple mutant combinations by growth on appropriate selective media, followed by PCR analysis. However, first, to investigate the role of the atToc90 protein *in vivo*, I used the *Arabidopsis* knockout mutants and conducted a comprehensive comparative study of the mutant phenotype with wild type. There are three alleles: *toc90-1* (1236-C11), *toc90-2* (N566449), and *toc90-3* (NG19434) (Fig. 2.1). The three mutants were confirmed as heterozygous by plating an appropriate selective medium (phosphinothricin for *toc90-1*; kanamycin for *toc90-2* and *toc90-3*) and by PCR analysis using gene and T-DNA specific primers (Table 3). To confirm that the mutants were truly knockout mutants, the absence of the atToc90 mRNA was confirmed by RT-PCR (see Chapter 4; Fig. 4.2) and the absence of the atToc90 protein was confirmed by immunoblotting (see Chapter 4; Fig. 4.2). Carefull analysis of the three single knockout mutants did not reveal any detectable differences from

the wild type under standard growth conditions or at any stage of development. For a more detailed analysis of the mutant phenotypes, see Chapter 4.

2.2.2 Double mutant studies

The study of the *toc90* double mutants was started by crossing *toc90-1* with various mutants shown in Table 1. Phenotypic analysis was made in the F4 generation, using plants that were 24 days old following growth on soil. The phenotypes of the double mutants were compared with those of the single relevant mutants and with that of wild type.

Three of the single mutants (*toc33*, *toc132-2*, and *toc75-III-3*) display a clear visible pale phenotype. When they were crossed with *toc90-1*, the resulting double homozygote mutants exhibited identical phenotypes to the single mutants (Fig. 2.3). Some of the double mutants have also been described in the past by Kubis et al. (2004). My data confirmed previous findings, and suggested that there is no significant functional redundancy between atToc90 and several other TOC proteins.

2.2.2.1 The *toc90-1 toc159* double mutant displays a more severe phenotype than *toc159*

Among the different single mutants studied here, *toc159* exhibits the most severely chlorotic phenotype in fact, it is albino. The *toc90 toc159* double homozygote was grown to maturity alongside *toc159* single mutants on medium containing 3% sucrose to aid growth, as the mutant is not able to grow photoautotrophically. In the early stages of development, the double and the single mutant do not exhibit different phenotypes. When both genotypes were about 32 days old, a phenotypic difference became evident (Fig. 2.4A). To characterise the severity of the double homozygote, chlorophyll measurements were conducted. The double mutant contained reduced chlorophyll concentrations compared with the single *toc159*, which is also visible by eye. This result is in contrast with the finding that Kubis et al. (2004) reported where no phenotypic difference was observed. To confirm the results, *toc90-3*, an other allele of atToc90, was crossed with the *toc159* (Col-0) and double homozygous plants were identified in similar fashion. These mutants were studied in the same way and the results indicated a clear difference between the single and double knockout mutant.

In summary, my double mutant studies provided clear evidence that there is no functional redundancy between the atToc90 and the majority of the TOC components that are shown in

Table 1. However, there was clear evidence for functional redundancy between atToc90 and atToc159.

2.2.3 *Arabidopsis thaliana* Toc90 triple mutants reveal significant functional redundancy

As was shown in Section 2.2.1, with the exception of *toc90-1 toc159*, no visible phenotypic difference from the control was observed in several *toc90* double knockout mutants. For this reason, *toc90-1* was crossed with several double mutants in order to extend the search for any possible distinct phenotypes (Table 2). All the resulting crosses were analysed by using the respective antibiotic resistant markers (where applicable) and by PCR testing using specific primers (Table 3).

2.2.3.1 Analysis of a *toc90-1 toc132-2 toc120-2* triple homozygous mutant

The *toc90-1 toc132-2 toc120-2* triple homozygote mutant was scored after 10 days of growth *in vitro*. At this early stage of development the visible phenotype of the triple homozygote plants was very clear (Fig. 2.5A). Plants of both genotypes were rescued and grown alongside each other on 3% of sucrose. Kubis et al. (2004) have shown that the double homozygote, *toc132-2 toc120-2*, has a very strong visible phenotype, almost as severe as of the *toc159* mutant. Unlike *toc132-2 toc120-2*, the *toc90-1 toc132-2 toc120-2* triple homozygote is not able to survive to maturity on soil. The severity of the triple homozygote's phenotype clearly demonstrates the existence of a functional overlap between atToc90 and atToc132/atToc120. To confirm our findings, the *toc90-3* single mutant was also crossed with *toc132-2 120-2*. Again, in the F3 progeny of the crosses, the triple mutant was compared and the results confirmed the previous findings (Fig. 2.5A).

This functional redundancy was even more apparent after I conducted chlorophyll measurements. Plants from both genotypes were grown on 3% sucrose for 24 days and then collected and used to perform dimethylformamide (DMF) chlorophyll measurements. The chlorophyll levels of the triple homozygote mutant were significantly lower than those of the double mutant control (Fig. 2.5B)

2.2.3.2 Analysis of a *toc90-1 toc132-2 toc120-2* heterozygous mutant

After obtaining significant results from the analysis of the *toc90 toc132 toc120* triple homozygous mutant, the heterozygous form of the *toc90-1 toc132-2 toc120-2* (hom/hom/het) triple mutant was also analysed. Kubis et al. (2004) have described that the pale phenotype of the *toc132-2 toc120-2* heterozygote is very clear even at the seedling stage. The phenotype of the *toc90-1 toc132-2 toc120-2* heterozygous mutant (genotype: *toc90/toc90; toc132/toc132; +/-toc120*) is significantly more severe than that of the control *toc132-2 toc132-2; +/-toc120-2* heterozygote (Fig. 2.6A). Repeating this analysis using the *toc90-3* allele showed the same results. As in the case of the triple homozygous mutant, the results with the heterozygous mutant strongly suggest that there is a functional overlap between atToc90 and atToc132/atToc120.

My experimental observations were confirmed once again by making chlorophyll measurements. Significantly reduced chlorophyll levels were present in 24 days old plants of the heterozygous triple mutant compared with the double heterozygote (Fig. 2.6B).

2.2.3.3 Analysis of a *toc90-1 toc159 toc120-2* triple homozygous mutant

The other triple mutant which was studied was *toc90-1 toc159 toc120-2*. As was stated in Section 2.2.1, there is a clear visible difference between the single *toc159* mutant and the double homozygous mutant, *toc90-1 toc159*. Interestingly, the double homozygous mutant *toc159 toc120-2* exhibited a similar phenotype to *toc90-1 toc159*. However, the most severe phenotype was observed in the triple homozygote, *toc90-1 toc159 toc120-2*, where the plants were extremely small (Fig. 2.7A). To confirm the results, the *toc90-3* allele was similarly crossed with *toc159 toc120-2*, and analysis of the triple mutant provided identical results (Fig. 2.7A).

Chlorophyll measurements were taken and the chlorophyll levels of the triple mutant were found to be significantly lower than those of the other genotypes (Fig. 2.7B). The albino triple mutant can not survive in soil, like all the other albino homozygous genotypes, but does have survival chances when it is rescued to 3% sucrose. The results suggest that there is a functional redundancy amongst atToc90, atToc159 and atToc120

2.2.3.4 Analysis of a *toc90-1 toc33 toc34-2* triple mutant

Finally, the *toc90-1 toc33 toc34-2* (hom/het/hom) triple mutant was compared with the *toc33 toc34-2* (het/hom) double mutant. Kubis et al. (2003) have shown that the *toc33 toc34-2* double homozygote is embryo lethal, and only the *+toc33; toc34 toc34* survive. The latter genotype exhibits a severe phenotype but can nonetheless survive to maturity on soil. To quantify the severity of the pale phenotype in the triple mutant, I conducted chlorophyll measurements. Comparing the triple mutant with the double mutant, the former was found to be smaller and paler in appearance (Fig. 2.8A). However, a small but significant difference in the chlorophyll levels was also observed. The triple mutant presents a slightly lower chlorophyll level than the double mutant (Fig. 2.8B).

To corroborate the results, *toc90-3* was also crossed with *+toc33; toc34 toc34*, and analyses of the resulting triple mutant gave identical results (Fig. 2.8A). The results indicate a functional overlap between the atToc90 and atToc33/ atToc34.

The other three triple mutants that were analysed (Table 2), after careful phenotypic analysis, did not exhibit any obvious difference when were compared with the appropriate controls (data not shown). In summary, the data indicate that atToc90 is important for chloroplast biogenesis. Even though atToc90's role is unknown, it seems that it shares a functional relationship not only with the other orthologues of Toc159, but clearly also with atToc33 and atToc34.

2.2.4 Analysis of atToc90 function by overexpression

2.2.4.1 Generating new atToc90 overexpression lines.

To support the findings from the double and triple Toc90 mutant studies, transgenic complementation studies were conducted. For this work, the Toc90 protein was expressed under the control of the constitutive cauliflower mosaic virus (CaMV) 35S promoter in two different mutant backgrounds: (1) the *toc159* single mutant background; (2) the *toc132-3 toc132-3;+toc120-2* double heterozygous mutant background. For this experiment, was used the full length sequence of atToc90, as was described by Hiltbrunner et al. (2004) (accession number W43716).

The full length EST clone (H4C12T7) has a 2379 bp open reading frame (ORF). The ORF codes for a protein of 793 amino acids with a molecular mass of 89.338 kDa. The *atTOC90* cDNA was cloned into the pDONR207 donor vector after PCR amplification using specific

primers (Table 4). The presence of the insert was confirmed by digestion with *HspI* (cleaves at a position 307 bp) and *PstI* (cleaves at a position of 2759 bp) restriction enzymes. The results were confirmed by sequencing (detailed explanation of how constructs were made in Chapter 6)

The desired product was finally introduced to the pB2GW7 vector (spectinomycin resistant) by Gateway recombination cloning. The presence of the insert was confirmed by restriction analysis using *SacI* and *XhoI*. The resulting complementation vector was confirmed by sequencing.

The complementation constructs were then introduced into *Agrobacterium* strain GV3101 and then used to transform *toc159* heterozygotes and *toc132-3/toc132-3*; *+/toc120-2* by the floral dip method (Clough and Bent, 1998). Transformants were identified by plating T1 seed on selective medium, and then segregation was analysed in the T2 generation. Only single-insertion lines were carried forward. Transgene overexpression was estimated by RT-PCR. RNA was extracted from 14 days old T2 transgenic plants grown on medium containing the necessary antibiotic.

2.2.4.2 Identification and genotyping analysis of the transformants

After floral dipping, multiple (>10) phosphinothricin and kanamycin resistant primary transformants (T1) were identified for the transgenic lines in the background of *toc159*.

The first PCR performed confirmed that the T1 transgenic lines analysed were heterozygous for the *toc159* allele. One pair of *atTOC159* gene specific primers utilized were located on opposite sides of the T-DNA insertion in *toc159* (forward and reverse, Table 3). Another pair of primers consisted of one primer specific for the left border of the T-DNA insertion, and a *atTOC159* gene specific primer. All transgenic lines were found to carry the *toc159* mutant allele (as well as the wild type *atToc159* allele), as revealed by the positive amplification result for the first primer pair and the positive amplification result for the second primer pair.

T2 transgenic plants carrying the 35S-*atTOC90* construct in the *toc159* background were scored on medium containing phosphinothricin to identify the 35S transgene homozygotes. From these four lines were selected by RT-PCR based on the extent of transgene overexpression relative to the wild-type; It is very important here to note that after the identification of the desired transgenic lines which are expressing high levels, seeds were sown to find homozygous plants. This was done by sowing seeds from the transgenic lines

S2, and S8 in MS media containing kanamycin and phosphinothricin. About 20 petri dishes for each line were used to identify the homozygous. After careful phenotypic analyses, plates showing 100% resistance in the antibiotics mentioned above were selected as homozygous. The selected lines were: S2-3, S8-5, and S8-13. RNA was extracted from 14 day old T2 transgenic plants grown on medium containing phosphinothricin to select for the 35S construct and kanamycin to select for the *toc159* mutation. Primers for RT-PCR were selected to be upstream and downstream of the *toc90-1* T-DNA insertion (so as not to amplify the native gene) and the data were normalized using equivalent data for the translation initiation factor gene *eIF4E1* (Rodriguez et al., 1998) (Table 5) (Fig. 2.9A).

The analysis of the second set of transgenic lines in the background of *toc132-3 toc132-3;+/toc120-2* was performed in similar fashion. Multiple (>20) phosphinothricin and sulfadiazine resistant primary transformants (T1) plants were identified and genotyped by PCR. The T2 generation seeds were used to identify the homozygous 35S-*atTOC90* plants. RNA was extracted from 14 day old T2 transgenic plants grown on medium containing phosphinothricin for the construct. As above, two lines were selected based on the degree of transgenic overexpression (Fig. 2.10A); the selected lines were P5 and P20.

2.2.4.3 Phenotypic analysis of the transformants

As controls for the phenotypic analysis of the 35S-*atTOC90* (full length cDNA clone, H4C112) transformants in the background of (a) *toc159* and (b) *toc132-3 toc132-3;+/toc120-2*, I used 35S-*atTOC90* transgenic plants analysed by Kubis et al. (2004). Those transgenic plants were constructed with the use of cDNA clone RZL46g05 (accession number AV548084) which was truncated at the 5' end and encodes a protein that is 14 residues shorter (Kubis et al., 2004).

Transgenic plants with the full length *atTOC90* construct displayed partial complementation of the phenotype of *toc159*, while transgenic plants with the truncated construct showed no complementation (Fig. 2.9A). To confirm that these differing results were not due to different levels of overexpression mediated by the two different constructs, I analysed the points by RT-PCR (Fig. 2.11C) and by immunoblotting (Fig. 2.11D), (see also Section 2.2.4.4 for more detailed discussion). Lines that were homozygous for the 35S-*atTOC90* (full length) transgenes and the *toc159* mutation, had levels of transgene overexpression that was not significantly different from those in the transgenic 35S-*atTOC90* plants carrying the truncated construct (Fig. 2.11A). Taking into account the above results,

and also the earlier study of the double knockout mutant, *toc90-1 toc159*, my data strongly support the conclusion that *atToc90* and *atToc159* share significant functional redundancy. In support of this, after growth *in vitro* for 14 days, complemented seedlings of this construct can grow to maturity on soil and even produce new seeds (Fig. 2.11B).

In contrast, the results obtained from the analysis of the 35S-*atTOC90* lines in the *toc132-3 toc132-3;+/toc120-2* background did not reveal any partial or full complementation, with either construct (Fig. 2.11A). A line that was homozygous for the 35S-*atTOC90* (full length) transgene (P20), had significantly higher levels of transgene overexpression than any of the other transgenic 35S-*atTOC90* lines. Chlorophyll measurements were conducted on this line but no significant difference was found. From the above findings it seems that *atToc90* and *atToc132 atToc120* do not share a significant functional overlap. This result was surprisingly different from those I obtained earlier from the studies of the triple mutants, *toc90-1 toc132-2 toc120-2* and *toc90-1 toc90-1; toc132-2 toc132-2; +/toc120-2*.

2.2.4.4 Protein expression analysis

To confirm that the two constructs were expressing the expected protein, total protein samples were extracted from 10 day old seedlings of representative lines for each construct, as well as from wild-type plants. These extracts were analysed by immunoblotting using an *atToc90* specific polyclonal antibody (Fig. 2.12c). The antibody was made by Dr Sybille Kubis. In parallel the same protein samples were analysed by staining with Coomassie Brilliant Blue R250 (Fisher Scientific) to confirm that equal amounts of each sample were loaded. As expected, three of the partially complemented lines carrying the full length construct were found to overexpress the *atToc90* protein the correct size (~100 kDa) (Fig. 2.12c). This indicates that the construct is efficiently expressed and that the product is more likely targeted to the chloroplast. Also, seedlings carrying the truncated construct showed a similar high level of expression, confirming the efficiency of the construct. Similar results were obtained with the lines in the *toc132 toc120* background.

The experiment has been repeated twice with fresh total protein samples from the same representative lines in an attempt to confirm the findings. All the different biological and technical replicates produced the same results as shown in Fig. 2.12c.

2.3 Discussion

Several detailed genetic studies by Kubis et al. (2004) and Ivanova et al. (2004) provided no evidence for a significant role of atToc90 in chloroplast biogenesis as a component of the TOC complex. In {Kubis, 2004 #149}, *toc90* homozygotes were indistinguishable from the wild-type with respect to phenotypic appearance, growth and development, and chlorophyll accumulation. Also, there was no obvious effect of the *toc90* mutation in the *toc132*, *toc120* and *toc159* backgrounds, and so it was concluded that atToc90 does not share any substantial functional redundancy with these components. Hiltbrunner et al. (2004) have reported that atToc90 interacts genetically with atToc159, and more recently, Infanger et al. (2011) suggested the ability of atToc90 to support the import of atToc159 client proteins.

Overall, most of the double *toc90* mutants that I analyzed led to confirmation of previous findings. However, my experiments showed a clear functional redundancy between atToc90 and atToc159 as a *toc90-1 toc159* double mutant was even sicker than the albino *toc159* single mutant. Moreover, this result was confirmed in a study of the triple mutant *toc90-1 toc159 toc120-2*, which showed an extremely severe albino phenotype, indicating functional overlap between atToc90, atToc159 and atToc120.

The results of the studies on the double and triple *toc90* mutants were further supported by the results from the complementation study based on the overexpression of *atTOC90* using the full length cDNA clone (H4C12), which was first reported by Hiltbrunner et al. (2004). Kubis et al. (2004) have reported that the overexpression of atToc90 was inactive in their *toc159* complementation studies. In my complementation studies, there was clear evidence of partial complementation by *35S-atTOC90* in the *toc159* background. In my lines, the expression of *atTOC90* was almost at the same level as it was in the lines of Kubis et al. (2004). A likely explanation for these different results might be the importance of the usage of the full length *atTOC90* cDNA. An alternative suggestion was made by Infanger et al. (2011), who suggested that the success in their *toc159* complementation studies was due to the fact that they used the Wassilewskija ecotype instead of Columbia that Kubis et al. (2004) used. Infanger et al. (2011) also showed that the overexpression of *atTOC90* can partially complement the albino knockout of *atTOC159* and restore photoautotrophic growth.

As was mentioned in Section 2.2.4.3, it is surprising that my complementation studies using *35S-atTOC90* in the *toc132 toc120* background did not produce a positive result (*i.e.*, no partial complementation was found). The complementation studies could not confirm the

clear results from the *toc90 toc132 toc120* mutants. A possible explanation to this might be that the phenotypic additivity seen in the *toc90 toc132 toc120* triple mutant was not due to redundancy between the relevant proteins, but rather due to disruption of different import pathways (*i.e.* for photosynthetic and non-photosynthetic preproteins) leading to a deficiency in a much broader range of chloroplast proteins.

Hiltbrunner et al. (2004) showed that synthetic atToc90 was bound to chloroplast membranes under protein import assay conditions and a small portion of the protein specifically co-immunoprecipitated with Toc75, suggesting that atToc90 functions as a component of the chloroplast protein import machinery. My study in the respective double mutants, *toc90-1 toc75-III-3* and *toc90-1 toc75-IV-1*, did not reveal any different phenotypes from the single mutants, *toc75-III-3* and *toc75-IV-1* (Stanga et al., 2009; Baldwin et al., 2005). A difference could be more expected in the first case because of the distinct pale phenotype of *toc75-III-3* but that was not seen.

Analysis of the double mutant *toc90-1 toc33* showed that the phenotype remained the same as in the single *toc33* mutant. However, when was analysed the *toc90 toc33 toc34* triple mutant, it was observed a significant effect of the *toc90* mutation, in that the triple mutant was sicker than the *toc33 toc34* double mutant. This result also suggested a functional redundancy between atToc90 and atToc33/atToc34. Like the other genetic results, these findings suggest that atToc90 cooperates with proteins that mediate the import of the most highly-abundant photosynthetic preproteins (*i.e.* atToc159 and atToc33) as well as with proteins like atToc132, atToc120 and atToc34, that have specificity for low abundance non-photosynthetic preproteins. Interestingly, when it was compared the triple mutant *toc90-1 toc159 toc33* with the double mutant *toc159 toc33*, could detect no phenotypic difference (data not shown). The same results were obtained after comparison of the triple mutant *toc90-1 toc159 toc34-2* with the double homozygote *toc159 toc34-2* (data not shown). Further work will be required in order to explain these unexpected results.

From the results above it has been demonstrated that all four Toc159 homologues in *Arabidopsis* play an important role in chloroplast biogenesis, but still a distinct function for the atToc90 protein remains unclear. It was shown by Ivanova et al. (2004) that these four homologues differ in the length of their N-terminal acidic domains, and recent evidence from Inoue et al. (2010) suggests the involvement of this domain in specialization and specificity.

The lack of an A-domain in atToc90 may allow it to act with less specificity in more than one import pathway.

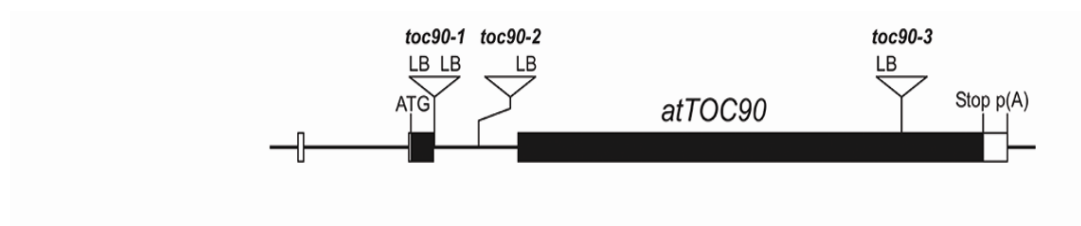


Figure 2.1: Schematic diagram showing the structure of the *Arabidopsis* Toc90 gene and the location of each T-DNA insertion.

atToc90 has three mutant alleles: *toc90-1*, *toc90-2* and *toc90-3*. Black boxes represent the exons while the untranslated regions are represented by white boxes. The thin lines between the boxes represent the introns. ATG is the translation initiation codon. LB, represents the left border T-DNA insertion site and p(A) represents the polyadenylation site.

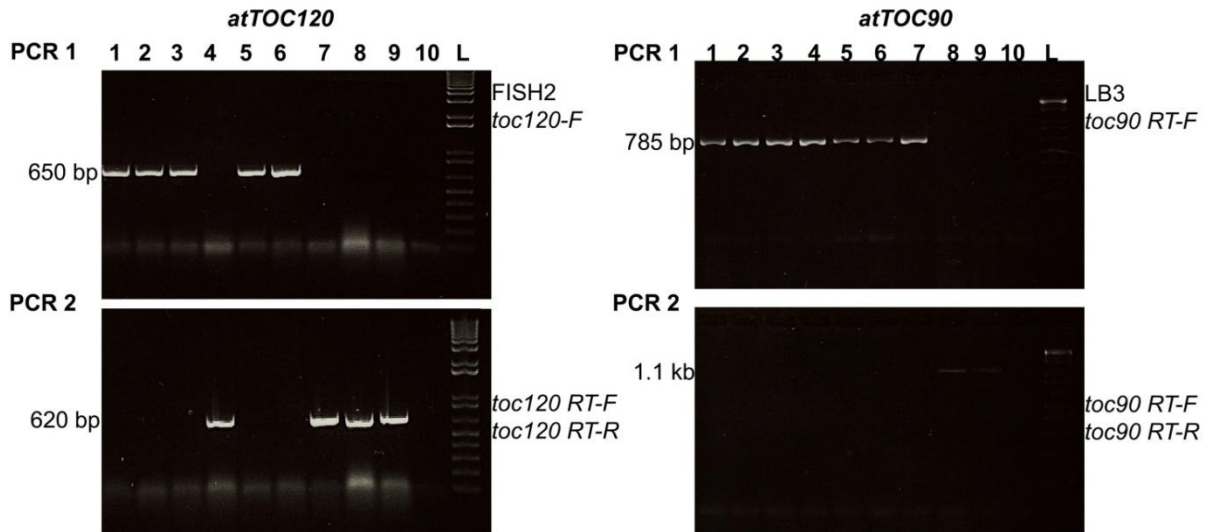


Figure 2.2: PCR gel analyses of the *toc90-1 toc120-2* double mutant.

DNA was extracted from nine F1 *toc90-1 toc120-2* plants (leaves) to confirm their zygosity. In the left side of the figure a PCR (PCR 1) was conducted to confirm the T-DNA insertion of *atTOC120*. The primers were used for this PCR was FISH2 and *toc120-F* as it is indicated in the right part of the first PCR. The expected size is 650 bp as it is shown in the left part. Five out of nine samples indicated that they have the *atToc120* T-DNA insertion. To further examine if the plants are homozygous, heterozygous for the *atTOC120* or wild-type, a second PCR was conducted (PCR 2). The primers were used for PCR 2 were *toc120 RT-F* and *toc120 RT-R* with the expected size to be at 620 bp. The results showed that samples 1, 2, 3, 5 and 6 were homozygous for the *atTOC120*. Sample 4, 7, 8, and 9 were wild-type and sample 10 was used as a control and was H₂O. In the right side of the figure appear the results of the testing; in the upper part which samples have the T-DNA insertion of *atTOC90* by using the LB3 and *toc90 RT-F* primers with an expected size of 785 bp, and in the lower part in PCR 2 was tested the zygosity. The primers which were used in PCR 2 was *toc90 RT-F* and *toc90 RT-R* with an expected size of 1.1 kb. The results showed that samples 1 to 7 were homozygous, samples 8 and 9 were wild-type and sample 10 was the control (H₂O). From all the above was concluded that samples 1, 2, 3, 5, and 6 were the double homozygote *toc90-1 toc120-2* plants.



Figure 2.3: The *tooc90* knockout mutation does not interact genetically with many other TOC component mutations.

Homozygous single and double mutants (24 days old). Plant were germinated *in vitro* and transferred to soil after 14 days of growth on Murashige and Skoog medium (MS).

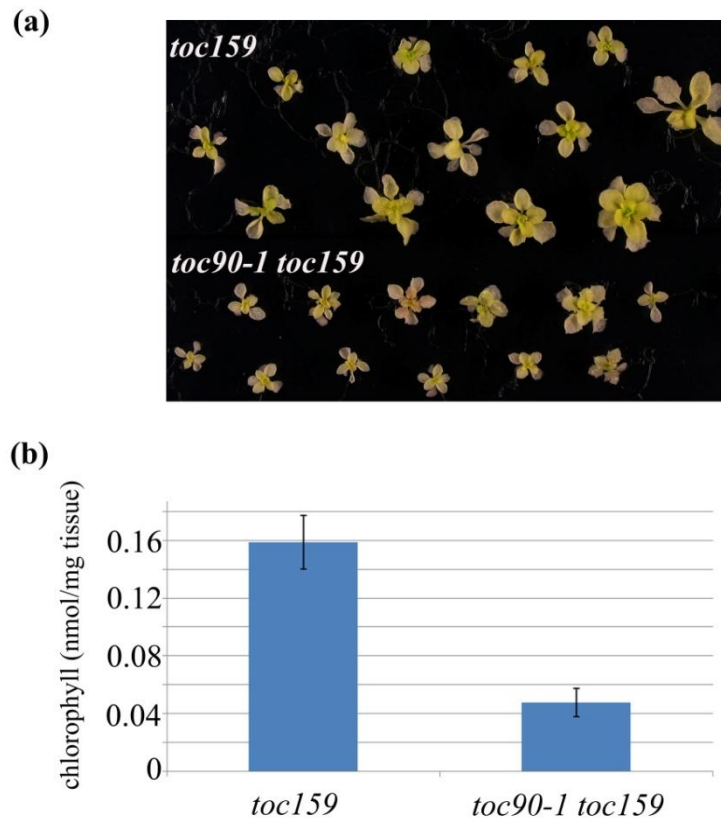


Figure 2.4: Characterization of the *toc90-1 toc159* double knockout mutant.

(a) Phenotypic analysis of the *toc90-1 toc159* double mutant. Single and double mutants were grown together on 3% sucrose for 32 days. (b) Chlorophyll levels show a clear difference between the single knockout mutant, *toc159*, and the double homozygote, *toc90-1 toc159*. Chlorophyll measurement was performed photometrically following extraction in dimethylformamide (DMF); 30 plants from each genotypes were selected for this experiment and the chlorophyll concentration is presented in nmol/mg tissue. The experiment was repeated more than two times.

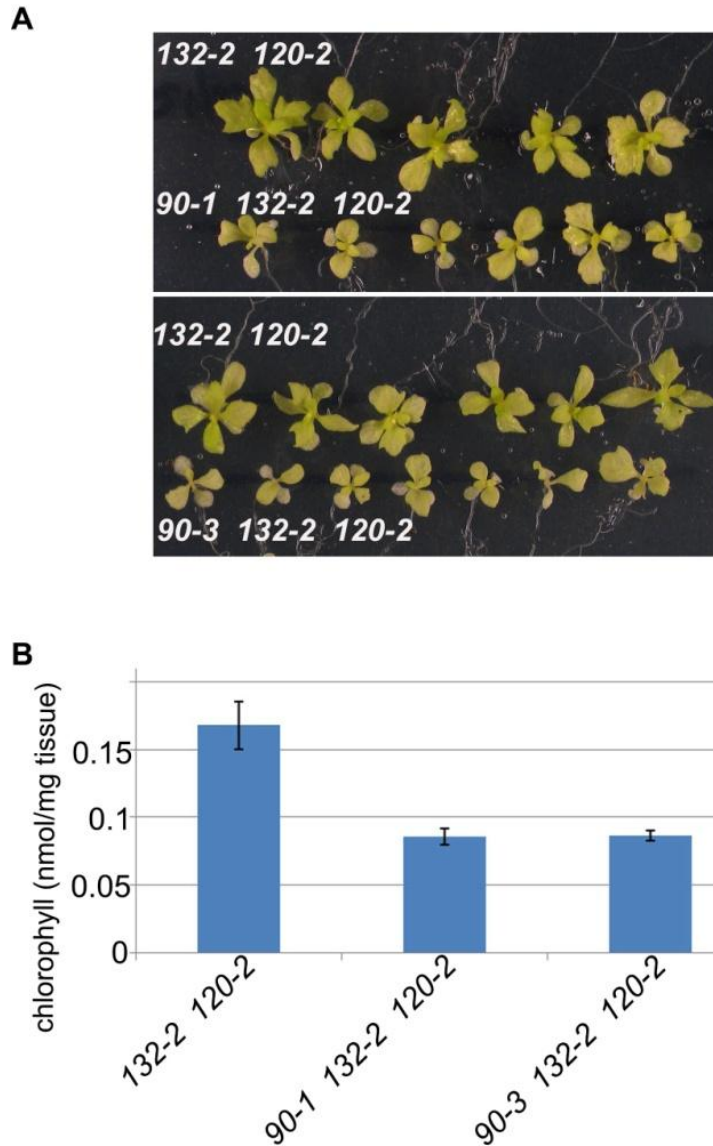


Figure 2.5: Characterization of the *toc90-1 toc132-2 toc120-2* triple homozygous mutant. **(A)** Upper photo is revealing the phenotypic differences between the *toc90-1* triple mutant and the appropriate controls. Lower photo shows a repeat of the experiment with the *toc90-3* allele, confirming the results obtained with the *toc90-1*. All the genotypes have been grown for 12 days in MS media and then transferred in petri-dish plates containing 3% of sucrose. The age of all the genotypes is 32 days after emergence. **(B)** Chlorophyll data revealing the clear difference between the *toc90-1* and *toc90-3* triple mutant and the appropriate controls. Chlorophyll measurements were performed using the DMF method.

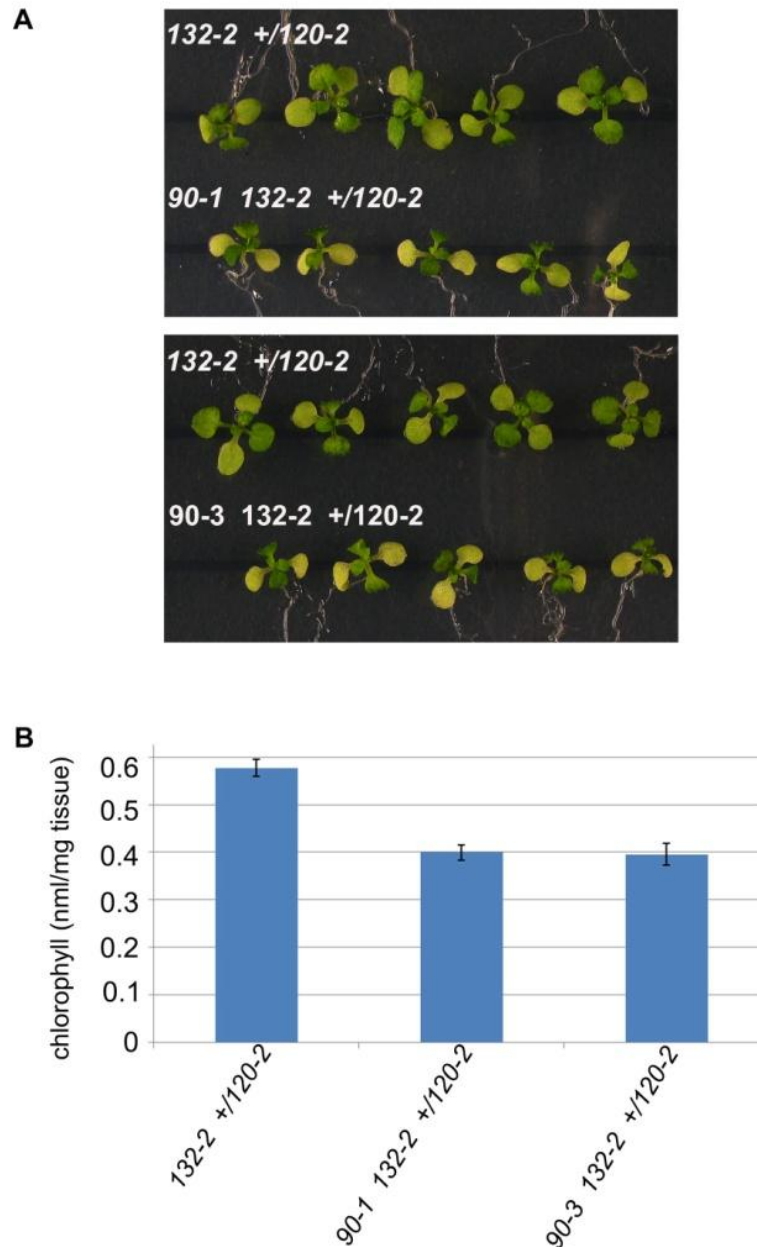


Figure 2.6: Characterization of the *toc90-1 toc132-2 toc120-2* triple heterozygous mutant.

(A) Upper photo is revealing the phenotypic differences between the *toc90-1* triple mutant and the appropriate controls. Lower photo shows a repeat of the experiment with the *toc90-3* allele, confirming the results obtained with the *toc90-1*. All the genotypes have been grown for 12 days in MS media and then transferred in petri-dish plates just MS media. The age of all the genotypes is 32 days after emergence. (B) Chlorophyll data revealing the clear difference between the *toc90-1* and *toc90-3* triple mutant and the appropriate controls. Chlorophyll measurements were performed using the DMF method when all the genotypes were 12 days.

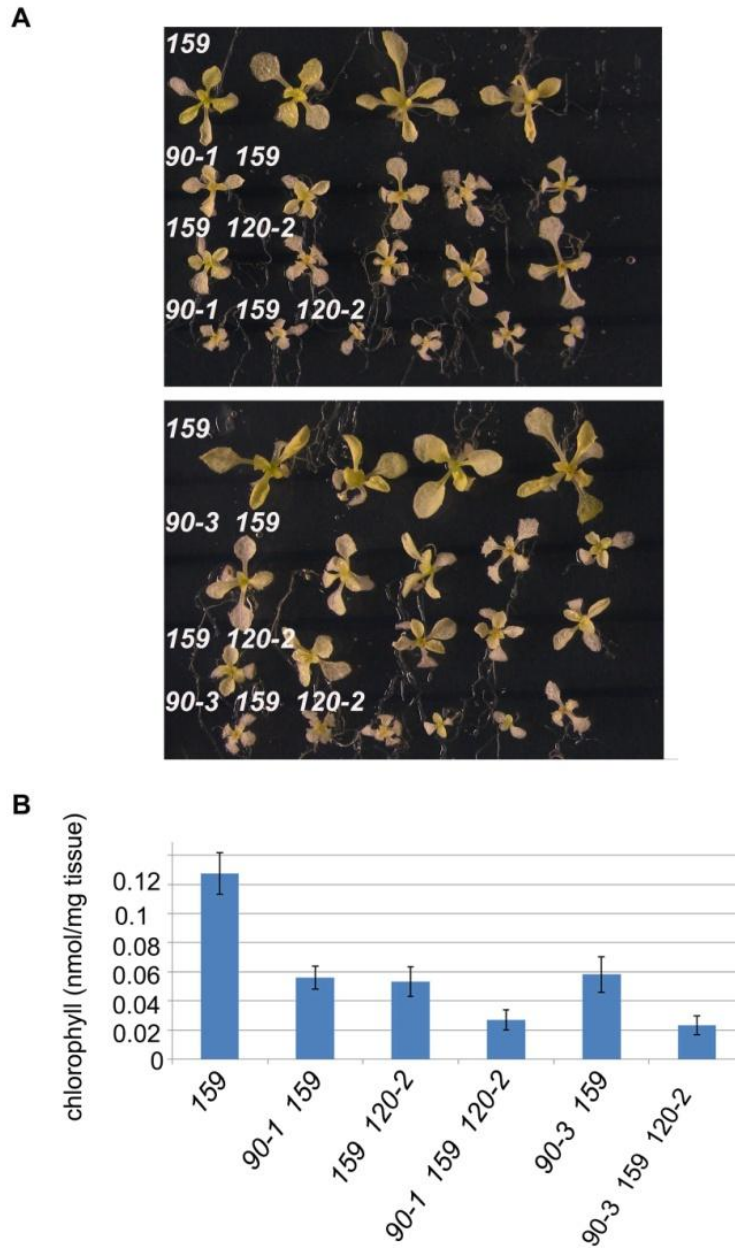


Figure 2.7: Characterization of the *toc90-1 toc159 toc120-2* triple homozygous mutant.

(A) Upper photo is revealing the phenotypic differences between the *toc90-1* triple mutant and the appropriate controls. Lower photo shows a repeat of the experiment with the *toc90-3* allele, confirming the results obtained with the *toc90-1*. All the genotypes have been grown for 12 days in MS media and then transferred in petri-dish plates containing 3% of sucrose. The age of all the genotypes is 32 days after emergence. (B) Chlorophyll data revealing the clear difference between the *toc90-1* and *toc90-3* triple mutant and the appropriate controls. Chlorophyll measurements were performed using the DMF method. Chlorophyll measurements were performed using the DMF method when all the genotypes were 10 days.

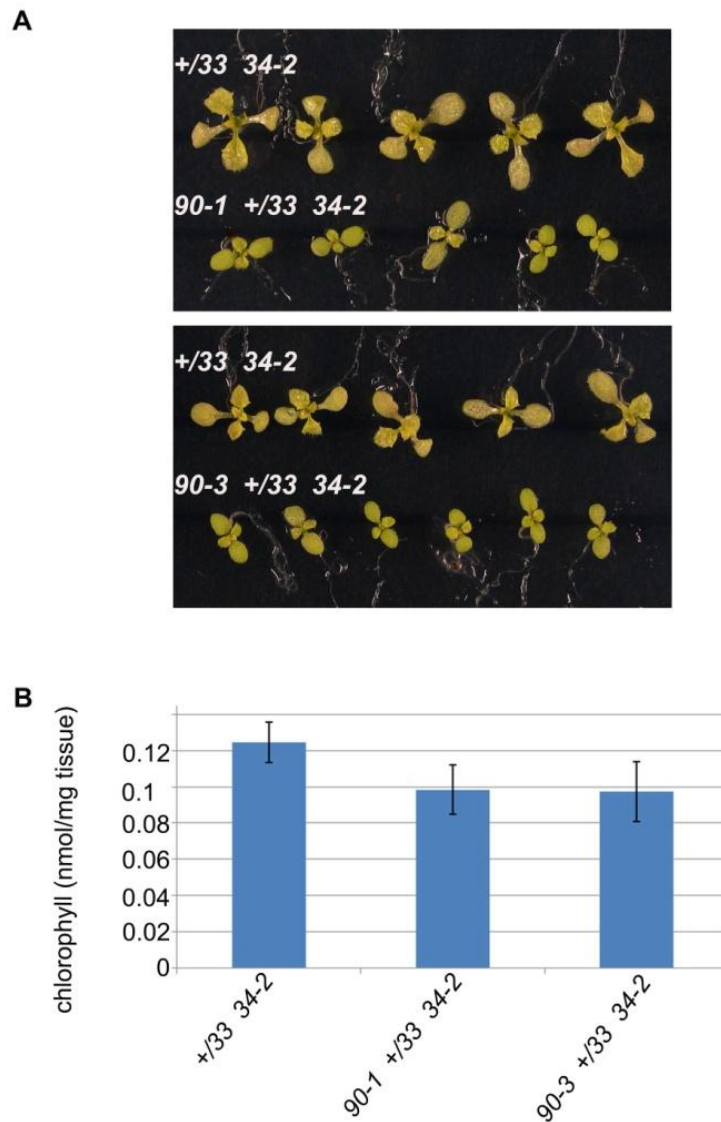


Figure 2.8: Characterization of the *toc90-1 +/toc33 toc34-2* triple heterozygous mutant.

(A) Upper photo is revealing the phenotypic differences between the *toc90-1* triple mutant and the appropriate controls. Lower photo shows a repeat of the experiment with the *toc90-3* allele, confirming the results obtained with the *toc90-1*. All the genotypes have been grown for 12 days in MS media and then transferred in petri-dish plates containing 3% of sucrose. The age of all the genotypes is 24 days after emergence. (B) Chlorophyll data revealing the clear difference between the *toc90-1* and *toc90-3* triple mutant and the appropriate controls. Chlorophyll measurements were performed using the DMF method when all the genotypes were 12 days.

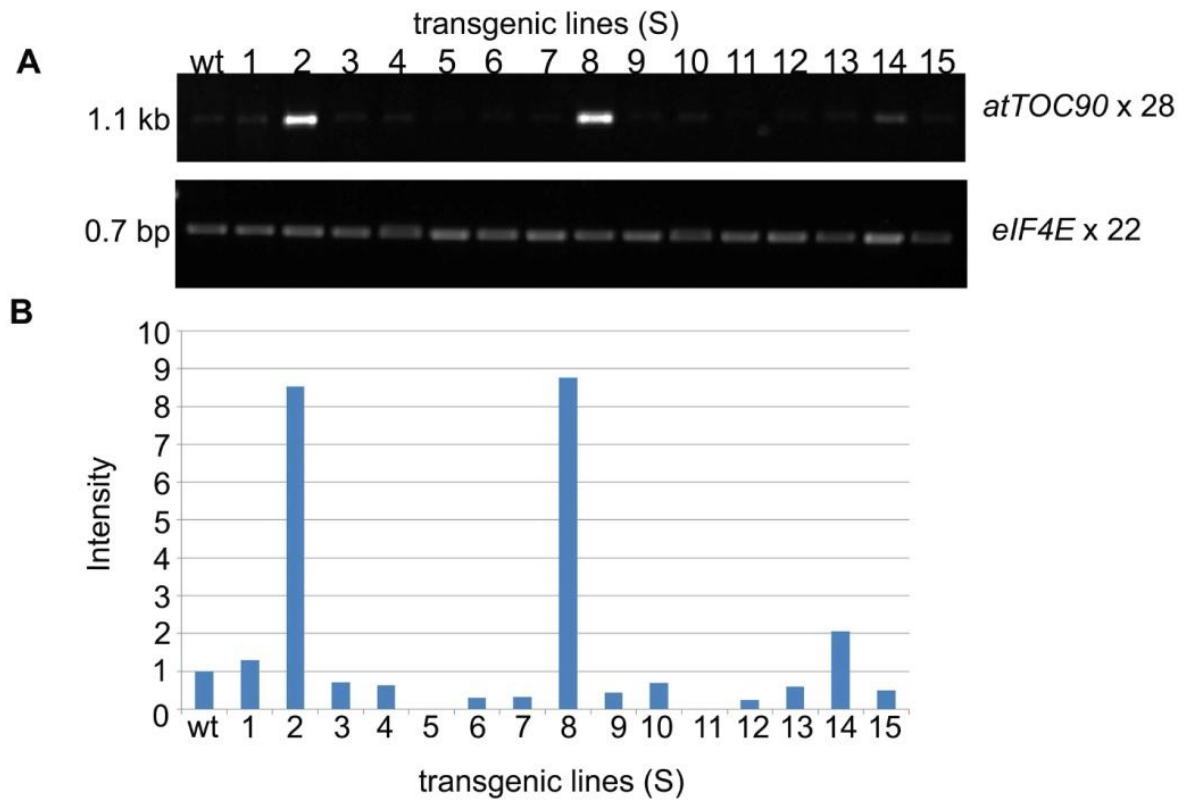


Figure 2.9: RNA levels for the 35S-*atTOC90* full length in the background of *toc159*.

(A) Twenty microgram samples of total RNA isolated from the *toc159* mutant transgenic lines were analysed by RT-PCR. Total RNA was extracted from 14 day old transgenic seedlings and wild-type grown in vitro. PCR reactions were designed to identify the levels of transgene overexpression. *eIF4E* was used as a loading control. PCR was terminated after 22 cycles for *eIF4E* and 28 cycles for *atTOC90*. After electrophoresis and staining the bands were quantified using AIDA software. (B) Relative levels of expression of 35S-*atToc90* were normalized to *eIF4E* and to wild-type.

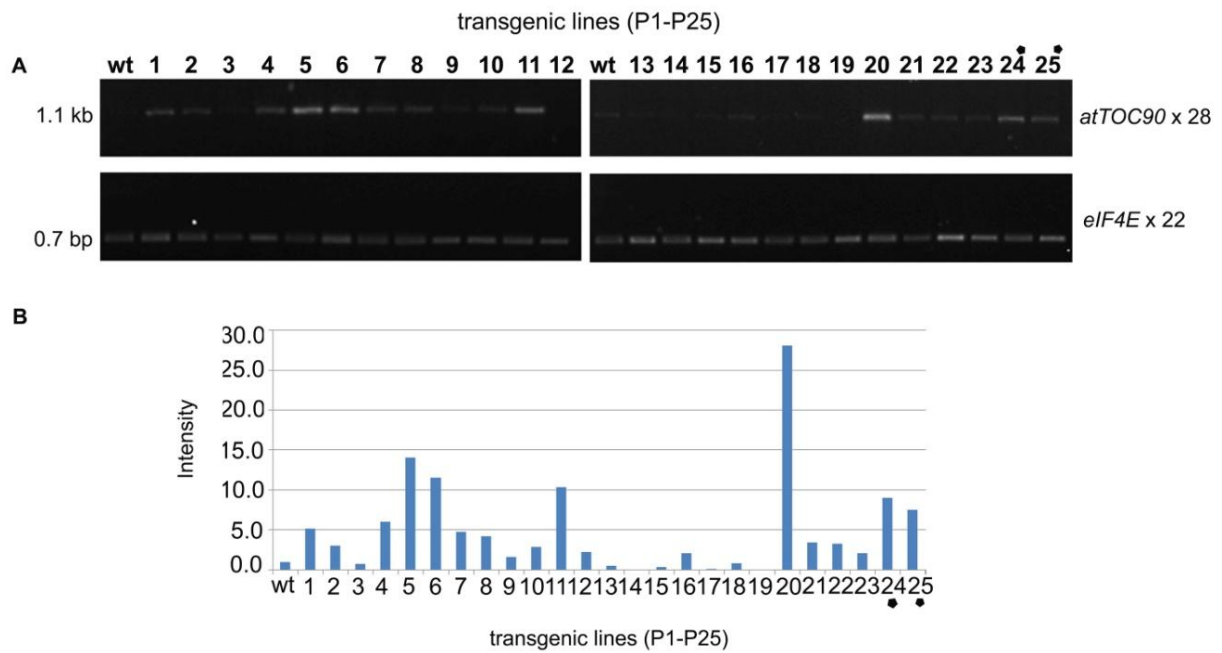


Figure 2.10: RNA levels for the 35S-*atTOC90* in the background of *toc132-2 toc120-2*.

Analysis of the *toc132 toc120* transgenic lines was conducted in similar fashion. **(A)** Twenty microgram samples of total RNA isolated from the *toc159* mutant transgenic lines were analysed by RT-PCR. Total RNA was extracted from 14 day old transgenic seedlings and wild-type grown in vitro. PCR reactions were designed to identify the levels of transgene overexpression. eIF4E was used as a loading control. PCR was terminated after 22 cycles for eIF4E and 28 cycles for atToc90. After electrophoresis and staining the bands were quantified using AIDA software. Samples 24 and 25 are transgenic lines in the truncated form of atToc90 and were included as controls. **(B)** Relative levels of expression of 35S-*atToc90* were normalized to eIF4E and to wild-type.

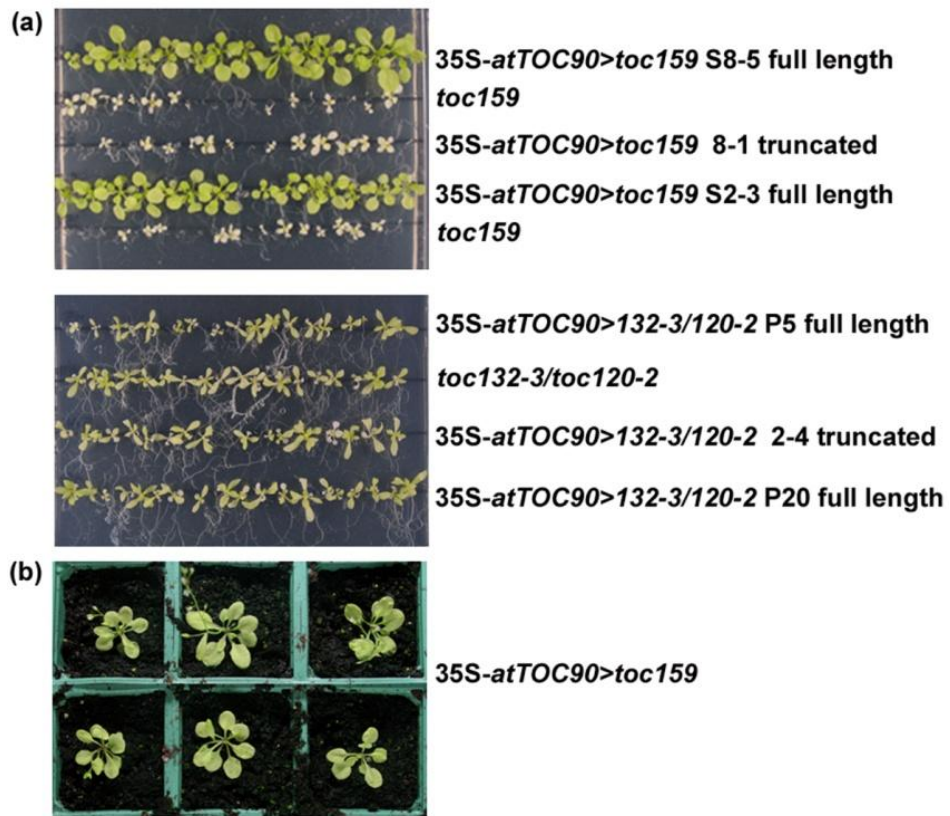


Figure 2.11: Phenotypic and mRNA analysis together of the 35S-*atTOC90* lines in the background of *toc159* and *toc132-3 toc132-3; +/toc120-2*.

(A) Representative 35S-*atTOC90* full length (S2-3, S8-5) and 35S-*atTOC90* truncated (8-1) line in the *toc159* background (Kubis et al. 2004) growing alongside the single *toc159* knockout mutant are shown. Plants were grown on Murashige and Skoog medium with 0.5% sucrose. Also, representative 35S-*atTOC90* full length (P5, P20) into the *toc132-3 toc132-3;+/toc120-2* background, growing alongside with the double *toc132-3 toc132-3;toc120-2toc120-2* homozygote plants and the 35S-*atTOC90* truncated form (2-4) of *atToc90* in the same background. (B) 35S-*atTOC90* *toc159* homozygous plants were transferred to soil and they can grow to maturity and produce new seeds.

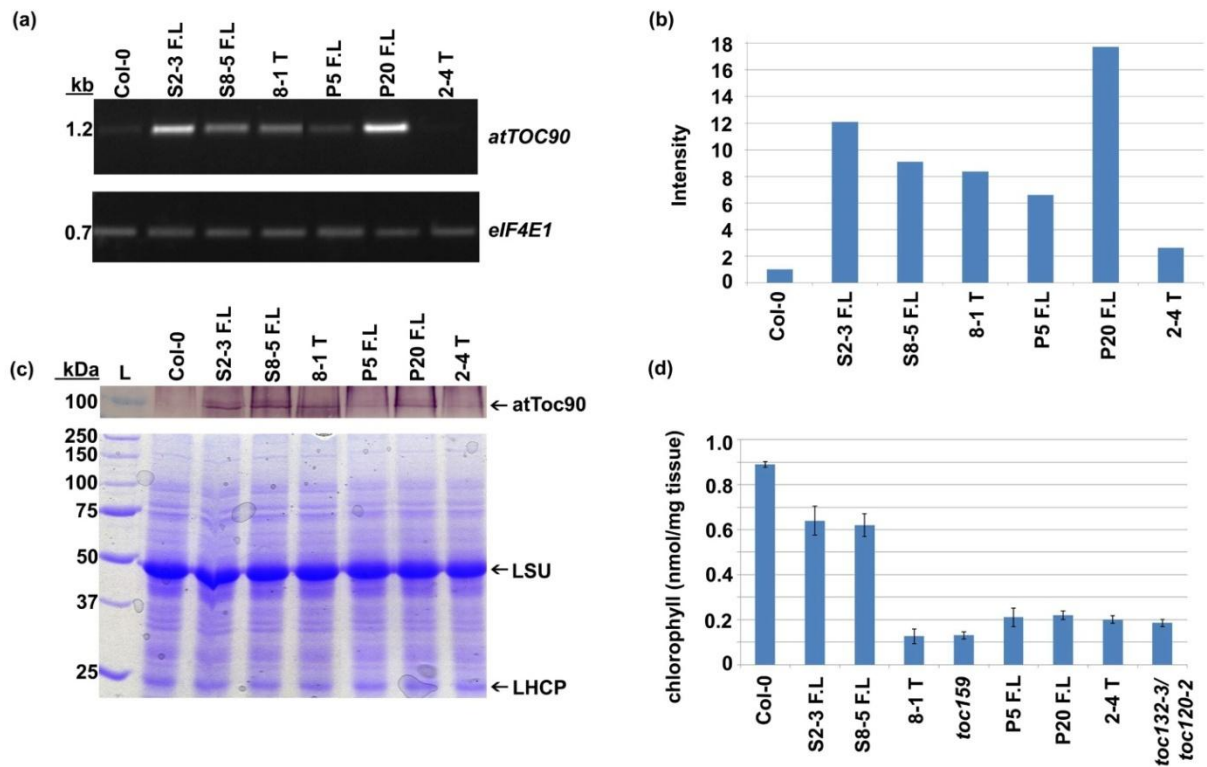


Figure 2.11: Phenotypic and mRNA analysis together of the 35S-*atTOC90* lines in the background of *toc159* and *toc132-3 toc132-3; +/toc120-2*

(a) Total RNA was extracted from transgenic 35S-*atTOC90* plants of the two backgrounds, along with wild-type, that had been grown for 14 days *in vitro*. RT-PCR was constructed using *Toc90* primers designed to identify just transgene overexpression, and the bands were normalized to *eIF4E1*. PCR was terminated after 26 cycles for *Toc90*, and 22 cycles for *eIF4E1*. The graph below the PCR results represents the overexpression levels normalized to *eIF4E1* and to the wild-type levels. (b) represents the overexpression levels normalized to *eIF4E1* and to the wild-type levels (c) Total protein was extracted from plants of the same transgenic lines. Thirty micrograms of protein was loaded and stained with Coomassie Brilliant Blue R250 to confirm equal loading. Immunoblotting analysis of total protein extracts was performed using an antibody specific to atToc90. F.L denotes the full length construct (H4C112); T denotes the truncated construct R2L46g05). (d) Chlorophyll levels indicate the similarity in the chlorophyll levels between the full length construct and the truncated construct in the background of *toc132-3 toc132-3; +/toc120-2*

Chapter 3

Purification and characterization of TOC complexes containing atToc33 and atToc34 from *Arabidopsis* chloroplasts.

3.1 Introduction

3.1.1 Multiple isoforms of the TOC receptors in *Arabidopsis thaliana*.

Chloroplast protein import is facilitated by multimeric translocation complexes in the outer envelope (TOC complex) and the inner envelope (TIC complex). In *Arabidopsis* there are two homologues for Toc34, atToc33 and atToc34, and four Toc159 homologues, atToc159, atToc132, atToc120 and atToc90, as it was described in the Introduction. Utilising knockout mutants for each of the different homologues, Kubis et al. (2003;2004) and Constan et al. (2004) conducted comprehensive and comparative studies of the two Toc34 and four Toc159 homologues. Using import studies, proteomics and transcriptomics, the understanding of the substrate specificity of the chloroplast protein import was advanced significantly. Detail characterization of the *ppi1* mutant, the atToc33 knockout mutant, showed that it is specifically defective in the expression, import and accumulation of photosynthetic proteins, suggesting a higher importance of atToc33 for the import of photosynthetic precursors. In the same way, Toc34 is thought to have specificity for non-photosynthetic proteins, while the Toc159 homologues exhibit similar specialization. Detailed genetic studies of the Toc159 homologues revealed that the *toc132 toc120* double homozygotes exhibit a severe phenotype that is superficially similar to *ppi2* (the atToc159 knockout), indicating that an important role is shared by the atToc132 and atToc120, which is distinct from that of atToc159. In agreement with this overexpression of *atTOC159* failed to rescue the *toc132 toc120* double mutant, whereas overexpression of either *atTOC132* or *atTOC120* could (Kubis et al., 2003; Kubis et al., 2004; Constan et al., 2004). The atToc159 isoform is believed to act with atToc33 in photosynthetic preprotein import, whereas atToc132 and atToc120 act with atToc34 in non-photosynthetic import.

All the above strongly support a model whereby the different Toc34 and Toc159 isoforms exhibit specialized functions in the import of subsets of precursors. The existence of distinct receptor systems may ensure that the import of less abundant, but equally important non-photosynthetic, constitutive precursors is not out-competed by the bulk flow of highly abundant, photosynthetic proteins (Jarvis and Robinson, 2004).

In this chapter I aimed to investigate the composition of distinct TOC complexes using the Tandem Affinity Purification (TAP) method, which allows the efficient purification of protein complexes under native conditions (Puig et al., 2001; Rigaut et al., 1999). By tagging atToc33 and atToc34 I was expecting to elucidate the association preferences of the various

TOC component isoforms, and the composition of the different TOC complexes which was mentioned above.

3.1.2 TAP (Tandem Affinity Purification) – tagging.

The method of TAP (tandem affinity purification)-tagging allows a high yield, high purity and rapid purification of protein complexes by the use of a small protein or peptide attached to the target protein (Rohila et al., 2004; Puig et al., 2001). The TAP tag contains the calmodulin binding peptide (CBP), a tobacco etch virus (TEV) protease site, and tandem protein A domains (ProtA) (Fig. 3.3). The CBP tag allows efficient selection and specific release from the affinity column under mild conditions. In contrast, ProtA can only be released from matrix-bound IgG under denaturing conditions at low pH. Therefore, a specific TEV protease recognition sequence is inserted (Dougherty et al., 1989), which has been shown to allow proteolytic release of the bound material under native conditions (Senger et al., 1998). A fusion cassette encoding CBP, a TEV cleavage site, and a ProtA was constructed and named the tandem affinity purification (TAP) tag (Rigaut et al., 1999).

The TAP method involves the fusion of the TAP tag to the target protein and introduction of the construct into the host cell or organism, maintaining the expression of the fusion protein at its natural level. In other words, this two step purification method (Fig. 3.4) includes first the binding of the ProtA of the fusion protein into the IgG beads. After washing, the fusion protein will be incubated with TEV protease which will release later the target protein by cleavage under native conditions. The second step consists of the incubation of the eluted protein in a calmodulin-coated beads in the presence of calcium, before the release of the purified complex with EGTA (for a detailed description, see Materials and Methods).

For my work, was used the modified TAP vectors that have been described by Rohila et al. (2004), which are specifically optimized for use in plants. In most of my experiments, it was found that first stage purification using the Protein A domain and IgG matrix was sufficient, and that the second stage CBP-based purification (Fig. 3.4) was not necessary.

3.2 Results

3.2.1 Generation of transgenic plants expressing TAP tagged atToc33 and atToc34

For the TAP-tagging experiments the Toc34 receptor component of the core TOC complex was selected, (which as mentioned above has two homologues, atToc33 and atToc34) along with the fourth homologue of Toc159, atToc90. The atToc33 knockout mutant, *ppi1*, has a pale phenotype and aberrant chloroplasts. The atToc34 knockout mutant, *ppi3*, has no visible phenotype in aerial tissues, but root growth is retarded, indicating a relatively higher importance of this isoform in non-photosynthetic tissues. The atToc90 knockout mutant as it shown in Chapter 4, does not display any abnormal visible phenotypes. Nonetheless, the genetic experiments (specifically the triple mutants, *toc90 toc33 toc34*, *toc90 toc132 toc120*, and *toc90 toc159 toc120*) suggested a functional redundancy of atToc90 and homologues of both Toc34 and Toc159.

To generate the transgenic plants, were used the Gateway-based plant TAP vectors (Rohila et al., 2004). These vectors can be used to generate N-terminal (pNTAPi) and C-terminal (pCTAPi) fusions. Constructs encoding fusions between atToc33 and atToc34 and an N-terminal TAP-tag were generated by using Gateway technology, cDNAs of the two genes, and the pNTAPi vector. All constructs have been transformed using the floral dip method (Clough and Bent, 1998) into the respective knockout mutants, *ppi1 (toc33)* and *ppi3-2 (toc34)*. Because *ppi3* does not have an obvious phenotype in aerial tissues, the atToc34-NTAPi was also transformed into *ppi1* plants, to confirm the functionality of the constructs. The vector carries the CaMV 35S promoter, so an overexpression of atToc34 is sufficient to mediate *ppi1* complementation (Jarvis et al., 1998). This provided a confirmation that the atToc33 construct was functional.

3.2.1.1 Characteristics of plants expressing Toc33-NTAPi and Toc34-NTAPi.

Gentamycin and kanamycin resistant T1 seedlings were screened by PCR to detect both the *ppi1* T-DNA insertion and the Toc33-NTAPi transgene, and the *ppi3* T-DNA and the Toc34-NTAPi transgene, respectively. Gentamycin resistance was used as a selectable marker for the construct and kanamycin as a selectable marker for the *ppi1* and *ppi3* T-DNA insertions. Western blots were performed using peroxidase anti-peroxidase (PAP) antibody, which recognizes the protein A domain, for both TAP transgenic lines and, using anti-atToc33, and anti-atToc34 for the Toc33-NTAPi and Toc34-NTAPi lines, respectively. The immunoblots

produced signals at the expected sizes: 55 kDa for Toc33-NTAPi and 56.9 kDa for Toc34-NTAPi. T1 generation plants expressing Toc33-NTAPi and Toc34-NTAPi were selected and grown to produce seeds. Resulting T2 gentamycin-kanamycin resistant lines were grown on soil under normal growth conditions to perform chlorophyll measurements for the atToc33 lines or to measure root growth for the atToc34 lines (Fig. 3.1)

Chlorophyll was measured with DMF method, when atToc33-NTAPi plants have been 10 days after emergence, using wild-type and *ppi1* as controls. The measurements revealed similar chlorophyll amounts in Col-0 and the atToc33-NTAPi transgenic lines. These results indicated that Toc33-NTAPi had complemented the *ppi1* phenotype. Toc34-NTAPi seedlings were growing vertically for 14 days alongside with wild-type and *ppi3*. The results indicated that atToc34-NTAPi plants have complemented the retarded phenotype in root growth of the *ppi3* mutant (Fig. 3.4).

3.2.2 Small scale TAP tagging

Resulting T2 resistant lines in the selective resistant markers (see 3.1.1 and 3.1.2) were grown on petri dishes for 14 days after emergence to perform a small-scale purification of the TAP tag complex. The selected lines for chloroplast isolation were Toc33-NTAPi G2, Toc34-NTAPi G7, and Col-0 (wt plants) were used as control.

Chloroplast isolation was performed as described by Kubis et al. 2008 (see Material and Methods). Always was used fresh chloroplasts but frozen chloroplasts have been used in a same small scale TAP tagging and shown to work as well as fresh chloroplasts (data not shown). The starting amount of the fresh chloroplasts for each sample was 40×10^6 chloroplasts, which is equivalent to ~2 mg of protein. TAP tagging was performed (see Materials and Methods) in the following steps: (a) solubilization of the chloroplasts in solubilization buffer with 1% dodecyl- β -D-maltoside (DDM) plus protease inhibitors, (b) binding of the fusion protein with associated proteins to IgG beads for 2 hours in a cold room, (c) washing thoroughly for several times with 0.3% DDM plus protease inhibitors before incubating overnight with TEV protease, (d) before elutions, Ni-NTA was incubated to the samples for 30 minutes to bind the His-tagged TEV enzyme and final step (e) elutions of the samples.

After performing TAP purification all the collected samples were subjected to immunoblot analysis using antibodies raised against atToc33, atToc159 and atToc75 to detect whether

these TOC proteins co-purified with the TAP fusion proteins (Fig. 3.5). In my small scale TAP tagging experiments the goal was to optimize the purification method and then complete the basic complex characterization. The small scale experiments were performed several times using only the atToc33-NTAPi lines, and methodological improvements were achieved until finally the method was optimized and was ready for scaling-up procedure using more chloroplasts. The methodological improvements consists of; making our own home made IgG beads (following Pfanner laboratory protocol), instead of using IgG Sepharose 6 Fast Flow (GE Healthcare), usage of His-tagged TEV and not the commercial ProTEV (Promega), and finally adding Protein A Sepharose 4 Fast Flow (GE Healthcare) beads into the TEV eluted samples. This application had as a result to minimize the intensity of the heavy chain IgG, which are visible in Silver staining gels in the area of 50 kDa (Fig. 3.8).

3.2.3 Large scale TAP tagging

To perform a large scale TAP tagging experiment to enable proper characterization of the TOC complexes, a much larger number of chloroplasts was isolated (see Materials and Methods) from 14-day-old atToc33-NTAPi (33N) G2, atToc34-NTAP (34N) G7, and wild type Col-0 seedlings. The number of chloroplasts which was used in such large scale TAP tagging experiment was 550×10^6 chloroplasts, which is equivalent to ~27.5 mg of protein.

(a) atToc33-NTAPi G2 analysis:

Typical results for the atToc33-NTAPi analysis are shown in figure 3.6 and the whole technique is well described in Chapter 5 (Materials and Methods). Immunoblotting using atToc33 antibody showed a strong signal at a molecular mass of 55 kDa as was expected for the atToc33-TAP fusion protein. It was clear from the immunoblot that the binding step was successful as only a faint band appears in the post-binding lane. In the TEV eluate, a clear strong signal was detected at 40.1 kDa indicating the appearance of atToc33-CBP. In the final elution with SDS buffer essentially no band was detected either at 55 kDa or 40.1 kDa demonstrating that the purification was successful. As a negative control, chloroplast sample from Col-0 wild type was used, and with this I detected only a band at 33 kDa (corresponding to native atToc33) and only in the total solubilized lysate and post-binding samples (Fig. 3.6).

In the same experiment other antibodies were used: atToc159, atToc90, atToc75, atTic110, atTic40 and LHCP (Fig. 3.6). The first two antibodies (atToc159 and atToc75-III) are against known partners of atToc33 in TOC complexes, and so were used to demonstrate the

successful isolation of atToc33 complexes. The third antibody (atToc90) is against the protein of primary interest to me, as my thesis aims is to elucidate the function of this protein. The antibodies against Tic110 and Tic40 were used to assess whether TOC-TIC supercomplexes were isolated in my experiment, while the LHCP antibody was used as a negative control as this thylakoid protein should not be detected in TOC complexes. The results with atToc159 and atToc75-III antibodies clearly indicated the success of the experiment, as clear bands were visible in the TEV eluate (Fig. 3.6).

Interestingly, atToc90 is presence with a good visible band at 100kDa in the TEV elution sample. LHCP antibody was used as a control. Immunoblotting using α -atTic110 and α -atTic40 could detect a good band in the starting material and unbound protein samples, and a faint band was detectable in the TEV eluate of the Toc33-NTAPi but not in the wild type. This indicated that some TOC-TIC supercomplexes had been isolated. As expected, the LHCP protein was absent from the eluates, clearly indicating the specificity of the experiment. All the Western blots were repeated more than three times for the results to be confirmed.

(b) atToc34-NTAPi analysis:

Typical results for the atToc34-NTAPi analysis are shown in figure 5. The same procedure was performed for the atToc34-NTAPi G7 transgenic line. Immunoblotting using atToc34 antibody (Agriseria) showed a strong signal at a molecular mass of 56.9 kDa as was expected for the atToc34-TAP fusion protein in the starting material. A faint band in the unbound protein sample indicated that the binding step with the IgG beads was successful. In the TEV eluate a clear band at the size of 41 kDa indicated the presence of atToc34-CBP (Fig. 3.7), while in the final elution with SDS buffer no band was visible, indicating that TEV elution was successful. Unfortunately, there was no visible band corresponding to the native atToc34 protein to wild type samples. This might have been due to the antibody being rather weak or the fact that atToc34 a much less abundant protein than atToc33 making it less easy to be detected.

As previously described in paragraph (a), other antibodies were used in the same experiment to detect other TOC-TIC proteins that may have been co-purified. Among those was tested were atToc132, atToc120, atToc90, atToc75, atTic110, atTic40 and LHCP (Fig. 3.7). The atToc132, atToc120 and atToc75-III proteins are all known partners of atToc34, and so these antibodies were used to confirm the isolation of atToc34 complexes. The results clearly

indicated that all of these proteins were present in the atToc34-NTAPi TEV eluates. As with the atToc33-NTAPi experiment (Fig. 3.8), the TIC protein antibodies indicated that some TOC-TIC supercomplexes had been isolated, while the absence of the thylakoid LHCP protein from the TEV eluate sample clearly indicated the specificity of the experiment.

Again, most interestingly, atToc90 was present with a good visible band, although it was fainter than the band present in the atToc33-NTAPi TEV eluate sample (Fig. 3.7).

3.2.4 Silver staining and colloidal coomassie blue

After detailed immunoblotting analysis of samples were analysed by SDS-PAGE, followed by Silver and colloidal Coomassie staining techniques (see Materials and Methods) (Fig. 3.8). This was done in order to visualise the different proteins within the TEV eluted proteins for mass spectrometric analysis. In both staining methods, two bands corresponding to the IgG heavy and light chains, at around 50 kDa (faint) and 25 kDa (stronger signal) respectively, appeared in the TEV eluates. In addition to these bands, several other bands were observed in the silver stained gels (Fig. 3.8).

Areas of the colloidal Coomassie stained gels (with the same loading order as the silver stained gels) were excised and sent for the mass spectrometric analysis after digestion of the proteins with trypsin (detail analysis in section 3.2.5). Areas that were selected and excised for mass spectrometry are indicated in Table 1.

3.2.5 Mass spectrometric protein identification

To enable identification of the atToc33-NTAPi and atToc34-NTAPi associated proteins, a large scale TAP tagging purification was enabled as described above (see Section 2.3) followed by proteomics analysis.

Proteomics was carried out by the University of Leicester Proteomics Facility (PNAFL, University of Leicester). Bands of interest were excised from the gel, and in-gel trypsin digestion was carried out upon each (Speicher et al. 2000). Each slice was destained using 200mM ammonium bicarbonate/20% acetonitrile, followed by reduction (10 mM dithiothreitol, Melford Laboratories Ltd., Suffolk, UK), alkylation (100 mM iodoacetamide, Sigma, Dorset, UK) and enzymatic digestion (sequencing grade modified porcine trypsin, Promega, Southampton, UK) using an automated digest robot (Multiprobe II Plus EX, Perkin Elmer, UK). After overnight digestion, each sample was acidified using formic acid (final

concentration 0.1%), and analyzed either by MALDI-ToF mass spectrometry or by LC-MS/MS.

LC-MS/MS was carried out using an RSLCnano HPLC system (Dionex, UK) and an LTQ-Orbitrap-Velos mass spectrometer (Thermo Scientific). Samples were loaded at high flow rate onto a reverse-phase trap column (0.3mm i.d. x 1mm), containing 5µm C18 300 Å Acclaim PepMap media (Dionex) maintained at a temperature of 37 °C. The loading buffer was 0.1% formic acid / 0.05% trifluoroacetic acid in water.

Peptides were eluted from the trap column at a flow rate of 0.3 µl/min and through a reverse-phase capillary column (75µm i.d. x 250mm) containing Symmetry C18 100 Å media (Waters, UK) that was manufactured in-house using a high pressure packing device (Proxeon Biosystems, Denmark). The output from the column was sprayed directly into the nanospray ion source of the LTQ-Orbitrap-Velos mass spectrometer.

The LTQ-Orbitrap-Velos mass spectrometer was set to acquire a 2 microscan FTMS scan event at 30000 resolution over the m/z range 400-1800 Da in positive ion mode. Accurate calibration of the FTMS scan was achieved using a background ion lock mass for polydimethylcyclsiloxane (445.120025 Da). Subsequently up to 20 data dependent CID MS/MS were triggered from the FTMS scan and performed in the LTQ-Velos ion-trap. The isolation width was 2.5 Da, normalized collision energy 35.0, Activation Q 0.25, Activation time 10 ms. Dynamic exclusion was enabled.

The raw data file obtained from each LC-MS/MS acquisition was processed using the Raw2MSM application (Olsen et al. 2005). Each file was in turn searched using Mascot² (version 2.2.04, Matrix Science Ltd.) against the UniProtKB/Swissprot database. The peptide tolerance was set to 5 ppm and the MS/MS tolerance was set to 0.6 Da. Fixed modifications were set as carbamidomethyl cysteine, and variable modifications were set as oxidised methionine. The enzyme was set to Trypsin/P and up to 3 missed cleavages were allowed. A decoy database search was performed.

Data was further processed using Scaffold (Searle and Scaffold, 2010) (version 3.0.9, Proteome Software). The Mascot.dat files were imported and searched using X!Tandem⁶ (version 2006.9.15.4, The Global Proteome Machine Organization). PeptideProphet (Keller et al. 2002) and ProteinProphet (Nesvizhskii et al., 2003) (Institute for Systems Biology) probability thresholds of 95% were calculated from each of the Mascot and X!Tandem decoy

searches and Scaffold was used to calculate an improved 95% peptide and protein probability threshold based on the data from the two different search algorithms.

Data received from the peptide analysis of each gel section or slices are presented in Table 1. The peptide profile showed some interesting results based on the model for substrate-specific protein import pathways. First, the mass spectrometry results actually confirmed the immunoblot data presented in Fig. 4. The most interesting results that is and be worthy of further analysis and discussion are that: (i) atToc132, atToc120 and atToc90 were co-purified with atToc33-NTAPi; (ii) atToc159 and atToc90 were co-purified with the atToc34-NTAPi. The high number of peptides identified indicates that this is not a mistake. This procedure was repeated more than three times to be sure that the results are accurate and reliable.

3.3 Discussion

By performing immunoblot analyses, I showed that atToc159, atToc75-III and atToc90 could be co-purified with atToc33-NTAPi. These findings were also confirmed by mass spectrometric analysis. Since not atToc33 but atToc34 was proposed to interact preferentially with atToc132 and atToc120 (Ivanova et al., 2004), it is interesting that the mass spectrometry results showed that both atToc132 and atToc120 were co-purified with atToc33-NTAPi.

I have also performed TAP tagging with atToc34-NTAPi. Immunoblot analysis showed that atToc132, atToc120, atToc75-III and atToc90 were co-purified with atToc34-NTAPi. Mass spectrometric analysis confirmed these findings. Most interestingly, I was able to detect atToc90 in these complexes. It is also noteworthy that atToc159 was unexpectedly detected in the atToc34 complexes by mass spectrometry.

My results indicate that the substrate specific import pathways model that was presented in the Introduction may not be entirely accurate. One possible explanation is that, while the different receptor isoforms may indeed have distinct client specificities, they perhaps are nonetheless associated together in large mixed TOC complexes. Another possible explanation is that the use of the strong, constitutive 35S promoter to drive expression of the TAP fusions in my work led to association of the fusion proteins with TOC components that they would not normally associate with in the wild type. Having said that, great care was taken when generating the TAP lines to select only those transformants that express the fusions at levels

close to the native level. Indeed, my own data (not shown) suggested that the fusion proteins are not strongly overexpressed.

Interestingly, in both TEV eluates I could detect some Tic110 and Tic40. After repeating the experiment several times I concluded that this result was not due to a contamination. However, my mass spectrometric results did not identify either TIC protein (or any chaperones) in the TEV eluates; Tic110 is known to recruit the chaperones Hsp93 and Cpn60 with the help of Tic40 (Kovacheva et al., 2007; Kessler and Schnell, 2006). Nonetheless, my immunoblot results suggest that I was able to purify at least some TOC-TIC supercomplexes, as was reported previously (Nielsen, 1997; Kouranov et al., 1998).

Mass spectrometry analysis revealed the presence of a small portion of actin (only a small number of peptides were identified) in the eluted TAP-tagged atToc33 protein complexes, but not in the eluted TAP-tagged atToc34 complexes. Unfortunately, I was unable to confirm the mass spectrometric results by immunoblotting because of a lack of the respective antibody. A possible link between TOC proteins and actin is interesting. Recent results from Jouhet and Gray, (2009), showed that there is an interaction between Toc159 and actin. Also, many other TOC-TIC components were identified after co-immunoprecipitation with antibodies to actin. The significance of this is uncertain but it may play a role in directing preproteins to the chloroplast surface from the cytosol.

The most interesting outcome of this work from the perspective of my thesis is that atToc90 was clearly shown to associate with both atToc33 and atToc34 complexes, by both immunoblotting and mass spectrometry. This is consistent with the genetic data presented in Chapter 2, which suggested a role for atToc90 in photosynthetic and non-photosynthetic protein import pathways. Equal amounts of chloroplasts were used to perform the large scale TAP-tagging experiments. Comparing the immunoblot results suggested that atToc90 is more abundant in the eluted TAP-tagged atToc33 protein complexes. However, as the immunoblots were conducted on different occasions, the results are not strictly comparable. In the future, it will be interesting to repeat the experiments simultaneously, to rigorously assess whether atToc90 is more abundant in atToc33 complexes than in atToc34 complexes. If true, this would be consistent with the notion that atToc90's role is primarily concerned with the import of photosynthetic preproteins (Hiltbrunner et al., 2004; Infanger et al., 2010).

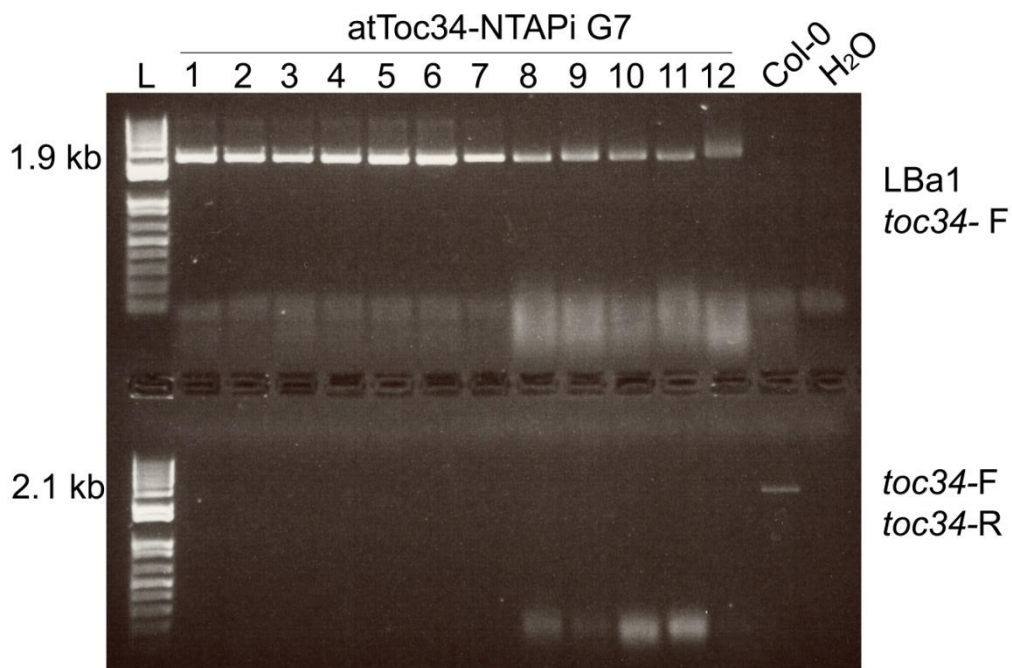


Figure 3.1: PCR gel analyses of atToc34-NTAPi G7 transgenic line.

DNA was extracted from nine T1 transgenic plants (leaves) to confirm their zygosity. In the upper part of the figure a PCR was conducted to confirm the T-DNA insertion of *atTOC34*. The primers used for this PCR were LBa1 left border and *toc34-F* as indicated in the right part of PCR gel. The expected size is 1.9 kb as shown in the left part. All the tested samples indicated that they have the atToc34 T-DNA insertion. To further examine if the plants are homozygous, or heterozygous for the *atTOC34*, a second PCR was conducted. The primers used were *toc34-F* and *toc34-R* with the expected size to be at 2.1 kb. The results showed that all the samples were homozygous for the atTOC34. For control was used Col-0 sample and H₂O.

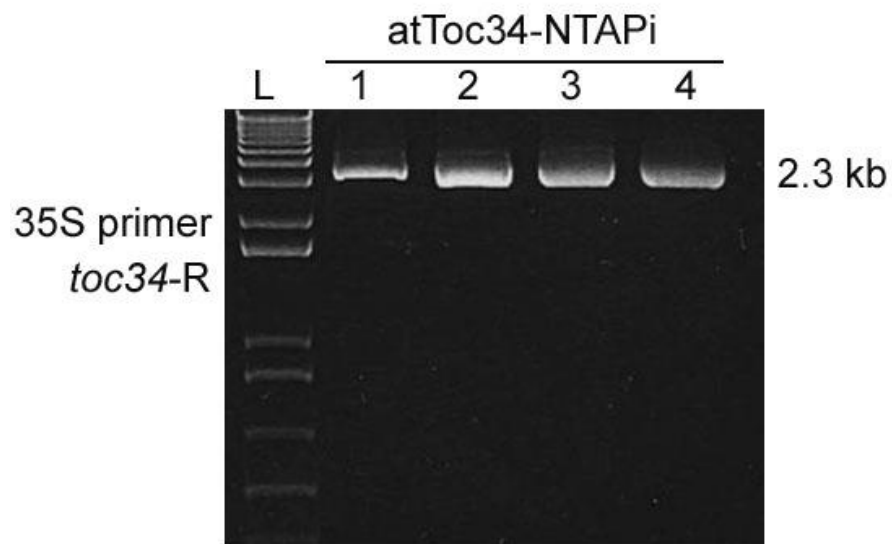


Figure 3.2: PCR gel analysis to confirm the function of atToc34-NTAPi G7 transgenic line.

DNA was extracted from nine T1 transgenic plants (leaves) to confirm the function of atToc34-NTAPi G7. The primers used for this PCR was 35S primer and *toc34-R* as it is indicated in the left part of PCR gel. The expected size is 2.3 kb as it is shown in the right part. In all four tested samples indicated that they are expressing the NTAP.

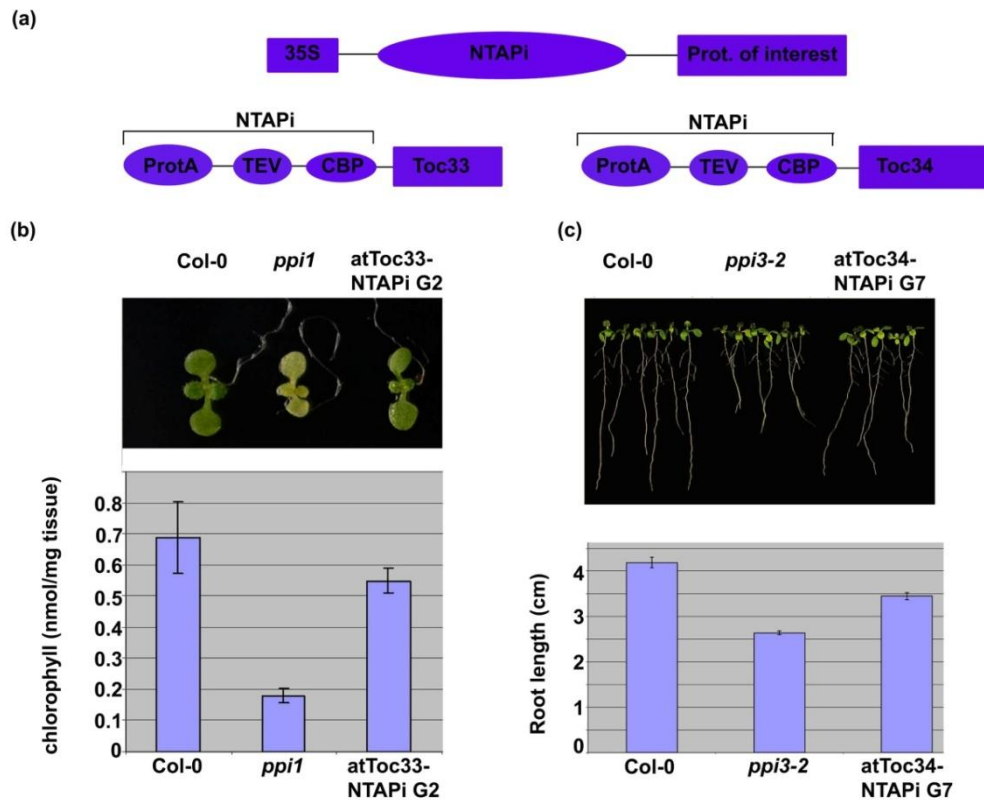


Figure 3.3: Structure of TAP tag expression cassette and analysis of atToc33-NTAPi and atToc34-NTAPi constructs.

(a) Schematic representation of a general NTAPi construct. The construct encoding fusions of the protein of interest, in our case fusions between atToc33 and atToc34 and an N-terminal TAP-tag were generated by using cDNAs of the two genes and the pNTAPi vector. The vector carries the CaMV 35S promoter. NTAPi is consisted from an IgG binding domain of *Staphylococcus aureus* Protein A (ProtA), a tobacco etch virus (TEV) protease cleavage site and another IgG binding domain, the calmodulin binding peptide (CBP) (b) Phenotypic analysis of the atToc33-NTAPi G2 construct. Transgenic plants of this NTAPi construct were growing *in vitro* for 14 days alongside wild-type and *ppi1* plants. Results are indicating that atToc33-NTAPi plants have complemented the *ppi1* phenotype. The result was confirmed after performing chlorophyll measurements with the DMF method in 10 days seedlings which showed similar chlorophyll amounts between Col-0 and atToc33-NTAPi G2 (c) atToc34-NTAPi G7 plants were growing vertically for 14 days alongside with wild-type and *ppi3-2*. The results show clearly that atToc34-NTAPi G7 plants have complemented the retarded phenotype in root growth of the *ppi3* mutant. Root length was quantified by analysis of multiple independent images using SigmaScan Pro software (SPSS Inc.). The values shown are means derived from approximately 8 individual measurements. Error bars indicate standard deviation.

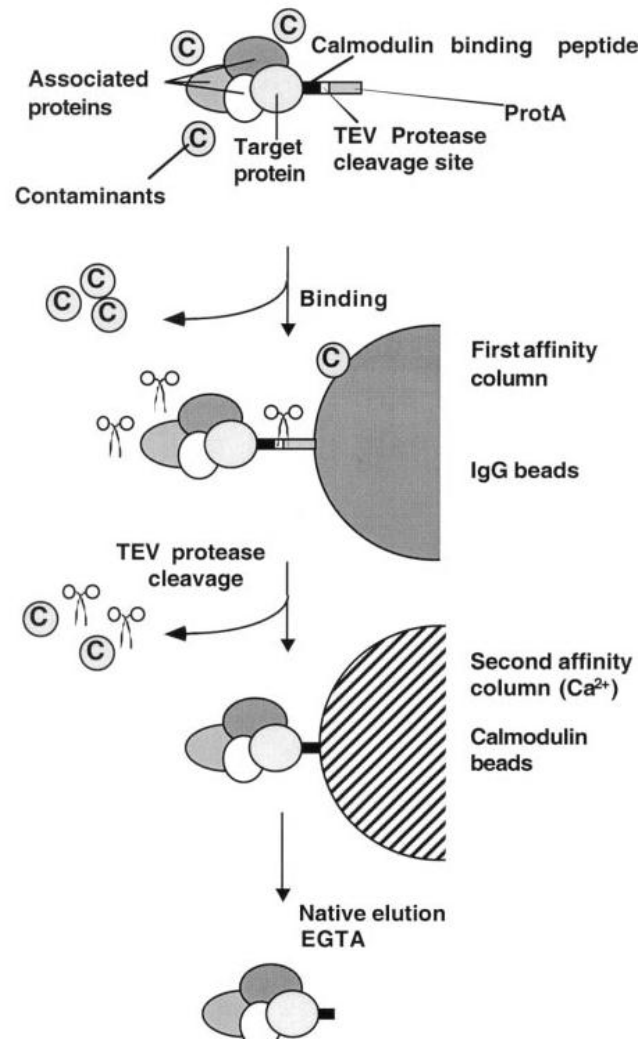


Figure 3.4: Schematic overview of the TAP tagging method.

The protein A has a very high affinity for IgG. The calmodulin binding peptide has high affinity for calmodulin. An extract containing the TAP-tagged target protein is mixed with IgG affinity resin before being incubated with TEV protease that will release the target protein by cleavage. This eluate may be used for a second affinity step where the target protein will bind to calmodulin in the presence of calcium, before release of the purified complex by EGTA which chelates calcium ions essential for calmodulin binding (Dziembowski and Seraphin, 2004). (Taken from Puig et al.2001)

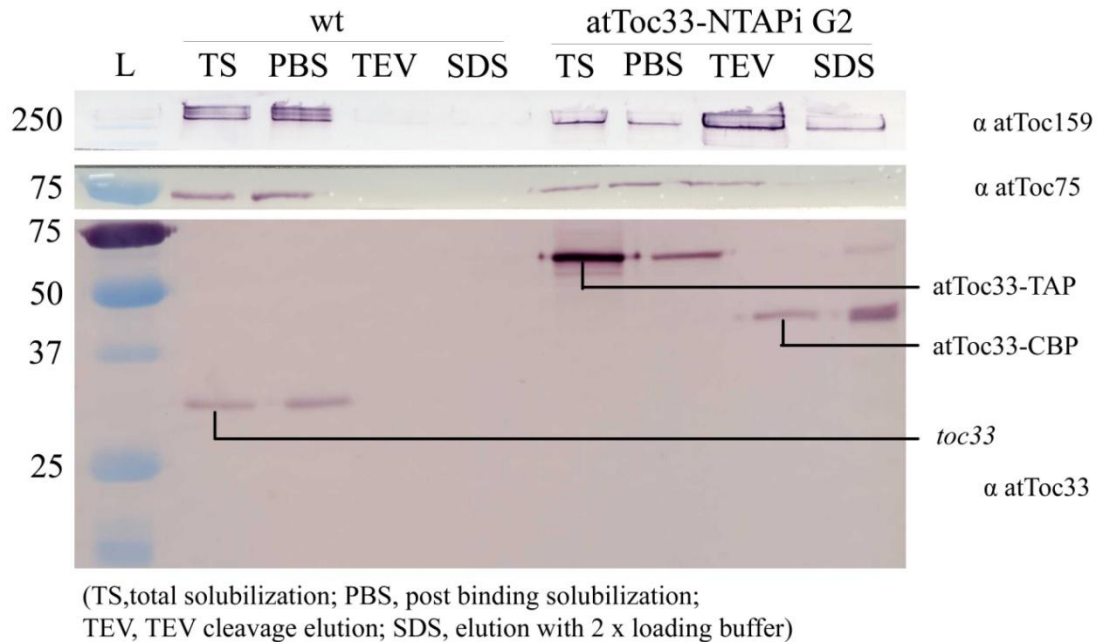
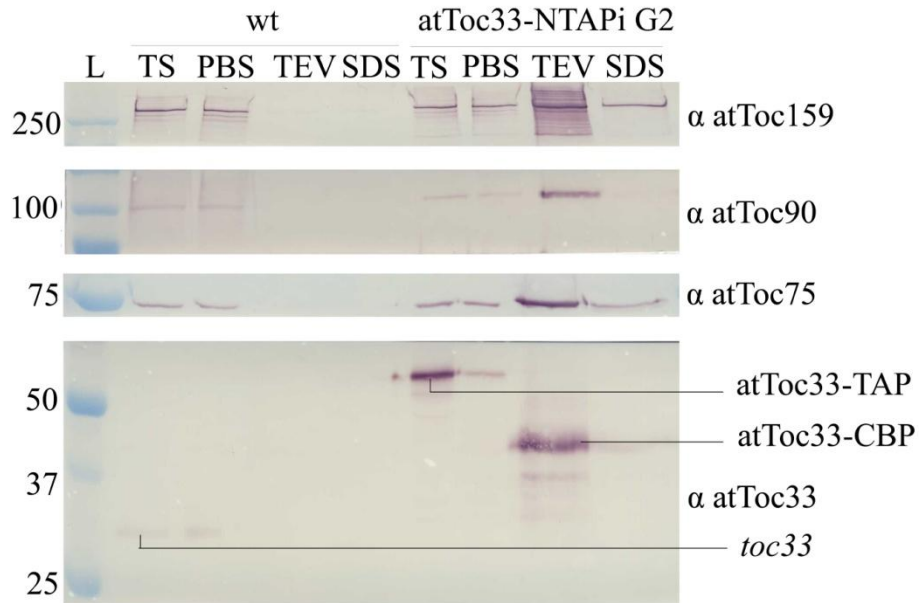


Figure 3.5: Small scale TAP tagging experiment using the atToc33-NTAPi (33N) G2 transgenic line and immunoblotting analyses of the results are shown.

Western blotting with atToc33 antibody shows a strong band for the atToc33-CBP protein at the expected size (40.01 kD) and a strong band of atToc33-TAP (approx. 50 kD) in the total solubilized lysate and post binding fractions for atToc33-NTAPi. I also identified a strong band corresponding to atToc33-CBP in the SDS elution sample, indicating that the elution after TEV cleavage was not complete. Native atToc33 were identified in the wild type total solubilized lysate and post-binding samples only. Antibodies raised against atToc159 and atToc75-III were used to confirm that other TOC proteins can be co-purified with the TAP fusion proteins, indicating the successful purification of TOC complexes



Other tested antibodies:

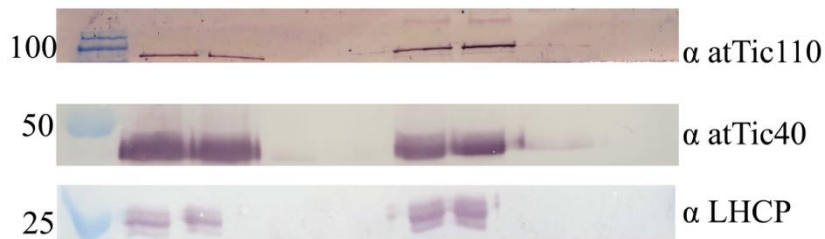


Figure 3.6: Large scale TAP tagging experiment using the atToc33-NTAPi (33N) G2 transgenic line and immunoblotting analyses of the results are shown.

Antibodies raised against TOC proteins were tested to confirm the co-purification of these proteins together with the TAP fusion. First was tested the α atToc33 antibody which was detected in the first two wild type samples Toc33 (TS and PBS) in the corresponding size. A strong band of atToc33-TAP (approx. 50 kD) was detected as expected in the total solubilized lysate. The binding of proteins (33N PBS) had almost 100% efficiency and that allowed more proteins to elute after the TEV elution; the atToc33-CBP protein at the expected size (40.01 kD). Although, was tested three more antibodies: α atToc75, α atToc90, and α atToc159. The most important among the findings was the detection of atToc90. Bands are in the expecting size and can prove that Toc75, Toc90, and Toc159 are part of the TOC complex. Finally, it was tested antibodies against two TIC proteins (atTic110 and atTic40). As a negative control it was used the LHCP antibody. Abbreviations in the figure are defined as follows: TS, total solubilisation; PBS, post binding solubilisation; TEV, TEV cleavage elution; SDS, 2 \times LB elution.

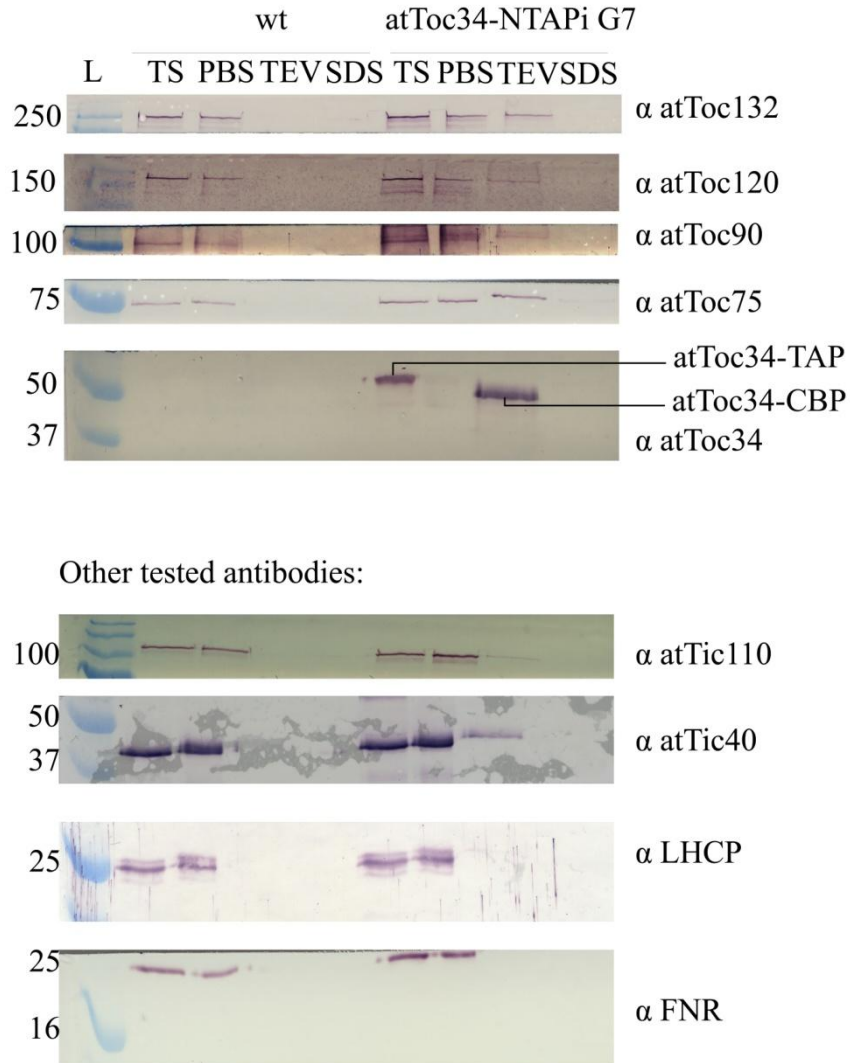


Figure 3.7: Large scale TAP tagging experiment using the atToc34-NTAPi (34N) G7 transgenic line and immunoblotting analyses of the results are shown.

Antibodies raised against TOC proteins were tested to confirm the co-purification of these proteins together with the TAP fusion. First was tested the α atToc34 antibody which was detected in the first two wild type samples Toc34 (TS and PBS) in the corresponding size. A strong band of atToc34-TAP (approx. 55 kD) was detected as expected in the total solubilized lysate. The binding of proteins (34N PBS) had almost 100% efficiency and that allowed more proteins to elute after the TEV elution; the atToc34-CBP protein at the expected size (41 kD). Although, was tested five more antibodies: α atToc75, α atToc90, α atToc120, α atToc132, and α atToc159. The most important among the findings was the detection of atToc90. Bands are in the expecting size and can prove that Toc75, Toc90, Toc120, Toc132 and Toc159 are part of the TOC complex. Finally, it was tested antibodies against two TIC proteins (atTic110 and atTic40). As a negative control it was used the LHCP and FNR antibody. Abbreviations in the figure are defined as follows: TS, total solubilisation; PBS, post binding solubilisation; TEV, TEV cleavage elution; SDS, 2 \times LB elution

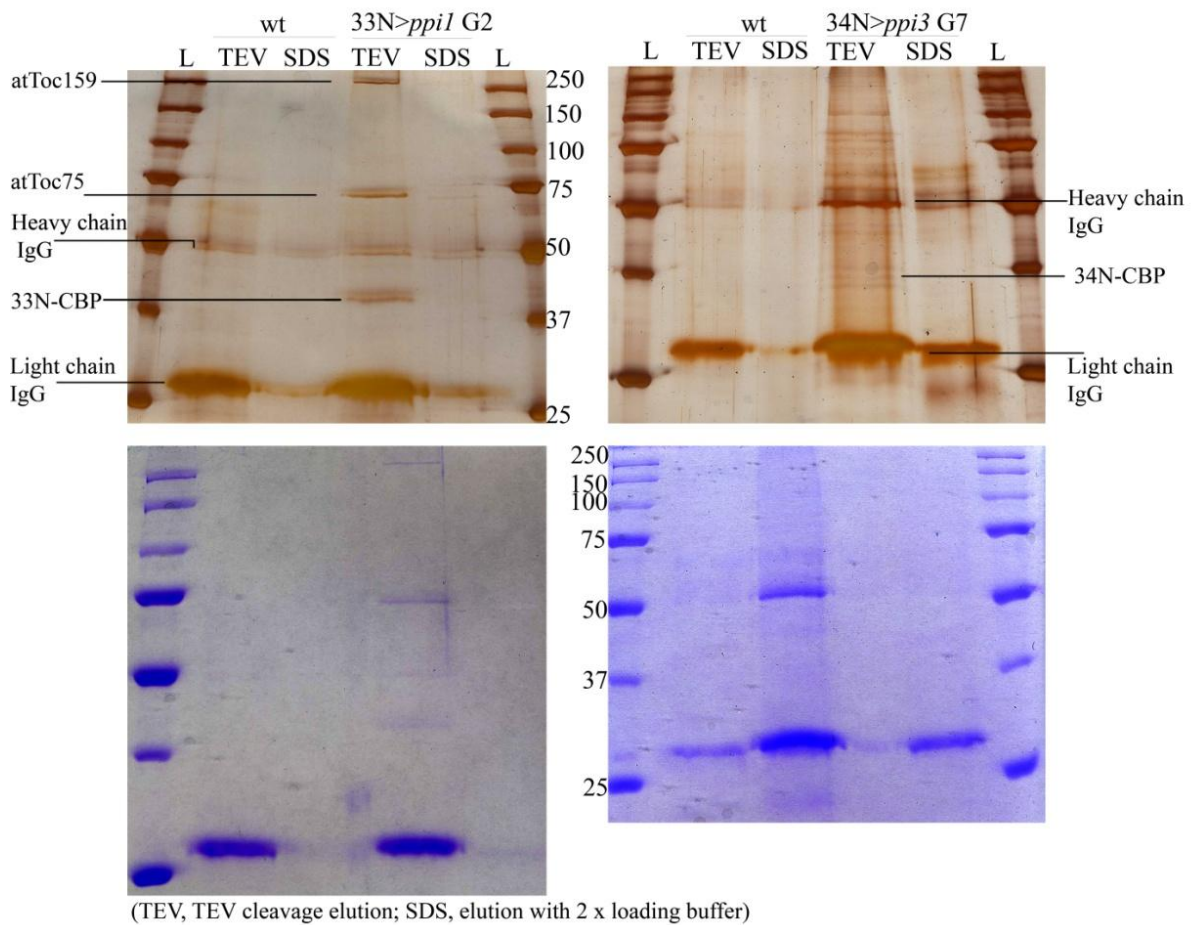


Figure 3.8: Silver and Coomassie staining of the TAP-tagged atToc33 and atToc34 complexes.

The TEV and SDS eluates were analysed by SDS-PAGE followed by silver (upper panel) and Coomassie staining (lower panel). Staining with Coomassie could not give a good visualization of the TOC bands because it is less sensitive than silver staining. Control eluates from Col-0 wild type were used as negative controls. However, Coomassie stain is more compatible with mass spectrometry. Areas from Coomassie stained gel were selected to be trypsin digested and made ready for mass spectrometry analysis. Areas that were selected and excised for mass spectrometry are indicated in Table 1

Table 3.1: Mass spectrometric analysis results for Toc33-NTAPi and Toc34-NTAPi.

TAP transgenic lines	Protein identification	kDa range of gel slice	Accession gene number	no. of representative peptides
33N-G2	atToc159	150-250 kDa	At4g02510	278
	atToc90	90-150 kDa	At5g20300	10
	atToc132	100-250 kDa	At2g16640	
	atToc120	100-250 kDa	At3g16620	6
	atToc75-III	75 kDa	At3g46740	18
	atToc33	30-50 kDa	At1g02280	11
	Actin 1	130-250 kDa	At1g49240	2
34N-G7	atToc159	150-250 kDa	At4g02510	223
	atToc90	90-150 kDa	At5g20300	9
	atToc120	100-250 kDa	At3g16620	12
	atToc75-III	60-80 kDa	At3g46740	14
	atToc34	25-50 kDa	At5g05000	22

Chapter 4

Possible involvement of the *Arabidopsis* atToc90 protein in leaf senescence

4.1 Introduction

Here in this chapter, the aim was to elucidate the function of *atToc90* and understand the relationship that *atToc90* has regarding leaf senescence. The idea of looking for a relationship between the *atToc90* and leaf senescence came after careful searches using Genevestigator (<http://www.genevestigator.com>) (Zimmermann et al., 2004), a very useful and easy accessible software tool for the analysis of publicly available gene expression data from Affymetrix microarray experiments. Genevestigator is a high performance search engine for gene expression. The high quality and well annotated data with high performance computing allowed running queries across thousands of datasets simultaneously. Therefore, it was interested to start looking which conditions affect the expression of *atTOC90* comparing with the other known TOC genes, as it shows in figure 4.1. Significant changes of *atTOC90* gene expression were observed in relation to senescence and osmotic treatments, line treatment with high concentration of NaCl, jasmonic acid, abscisic acid (ABA), and low nutrient supply. Though, as none of these treatments could show a significant change in my experiments between the *Toc90* knockouts and overexpressor lines (Fig. 4.1).

Few studies have shown any involvement of the TOC/TIC components in leaf senescence. Niwa et al. (2004) have reported that, in an *Arabidopsis thaliana* mutant that lacks the *atTic40* protein, cotyledon cells contain undeveloped plastids, and that a proportion of these are sequestered and partially degraded in the vacuoles. Such autophagy occurs under nutrient starvation conditions to recover resources for the cell, but can also serve as a quality control mechanism to remove abnormal organelles. It should be noted that it is quite possible that osmotic stress is related to senescence. For the below described physiological experiments of this chapter, was used three knockout mutants of *atTOC90* (*toc90-1*, *toc90-2*, and *toc90-3*), together with an overexpression 35S-*atTOC90* transgenic line in the background of Col-0 constructed with the full length sequence of *atTOC90* (see Chapter 2). As the control, was used wild-type plants (Col-0 ecotype).

In some species such as *Arabidopsis*, leaf age can be used as a predictor of the timing of senescence; the sequential senescence of rosette leaves coinciding with maximum inflorescence development. During its life cycle, a rosette leaf progresses through distinct developmental stages. Leaf chlorophyll and protein contents are often used as indicators of leaf senescence. Chlorophyll degradation is the first visible symptom of senescence, but by

the time yellowing of the leaf can be seen, the majority of the senescence process has occurred (Buchanan-Wollaston et al., 2003).

Environmental and endogenous factors interact in the onset and progression of leaf senescence. Environmental causes may accelerate leaf senescence by affecting physiological aging, reproductive development, and hormone levels. Plants also have mechanisms whereby leaf senescence can be induced by stresses such as nutrient availability, water deficit, and high light.

Senescence proceeds gradually in leaves and is characterised by three distinct phases. First is the initiation phase, the result of early signalling cascades that lead to changes in gene expression. These signalling cascades will determine whether leaf senescence is induced upon the stress conditions. These changes in gene expression lead to modifications in the endogenous concentrations of plant regulators such as plant hormones (ABA and cytokinin), reactive oxygen species (ROS) which by their localization and cellular concentration can regulate the expression of senescence associated genes (SAGs). Second is the re-organization phase where major metabolic and ultrastructural changes occur. These changes may include chlorophyll degradation, decrease of cell integrity, and decrease of photosynthetic activity. Last is the terminal phase of leaf senescence, thought to be the result of the accumulation of cell death inducing factors that lead to complete loss of cell integrity and death. This phase occurs only when nutrient remobilization has been accomplished.

Chloroplasts show the first symptoms of senescence associated decline in leaves. The modifications that take place in chloroplasts include the distortion of grana, decrease of chloroplast volume, and finally complete loss of chloroplast components (Krupinska et al., 2006). It has been suggested that conversion of chloroplasts to gerontoplasts may be reversible if the senescing tissue is exposed to an exogenous application of cytokinin to favour greening (Olah and Masaricova, 1998). Degradation of chloroplast proteins within the organelle is supported by the observation that chloroplasts contain a number of proteases, like caseinolytic protease (ClpP), DegP and FtsH (Adam and Clarke, 2002).

4.2 Results

4.2.1 Analysis of the *atToc90* knockout mutants and an overexpression line

Three *atToc90* knockout mutants were introduced briefly in Chapter 2. To assess the importance of *atToc90* for plant and chloroplast development, it was conducted a phenotypic analysis of these mutants, as well as of an *atToc90* overexpression line in the wild type background. The overexpression line was generated using the 35S overexpression construct carrying the full length *atTOC90* cDNA that was described in Chapter 2. The relevant overexpression transformant (line N1) was chosen after the careful analysis of approximately 20 transformants by RT-PCR (in much the same way that the overexpression lines in the mutant background were selected in Chapter 2), and was identified as being the line giving the highest level of overexpression (~8.5-fold higher than wild type) (data not shown). Careful analysis of the knockout and overexpressor genotypes revealed that they all exhibit a normal green phenotype like the wild-type, throughout development (Fig. 4.2A and 4.2B). To confirm that I was working with the true knockout and overexpression lines, RT-PCR and immunoblot experiments was conducted. From the results (Fig. 4.2C), one can see that both *atTOC90* mRNA and *atToc90* protein are absent from the three knockout mutants, and present at higher levels by comparison with the wild-type in the overexpression line (line N1).

The phenotypes of the three homozygous *atToc90* knockout mutants and the 35S-*atTOC90* N1 transgenic line were further analyzed by making chlorophyll fluorescence measurements (Fig. 4.3). When the plants were 22 days old, it was performed measurements on dark adapted leaves using a continuous excitation fluorimeter (Handy PEA, Hansatech). The obtained results showed no significant change in F_v/F_m (which provides an estimate of the photosystem II photochemical efficiency) or in the photosynthetic performance index (PI) calculated using the Hansatech software, in any genotype relative to wild type (Fig. 4.3). Chlorophyll measurements were not conducted with the SPAD meter, because SPAD readings cannot show the photosynthetic performance. From the visible indistinguishable phenotype was more or less expected that the chlorophyll levels to be the same for all genotypes.

Thus, my initial observations revealed neither a visible abnormal phenotype nor a photosynthetic defect in any of the lines, under standard growth conditions. As described in the sections below, I therefore went on to analyze the plants under various different

conditions that induce stress or senescence. For all these experiments I have used two of the homozygous knockout mutants (*toc90-1* and *toc90-3*) and one overexpression line (N1), unless stated otherwise.

4.2.2 Jasmonic acid treatment

Originally identified in fragment oils, methyl jasmonate (MeJA) and its precursor jasmonic acid (JA) were first shown to promote leaf senescence in detached oat leaves (Ueda and Kato, 1980). Jasmonates are widely distributed in plants as a class of plant growth regulators (Creelman and Muller, 1997). They were found to be strong promoters of leaf senescence (Chen et al., 1998; Ueda et al., 1981). Exogenously applied JA and MeJA led to decreased expression of photosynthesis related genes, increased degradation of Rubisco, and rapid loss of chlorophyll in barley leaves (Weidhase et al., 1987).

For the following experiments, both MeJA and JA were used. To investigate a potential role of atToc90 in leaf senescence, the homozygous *toc90* knockout mutants, the atToc90 overexpression line (N1), and wild-type plants was treated with JA. All the genotypes were grown for 14 days under standard growth conditions (20°C; 16 hours light / 8 hours dark) side by side on vertically oriented petri dishes, containing MS medium with or without 30 µM JA. The expected pale, senescent phenotype was observed in all the genotypes (He et al., 2002). Moreover, a short root phenotype was also observed in all the genotypes. Unfortunately, although I was not able to establish a clear relationship between the application of JA and senescence, no evidence for effect of atToc90 knockout or overexpression on the induced senescence could be detected (Fig. 4.4).

It is possible that the growth of plants on JA from germination was too harsh a treatment to detect potential subtle effects of the loss or overexpression of atToc90. JA is also known to promote senescence in detached *Arabidopsis* leaves (He et al., 2002), while exogenously applied MeJA generally has similar effects. Thus, it was analyzed the effect of MeJA in detached leaves of the above mentioned genotypes. After plants were grown on soil for 28 days, rosette leaves were detached and placed in small petri dishes containing water, with or without 100 µM MeJA, and incubated in the dark for 4 days. At the end of the incubation time, I noticed that the control leaves kept in only water had become paler, with clear signs of senescence. Unexpectedly, the leaves treated with MeJA were greener and contained more chlorophyll than the control leaves (data not shown). It is unclear why MeJA did not promote senescence in this experiment, as previous work showed increased senescence in response to

JA treatment under otherwise identical conditions (He et al., 2002). It is possible that better results would be obtained if the experiment was repeated with JA instead of MeJA. However, I decided to focus on dark treatment as a method for inducing senescence in my subsequent work.

4.2.3 Induction of leaf senescence in attached darkened leaves

As was mentioned at the beginning of this chapter, during leaf senescence, cells undergo many changes in metabolism and cellular structure. In *Arabidopsis*, some mutants have been associated with delayed leaf senescence, which can be seen by observing visual progression of leaf yellowing during incubation of detached leaves under dark conditions (Oh et al., 1997; Woo et al., 2001). Some mutants can keep their green phenotype under such stress conditions, and among them are the *ore* mutants and the *pph* mutant (see Chapter 1 for further information on these mutants). The functionality of the leaves of such “stay green” mutants can be assessed by measuring chlorophyll fluorescence.

Weaver and Amasino (2001) have reported that senescence can be induced in individually darkened *Arabidopsis* leaves but not when the whole plants are incubated under darkness. To investigate the role of atToc90 regarding senescence, I analysed the atToc90 knockout and overexpression lines by covering attached rosette leaves. In this experiment, I also included as a control the *pph* “stay green” mutant (Schelbert et al., 2009). After 14 days of growth *in vitro*, plants were transferred to soil and grown until they were 24 days old. Developmentally similar rosette leaves from all genotypes were then covered with aluminium foil for 4 days. After the period of the dark incubation, the leaves were uncovered. Fig. 5 shows representative leaves immediately after the dark incubation, together with control leaves which had been left to grow under normal conditions.

Wild-type covered leaves showed a substantial yellowing implying that senescence had occurred during the incubation. In fact, all the genotypes compared with their respective controls showed a paler phenotype at the end of the dark treatment. Interestingly, the *toc90* knockout mutants and the atToc90 overexpression line showed a less pronounced senescence phenotype, although they did not display a “stay green” phenotype to the same extent as the control *pph* mutant (Fig. 5A). To further characterize these phenotypic results, I conducted chlorophyll measurements (Fig. 5B). In response to the dark treatment, the chlorophyll levels of the wild-type had declined sharply (to <20% of the normal level). In contrast, the chlorophyll decline in the *toc90* knockout mutants was much less (to ~60% of the level in the

controls), implying that senescence had progressed more slowly. It is surprising that the 35S-*atTOC90* N1 transgenic line also exhibited reduced senescence following dark treatment (albeit to a lesser extent than in the *toc90* knockout mutants), as one might have expected to observe an opposite (or diametrically opposed) phenotype to that seen in the knockout mutants. This suggests that an excess of atToc90 can interfere with the protein's function in a similar way to its absence. The experiment has been repeated several times, and it confirmed that the attenuated senescence results are reproducible. It is also reassuring that two independent *toc90* knockouts gave identical results.

The next question I wanted to answer was whether the applied dark treatment was truly inducing senescence. To address this question, RNA from similarly treated leaves immediately was isolated after uncovering the leaves, and conducted RT-PCR analysis (Fig. 5C). It was expected that the less exposed to light the dark-treated leaves were, the more accurate this experiment would be. In this work, was tested the senescence associated genes, *PPH* and *SAG12*, as well as a gene encoding chlorophyll *a/b* binding protein (*CAB*) whose expression declines during senescence. It is well known that *SAG12* is a senescence specific gene in *Arabidopsis* (Gan et al., 1995), and it has been used as a molecular marker for leaf senescence. I also analysed the expression of the *atTOC90* gene, while the translation initiation factor gene *eIF4E1* was used as a control to normalize loading. For this experiment, was used the gene specific primers listed in Table 1 (see Appendix).

In the wild type, expression of both *PPH* and *SAG12* increased following dark treatment (Fig. 5C), supporting the notion that the treatment was inducing senescence. Similarly, the expression of *CAB* was reduced in the wild type following dark treatment, as expected. More interestingly, the dark-induced expression changes of *SAG12* and *CAB* were attenuated in the atToc90 knockout and overexpressor lines, just as they were in the *pph* "stay green" mutant control. Puzzlingly, however, the opposite trend was observed for *PPH*, as its expression increased even more in the atToc90 lines following dark treatment. In addition, as would be expected on the basis of the Genevestigator data presented in Fig. 1, the expression of *atTOC90* was increased in the dark-treated leaves. Expression of *atTOC90* was also elevated in the *pph* mutant, regardless of the growth conditions, further suggesting a link between atToc90 and senescence. Overall, these results indicate that the experimental conditions used were appropriate, and support the notion of a special role for atToc90 in relation to senescence.

4.2.4 Light stress treatment

In their natural environment, plants are exposed to fluctuating high light intensities and absorb high light energy. Excessive stimulation of the photosynthetic apparatus under high light stress leads to the production of ROS and to the photooxidative damage of the chloroplast (Szymanska and Kruk, 2010). In excess light-stressed plants, damaged chloroplasts initiate retrograde signalling to the nucleus (Pogson et al., 2008; Nott et al., 2004) to down-regulate the expression of photosynthetic genes and up-regulate stress defence genes to moderate oxidative stress (Rossel et al., 2007; Rossel et al., 2002; Koussevitzky et al., 2007). Thus, it can be seen that there is a degree of similarity between light stress response and senescence.

In an attempt to provide further evidence of a physiological role for atToc90, knockout and overexpressor plants were subjected to high light treatments. The plants were initially grown under standard conditions, as in the other experiments. Then, I started the light stress treatment when plants were 26 days old. Light stress treatment consisted of exposure of the plants to 2000 $\mu\text{mol}/\text{m}^2/\text{s}$ of white light for 4 hours daily, and it lasted for one week. At the end of each exposure period, the plants were returned to light of normal intensity light (100 $\mu\text{mol}/\text{m}^2/\text{s}$). The test plants were grown alongside identical plants that were not treated with high light, and these were used as controls for the comparative study. At the end of the light stress treatment (after 7 days), I photographed the plants and determined the chlorophyll levels of the treated and control plants (Fig. 6).

All high light-treated plants contained reduced chlorophyll levels by comparison with the control plants. In contrast with the wild-type, where the reduction in chlorophyll content was quite modest (~20%), the chlorophyll levels of the *toc90* knockout mutants and the overexpression line were considerable (~40%). This implies that the perturbation of atToc90 function reduces the capacity of the plant to deal with high light stress. It is interesting that, once again (see Section 2.3 above), I have observed that the knockout mutants and the overexpression line exhibit a similar phenotype under stress conditions, which as mentioned above is not completely intuitive. Perhaps proper atToc90 functions relies on there being an optimal concentration of the protein in the envelope. Although the phenotypic observations (see photographs in Fig. 6) were not as clear as the chlorophyll measurements, the experiment has been repeated more than two times, and the results were the same.

4.2.5 Osmotic stress treatment

Stress tolerance in plants has long been described as a coordinated expression of certain genes and the silencing of others (Hare et al., 1996). The expression of these genes is influenced by several environmental factors (Foolad, 2004). The data presented in Fig. 1 suggested that the *atTOC90* gene might have a role to play in response to osmotic stress. Thus, I conducted experiments to determine whether exogenous application of mannitol or polyethylene-glycol (PEG) has a different effect on the *toc90* knockout mutants and the 35S-*atTOC90* overexpression line. Seeds of the above-mentioned genotypes were sown in petri plates containing MS medium with different concentration of mannitol or PEG. The same genotypes were also grown on MS medium lacking mannitol or PEG, and these were used as controls. After stratification, the various petri plates were placed vertically in a growth cabinet for 14 days under standard conditions. After two weeks growth I measured the roots of both stressed and control plants and the results are shown in Fig. 7. The analysis revealed progressive inhibition of root growth, as well as of overall plant size, for all genotypes as concentration of the osmotic stressing agent (mannitol or PEG) was increased. However, there was not any significant difference between the wild type and the *atToc90* knockouts or the overexpressor. I measured root growth by analysing the photographs using SigmaScan Pro software, and the results confirmed my phenotypic observations. The experiment was repeated many times, and the results were found to be reproducible.

My conclusion from this experiment was that the *toc90* mutants and the *atToc90* overexpressor do not behave significantly differently from the wild-type under osmotic stress conditions. Thus, I was not able to detect a significant role for the *atToc90* protein in the plant's ability to deal with osmotic stress, despite what the Genevestigator data had suggested (Fig. 1). I also tried different approaches, such as the rescue of young seedlings from stress conditions to MS medium with no added mannitol or PEG, but all of the genotypes again responded in identical fashion (data not shown).

4.3 Discussion

The atToc90 protein is a member of the Toc159 family of chloroplast protein import receptors. While the other members of the family have well established roles in the import of photosynthesis related preproteins (atToc159) or housekeeping preproteins (atToc132 and atToc120) (Jarvis, 2008), the function of atToc90 remains ill defined. To shed light on the role of this protein, I identified and characterized atToc90 knockout mutants and an atToc90 overexpression line, but I could not detect any differences between them and the wild type under normal growth conditions.

Leaf senescence is a genetically regulated developmental programme during which many morphological, physiological and molecular events take place. One of the most obvious and important symptoms of leaf senescence is the visible yellowing, which correlates with the dismantling of chloroplasts, a reduction of chlorophyll content and photosynthetic activities, and the degradation of RNA and proteins. Analysis of publicly available microarray data had suggested a possible role for atToc90 in senescence. To investigate this possibility, I compared atToc90 knockout mutants and an atToc90 overexpression line with the wild type under various conditions that induce senescence or are somehow related to senescence. I investigated how the plants respond to exogenously applied stress factors, JA and MeJA, dark treatment, high light intensity stress, as well as osmosis stress (which also was suggested as a possible role for atToc90 by the microarray data).

Upon germination of the plants on medium containing JA, a severely senescent phenotype was observed in all genotypes, but unfortunately no difference could be observed between the wild type and the various mutants and overexpressor lines. It was possible that this treatment was too harsh, and so I then went on the use dark treatment to induce premature senescence in attached leaves. I confirmed that darkness can induce senescence in individually darkened leaves, and provided evidence that atToc90 plays a significant role in the process. Like those of the well studied *pph* (Schelbert et al., 2009) (which lacks an enzyme of chlorophyll breakdown called pheophytinase, responsible for dephytylating the Mg-free chlorophyll derivative, pheophytin), the leaves of the *toc90* mutants and the atToc90 overexpression line remained quite green following dark treatment, unlike the wild type leaves which turned yellow. This observation was supported by making chlorophyll measurements, while the analysis of gene expression changes in the leaves provided additional support for a possible special role of atToc90 during senescence.

Further work will be required to elucidate the nature of this putative role, but one possibility is that atToc90 is responsible for recognizing precursors of the many enzymes (*e.g.* chlorophyll breakdown enzymes, proteases and nucleases) that are induced during senescence and which presumably must be imported into the chloroplasts. In the future it will be interesting to conduct import assays with such preproteins using chloroplasts isolated from the *toc90* knockout mutants (Aronsson and Jarvis, 2002). During the course of this work I obtained antibodies from Professor John Gray (anti-LLS1 [lethal leaf spot1]) and Professor Stefan Hörtensteiner (anti-RCCR [red chlorophyll catabolite reductase]) (Gray et al., 2004; Pruzinska et al., 2005) to look at the protein levels in the *toc90* mutants by immunoblotting, but the efficiency of the antibodies was not good and I did not obtain clear results. This would be another interesting avenue of research to pursue. In the future it will be very interesting to perform these and other similar assay to investigate and confirm that atToc90 indeed plays a crucial role in leaf senescence.

While no evidence for a role of atToc90 in the plant's response to osmotic stress could be found, high light stress treatments did reveal a difference between the atToc90 mutants and wild type. In this case, however, rather than attenuating the chlorophyll reduction seen in the wild type (which is what we observed following dark treatment, as discussed above), the reduction of chlorophyll was even more pronounced in the mutants than in the wild type on this occasion. Again, further work will be required to elucidate the basis for this difference, but it is possible that the atToc90 receptor is required for the efficient import into chloroplasts of proteins that enable them to deal with the ROS and other stresses that are created under high light conditions (*e.g.* enzymes responsible for the biosynthesis of a range of antioxidant compounds) (Szymanska and Kruk, 2010).

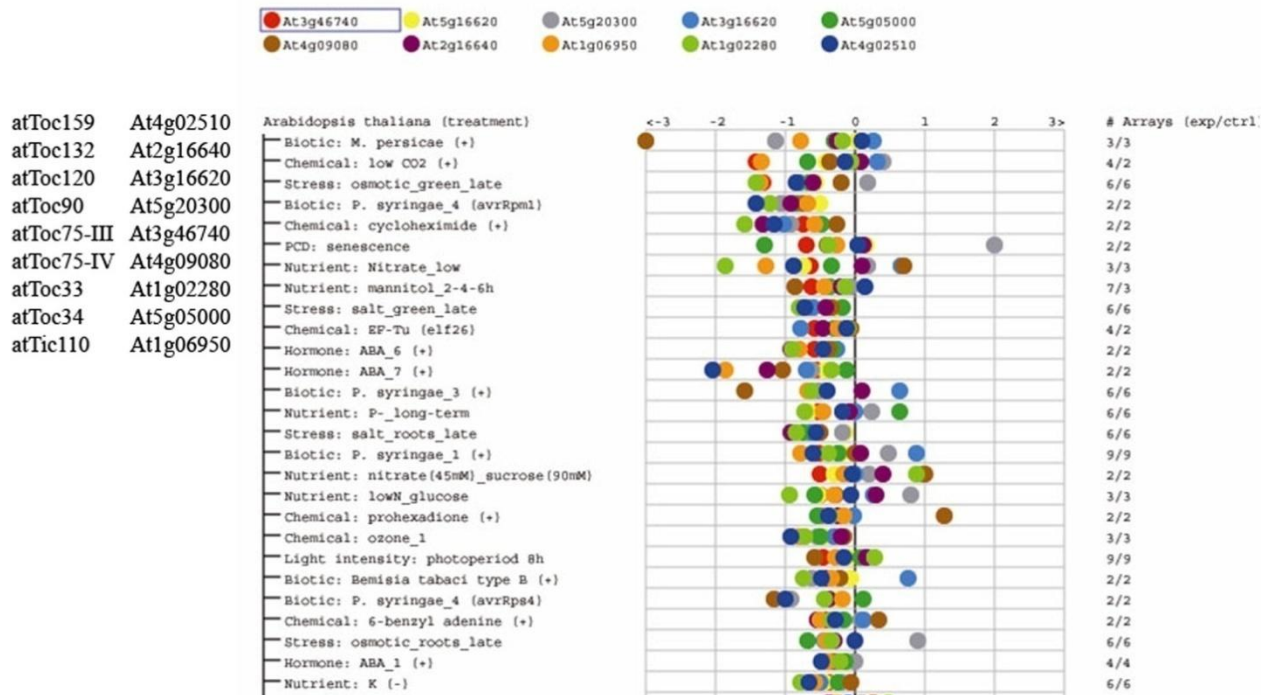


Figure 4.1: Analysis of the expression of major TOC and TIC genes using Geneinvestigator.

The AGI numbers of the TOC/TIC genes are provided at the left side of the figure, while colour coding of the data points is indicated at the top. The results show that the *atTOC90* gene (gray spots) is significantly up-regulated in response to senescence, osmotic stress, and nutrient deficiency. Experimental details about the relevant stresses were suggesting high expression of *atTOC90* when leaves were treated under dark conditions and in osmotic stress. For the osmotic stress were suggested treatments with high percentage of NaCl, polyethyleneglycol (PEG), and mannitol.

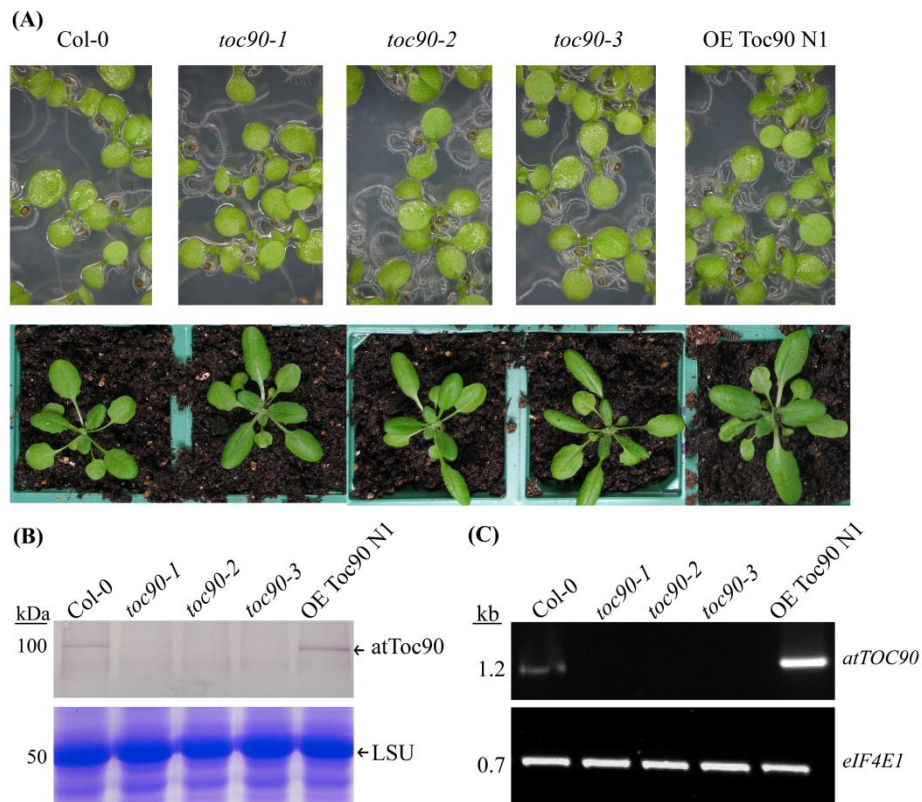


Figure 4.2: Visible phenotypes and molecular characterization of the three *atToc90* knockout mutants and a 35S-*atTOC90* transgenic line.

Wild-type Col-0, the three *atToc90* knockout mutants, and a 35S-*atTOC90* overexpression line (line N1) were grown side by side *in vitro*. (A) Typical 8 day old plants are shown; the images were taken using a Zeiss dissecting microscope. After 14 days growth *in vitro*, the plants were transferred to soil. The figure shows typical 22 day old plants on soil. The three knockout mutants and the overexpression line exhibit the same green phenotype as the wild type. (B) Analysis of protein expression; for immunoblotting, total protein was extracted from the same genotypes (grown for 14 days under similar conditions), and 20 μg samples were loaded per lane. After blotting to nitrocellulose, analysis used a specific antibody raised against an *atToc90* peptide. Samples of the three *atToc90* knockout mutants, wild-type and the *atToc90* overexpressor were separated by SDS-PAGE followed by Coomassie Brilliant Blue staining and used as loading control. (C) Analysis of mRNA in the different genotypes. For the RT-PCR, 5 μg samples of total RNA isolated from seedlings grown *in vitro* for 10 days in the light were each used to prepare a 20 μl reverse transcription reaction. Then, 1 μl of this was used as template in a 20 μl PCR reaction, of which half was loaded. PCR amplifications were performed using 23 cycles for *eIF4E1* and 32 cycles for *atTOC90*.

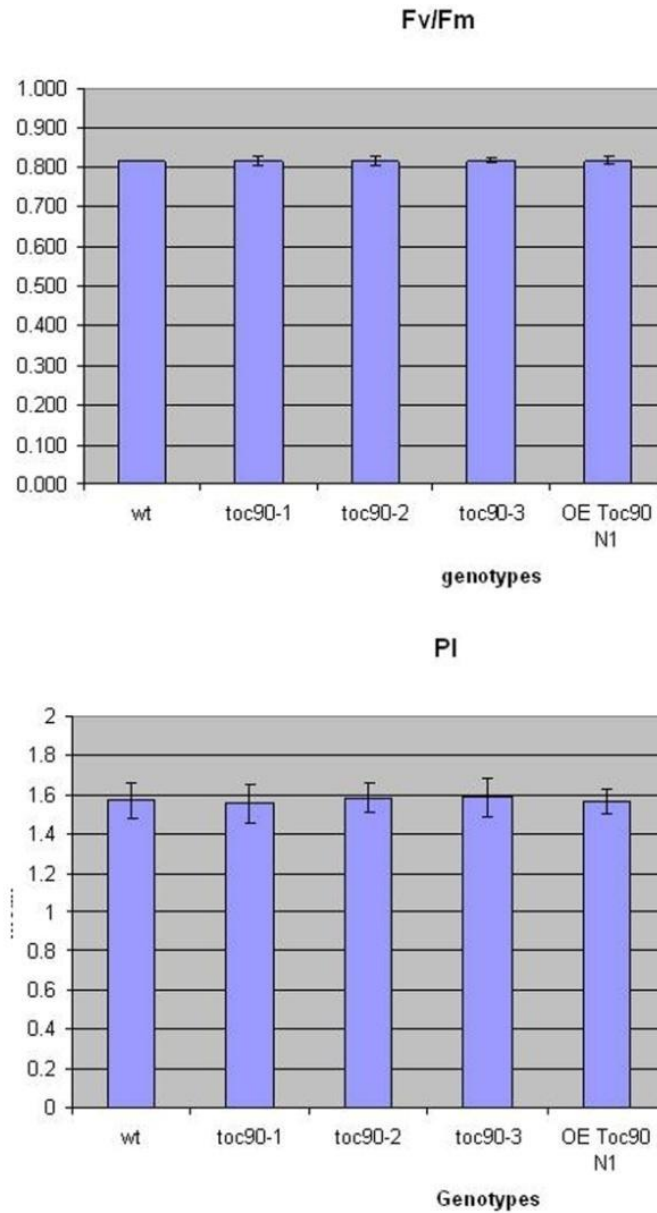


Figure 4.3: Analysis of photosynthetic parameters in the *atToc90* knockout and overexpressor lines.

Wild-type Col-0, two *atToc90* knockout mutants, and the 35S-*atTOC90* overexpression line N1 were grown side by side *in vitro* for 14 days, and then transferred to soil. After a total of 22 days growth, chlorophyll fluorescence was measured using a continuous excitation chlorophyll fluorimeter (Handy PEA, Hansatech). The parameters shown are F_v/F_m (A) and photosynthetic performance index, PI (B). The values shown are means derived from 2 individual measurements. Error bars indicate standard deviation.

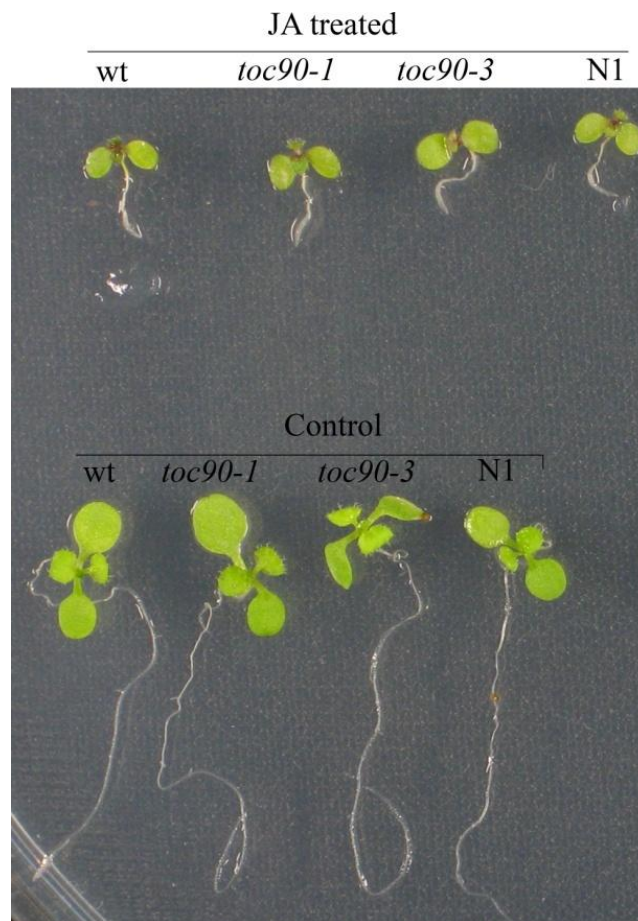


Figure 4.4: Treatment of the *atToc90* knockout and overexpressor lines with jasmonic acid.

Wild-type Col-0, two *atToc90* knockout mutants, and the *35S-atTOC90* overexpression line N1 were grown side by side in petri plates for 14 days under standard conditions, either on MS medium containing 30 μ M jasmonic acid (JA) or on standard MS medium. At the end of the growth period, representative plants from the control and JA-treatment plates were transferred to fresh plates for photography.

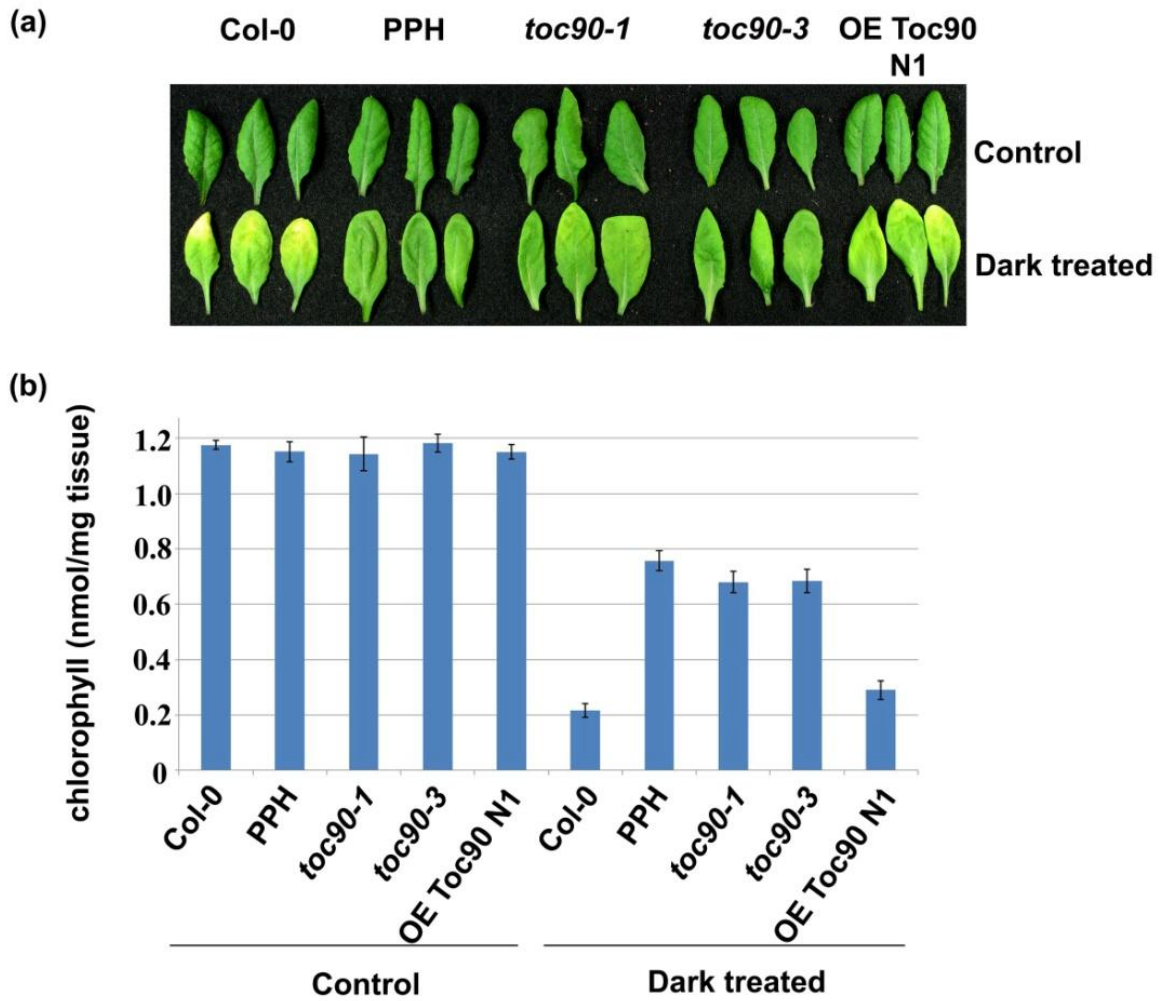


Figure 4.5: Induction of senescence in individual attached leaves of the *atToc90* knockout and overexpressor lines by dark treatment.

(a) Typical dark-treated and untreated control leaves of wild-type Col-0, the *pph* “stay green” mutant, two *atToc90* knockout mutants, and the 35S-*atTOC90* overexpression line N1 were detached from the plants and photographed. Individual rosette leaves were covered with aluminium foil, and kept in the dark for 4 days. (b) Chlorophyll levels in the dark-treated and control leaves were measured using a SPAD-502 meter (Konica-Minolta), and the values were converted to units of absolute chlorophyll content using a verified calibration curve (Qihua et al., 2011) The values shown are means derived from 3 individual measurements. Error bars indicate standard deviation.

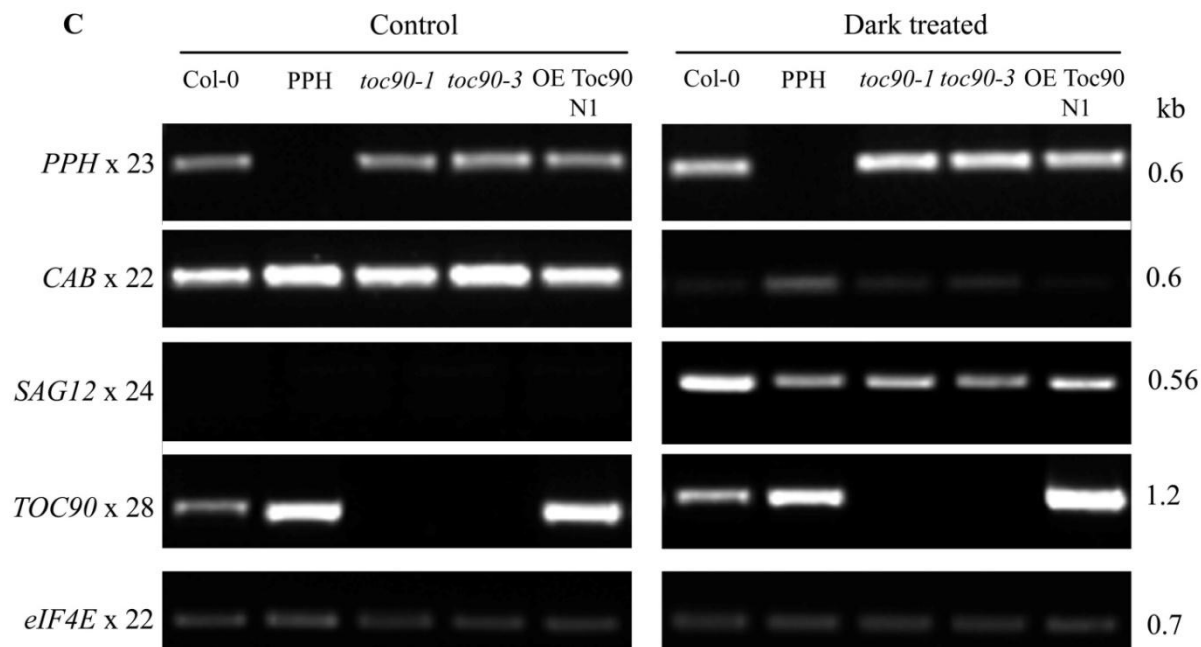


Figure 4.6: Analysis of mRNA from senesced individual attached leaves of the *atToc90* knockout and overexpressor line after dark treatment.

For the RT-PCR, 5 μ g samples of total RNA isolated from the senescent leaves (Fig. 4.5A) of each genotype to prepare a 20 μ l reverse transcription reaction. Then, 1 μ l of this was used as template in a 20 μ l PCR reaction, of which half was loaded. PCR amplifications were performed using the cycles indicated at the left of the figure. The expected products are indicated in the right part of the figure.

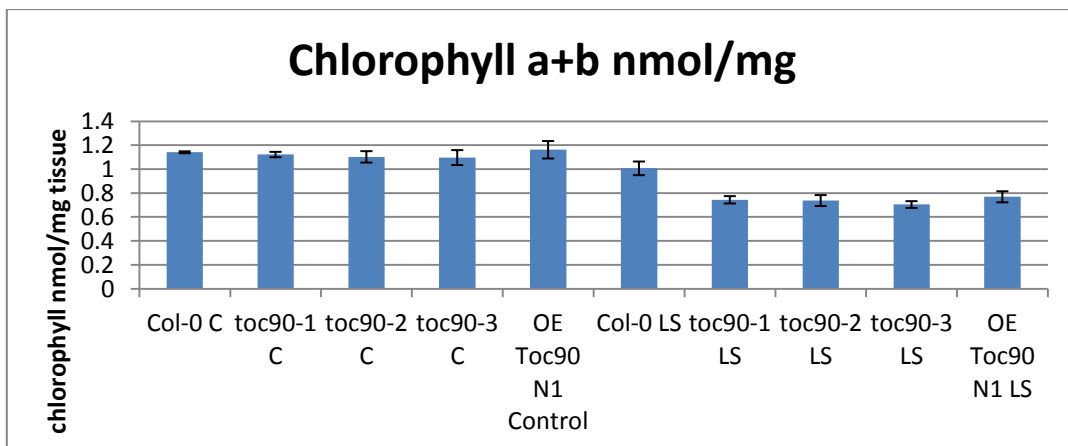
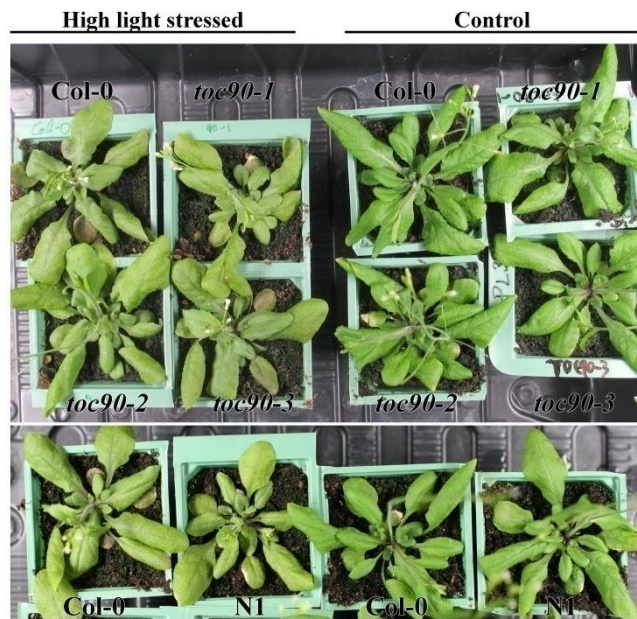


Figure 4.7: Treatment of the *atToc90* knockout and overexpressor lines with high light stress.

Wild-type Col-0, two *atToc90* knockout mutants, and the *35S-atTOC90* overexpression line N1 were grown side by side *in vitro* for 14 days, and then transferred to soil. After a total of 26 days growth under standard conditions ($100 \mu\text{mol}/\text{m}^2/\text{s}$; 16 hours light / 8 hours dark), light stress treatment commenced. Light stress treatment consisted of exposure of the plants to $2000 \mu\text{mol}/\text{m}^2/\text{s}$ white light for 4 hours daily, and it lasted for a week. At the end of the treatment, chlorophyll contents were measured using a SPAD-502 meter (Konica-Minolta), and the values were converted to units of absolute chlorophyll content using a verified calibration curve. The values shown are means derived from 3 individual measurements. Error bars indicate standard deviation.

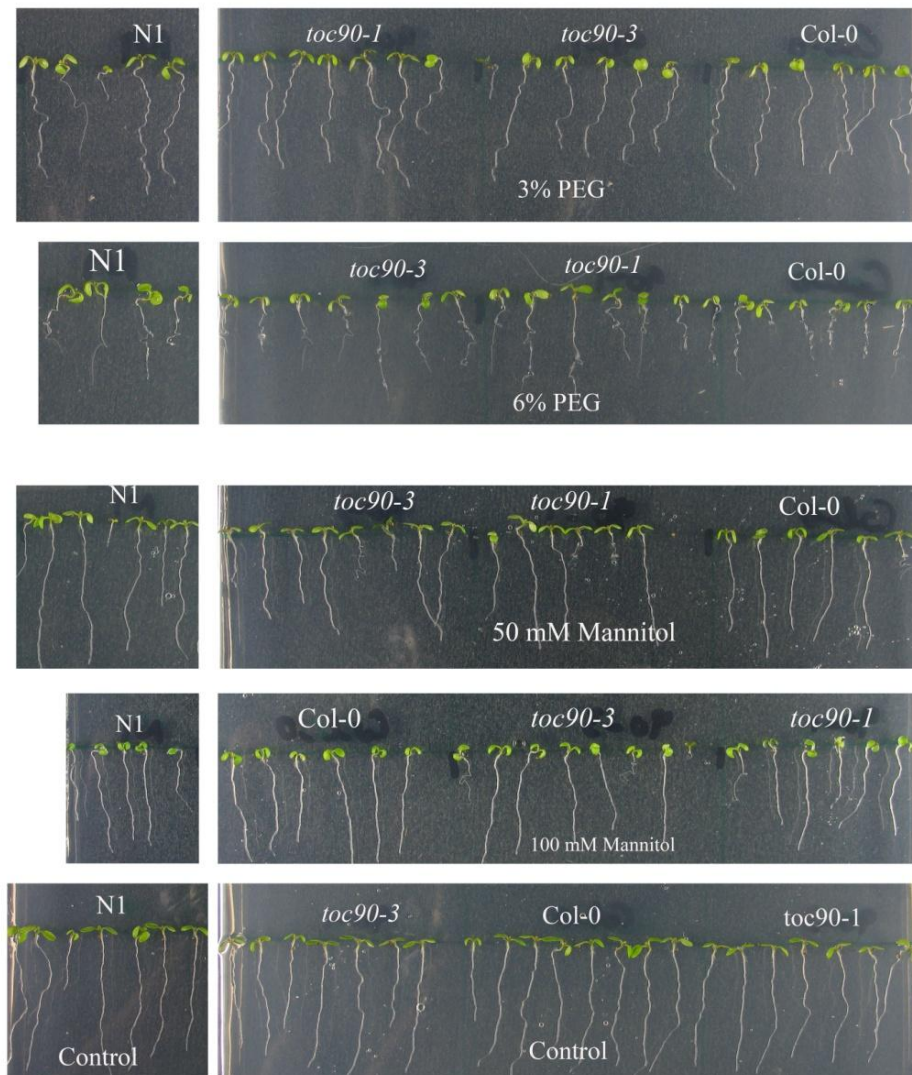


Figure 4.8: Treatment of the atToc90 knockout and overexpressor lines under osmotic stress conditions.

Wild-type Col-0, two atToc90 knockout mutants, and the 35S-*atTOC90* overexpression line N1 were grown side by side on vertically oriented petri plates for 14 days under standard conditions, either on standard MS medium or on MS medium containing different concentrations of mannitol (50 Mm and 100mM) or PEG (3% and 6%). At the end of the growth period, representative plants from the control and treatment plates were photographed. As a measure of growth under the different conditions, root length was quantified by analysis of multiple independent images using SigmaScan Pro software (SPSS Inc.). The values shown are means derived from approximately 8 individual measurements. Error bars indicate standard deviation.

Chapter 5

Materials and Methods

5.1 *Arabidopsis thaliana* plants growth conditions and manipulation

5.1.1 *In vitro* culture

Arabidopsis thaliana seeds to be germinated *in vitro* were surface-sterilised by shaking in: 70% (v/v) ethanol, 0.05% (v/v) Triton X-100 for 5 minutes; and then in 100% ethanol for 10 minutes. Sterilised seeds were dried on filter papers in a laminar flow hood and sown on Murashige and Skoog (MS) medium containing 0.5% (w/v) sucrose, 1×MS salts, 0.05% (w/v) N-Morpholino-ethanesulphonic acid monohydrate (MES), pH 5.7, 0.6% (w/v) agar (Murashige and Skoog, 1962).

When appropriate, the following antibiotics were used: kanamycin (50 µg/ml), gentamicin (110 µg/ml), phosphinotricin (15 µg/ml), spectinomycin (110µg/ml), hygromycin (15 µg/ml), cefataxin (50 µg/ml), and sulphodizine (4.5 µg/ml).

Plates were sealed with micropore tape (3M) which prevents contamination but allows air exchange. Seed dormancy was broken by stratification in the dark at 4°C between 2 and 4 days. Seedlings were grown at 20°C under long day conditions (16 h light, 8 h dark) in Percival growth cabinets (Percival Scientific) in which light intensity was approximately 120 µmol photon/m²/s of white light. Plants grown on selective MS medium were generally scored for resistance or sensitivity to the antibiotic after 7-10 days growth. When plants germinated *in vitro* were required to set seed, they were transplanted to soil after 12-14 days and allowed to grow to maturity in the greenhouse.

5.1.2 Soil culture

Arabidopsis thaliana plants were grown in soil composed of Levingtons F2 Seed and Modular Compost, silver sand and vermiculite (medium 2.0-5.0 mm, Sinclair). Generally, plants were grown at 20°C in a controlled temperature glasshouse under long day conditions. Humidity was also regulated.

Arabidopsis plants were generally grown in 24 cell compartment trays. Plants were kept covered with propagator lids for up to 5 days to maintain high levels of humidity. All plants were watered regularly from the base. *Arabidopsis* seeds were harvested by rupturing the siliques of dry plants over a sheet of paper, and the seed was sieved to remove dry plant material. All newly harvested seeds were placed in Eppendorf tubes 1.5 ml.

5.1.3 Cross-pollination of *Arabidopsis* plants

Arabidopsis thaliana plants to be used as parents in genetic crosses were germinated *in vitro*, transferred to soil as described above, and allowed to bolt. Best results were obtained using young, primary inflorescences, although secondary inflorescences were also employed. Crosses were carried out using fine point forceps. Between 3 and 4 flower buds were crossed per female parent, and 2 to 3 identical crosses were made (using distinct but genotypically identical plants) for each genetic experiment. Flower buds selected for crossing were the most mature of those whose stigmas were still fully enclosed within the sepals. The apical meristem and all unwanted buds were carefully removed from the inflorescence. Sepals and petals were also removed in order to gain access to the stamens. Each bud was then emasculated by the removal of the stamens. Emasculated flowers were cross-pollinated using at least two young open flowers from the required male parent. Inflorescences carrying the F1 seed were harvested directly, shortly after the siliques had begun to dehisce.

5.1.4 Chlorophyll measurements

To extract the chlorophyll from plant tissue, samples were placed in 1 ml of dimethylformamide (DMF) in 1.5 ml microcentrifuge tubes (Porra *et al.*, 1989), and mixed overnight on a shaker at 4°C. Due to the light sensitive nature of the chlorophyll, after collection of the plant tissue and immersion in DMF, the microcentrifuge tubes were concealed in a dark environment using aluminium foil. Approximately 15 mg of fresh plant tissue was incubated in 1 ml DMF. Less DMF and more plant tissue was used for plants containing less chlorophyll.

After chlorophyll extraction, measurements of the amount of chlorophyll contained within the DMF were made by photometry. The absorbance of the samples was measured at wavelengths 646.8 nm, 663.8 nm, and 750 nm. The accuracy of the measurements was maintained by running blanks (just DMF) as samples and comparing them to zero values. The amount of chlorophyll was calculated according to the following equations and total chlorophyll (nmol) was calculated per mg fresh weight tissue;

$$\text{Chlorophyll } \alpha = [13.43 \times (A_{663.8} - A_{750})] - [3.47 \times (A_{646.8} - A_{750})]$$

$$\text{Chlorophyll } b = [22.9 \times (A_{646.8} - A_{750})] - [5.38 \times (A_{663.8} - A_{750})]$$

5.2. Molecular biology techniques

5.2.1 Bacterial work

5.2.1.1 Growing bacteria

Escherichia coli (DH5 α) was cultured in liquid Luria Bertani broth (LB), (10 g/l yeast extract, 10 g/l peptone, 5 g/l NaCl, pH 7), in a shaking incubator or on LB-agar plates in a bacterial growth incubator, at 37°C. When applicable, 100 μ g/ml ampicillin or 50 μ g/ml kanamycin was applied.

5.2.1.2. *Escherichia coli* transformation.

Aliquots of chemically competent cells (Bioline) in 1.5 ml microcentrifuge tubes were thawed on ice for 10 minutes. Plasmid DNA (<20 μ l) was added to 50 μ l of cells, mixed gently, and incubated on ice for 15 min. Cells were subjected to heat shock at 42°C for 30 s, followed by 2 min incubation on ice. LB (0.8 ml) was added to each sample prior rescue of the cells by gentle shaking at 37°C for 1 h. An aliquot (100 μ l) of the transformed cells was spread on an LB plate containing the appropriate antibiotic. The remaining cells were pelleted by centrifugation at 5,000 \times g for 2 minutes and most of the supernatant was discarded. The cells were resuspended in the remaining solution (~100 μ l) and also spread on a selective LB-agar plate.

5.2.1.3. *Agrobacterium* transformation.

An *Agrobacterium* strain (GV3101) containing an appropriate plasmid DNA (~1-5 ng) was grown in 5 ml of LB medium containing Rifampicin (50 mg/ml) overnight at 28°C with gentle shaking at 200 rpm. A 2 ml aliquot of the overnight culture was added to 50 ml of LB medium in a 250 ml flask. The culture was grown at 28°C with vigorous shaking at 250 rpm until the OD₆₀₀ reached 0.5-1.0. The cell suspension was chilled on ice and centrifuged at 3,000 rpm for 10 min at 4°C. The supernatant was discarded and the cells were resuspended in 1 ml of 20 mM ice cold CaCl₂ solution. A 100 μ l aliquot of the cells was quickly dispensed into pre-chilled microcentrifuge tubes, frozen in liquid nitrogen (N₂), and stored at -80°C.

5.2.1.4 Transformation of *Arabidopsis thaliana* using the floral dip method

Transgenic plants were generated using an *Agrobacterium*-mediated transformation protocol based on the floral dip method (Clough and Bent, 1998). Approximately 30 *Arabidopsis* plants were grown in 10 cm² pots in a greenhouse or in a growth cabinet. The primary inflorescences were cut at the base when they reached ~5 cm in height to promote generation of secondary inflorescences. When young secondary inflorescences reached ~5-10 cm and had a few open flowers, the plants were dipped in solution containing *Agrobacterium*.

Five millilitre LB cultures of *Agrobacterium* were set up from fresh streak plates two days prior to dipping and grown to saturation. The day before dipping, large overnight cultures (250 ml of culture for four pots) were inoculated in conical flasks by diluting the saturated culture 1:100 in fresh LB medium containing the appropriate antibiotic selection. The following day, when the overnight cultures reached an OD₂₆₀=1.8 (~14 hours after inoculation), the cells were collected by centrifugation at 5,000 rpm for 10 min in a Sorvall rotor (SLA 1500), at room temperature. The cells were gently resuspended in 3 volumes of infiltration medium; 2.2 g/l MS salts, 0.5% (w/v) sucrose and Silwet (50-100 µl/l) (Lehle Leeds).

The above-ground parts of *Arabidopsis* plants were submerged, upside down, in the bacterial solution for 10 min. Transformation occurs in the ovules of the developing flowers after the female and male gametophyte cell lineages form, but before the embryo develops a single cell (Clough and Bent, 1998). After 10 minutes, excess liquid was drained on tissue and the pots were loosely wrapped in plastic film to retain humidity, allowing the motile bacteria more time in which to enter the buds. Two days after dipping the plastic film was removed and the plants were allowed to set seed. The seed was bulk harvested and the first generation was screened for transformants (T1). Screening for T1 seeds was performed on MS medium supplemented with cefotaxime (200 µg/ml), an antimicrobial agent that inhibits the growth of *Agrobacterium*.

5.2.1.5. Plasmid preparation from bacterial growth overnight cultures

Aliquots (5 ml) of LB containing the appropriate antibiotic, in glass 25 ml universal tubes were inoculated with single bacterial colonies (*E. coli* or *A. tumefaciens*) and growth was allowed to proceed overnight at 37°C and 28°C respectively, in a shaking incubator. All subsequent steps were carried out in an 1.5 ml microcentrifuge tubes. Cells (between 1.5 and

3.0 ml overnight culture) were pelleted by centrifugation at 5,000 rpm for 2 minutes in a bench-top microcentrifuge, and then resuspended in 100 µl solution I (50 mM D-glucose, 25 mM Tris-HCl, pH 8.0, 10 mM EDTA). Incubation at room temperature for 5 min was followed by the addition of 200 µl solution II (0.2 M NaOH, 1 % (w/v) SDS; freshly prepared); samples were mixed by inversion. Incubation on ice was allowed to proceed for 5 minutes prior to the addition of 150 µl solution III (3 M potassium, 5 M acetate, pH 4.8; solution III was prepared by adding 11.5 ml glacial acetic acid and 28.5 ml distilled water to 60 ml 5 M potassium acetate). Samples were mixed by inversion, incubated on ice for 5 minutes and then centrifuged for 10 minutes in a bench-top microcentrifuge. Supernatants were transferred to fresh tubes containing 1 ml ice cold ethanol. Samples were mixed by inversion and allowed to incubate on ice for 5 min. Plasmid DNA was collected by centrifugation at 13,200 rpm for 5 min, washed with 70% (v/v) ethanol, dried briefly in a vacuum desiccator, and then resuspended in 40 µl TER (10 mM Tris, 1 mM EDTA, 10 µg/ml RNase).

5.2.1.6 Preparation of high quality plasmid DNA

High quality plasmid DNA was prepared from *E. coli* cultures using the Qiagen QIAprep Spin Miniprep Kit, following the guidelines provided by the manufacturer.

5.2.1.7 Quantification of DNA and RNA

Spectrophotometry was used to calculate the approximate concentrations of double stranded DNA and RNA solutions. A sample of DNA or RNA solution was diluted either 1:100 or 1:200 in distilled water (diH₂O). The spectrophotometer was calibrated using diH₂O in a thoroughly rinsed cuvette. Measurements were made for each sample at wavelengths 260 nm and 280 nm. Concentrations were calculated using the equations:

OD unit 260 nm = 50 ng/µl of DNA

OD unit 260 nm = 40 ng/µl of RNA

5.2.2 Nucleic acid and protein preparation

5.2.2.1 Plant DNA extraction

A quick method was used to obtain DNA from plant tissue for PCR. Approximately 0.15g of plant tissue, previously collected in liquid N₂ and stored at -80°C, was supplemented with

liquid N₂ and ground to a fine powder in a 1.5 ml microcentrifuge tube using a small pestle of the appropriate size. The powdered tissue was suspended in 0.5 ml EB [200 mM Tris, pH 7.5, 250 mM NaCl, 25 mM EDTA, 0.5% (w/v) SDS] and vortexed briefly to disperse large clumps. Each sample was carried individually until this point and then stored on ice until all other samples were ready to proceed to the next stage. Samples were centrifuged for 5 min at 4°C, and subsequently the supernatants were transferred to a fresh 1.5 ml microcentrifuge tube containing 0.5 ml isopropanol (IPA). After 30-60 min incubation at -20°C, the samples were centrifuged for 10 min at 4°C. The supernatants were discarded and the pellets washed with 1 ml ice cold 70% (w/v) ethanol. The pellets were dried for approximately 15 min on the bench and dissolved in 50 µl sterile diH₂O. After overnight dissolution at 4°C, the samples were centrifuged for 2 min and the supernatant transferred to a fresh tube.

5.2.2.2 Plant RNA extraction

RNA was extracted from ~0.15 g plant tissue samples that had previously been collected in liquid N₂ and stored at -80°C. For RNA extraction the Plant Mini Kit 50 (Qiagen) was used following the guidelines of the manufacturer.

After the amount of plant material was determined (~100 mg), the tissue was placed in liquid nitrogen and grinded thoroughly with a mortar. When the liquid nitrogen was evaporated, 450 µl of buffer RLT (Qiagen) containing β-mercaptoethanol (β-ME) was added and then the samples were vortexed vigorously. A short period of 1-3 minutes at 56°C helped the tissue to be disrupted. The lysate was transferred to a QIAshredder spin column which was placed in a 2 ml collection tube, provided by the manufacturer, and centrifuged for 2 min at full speed. At the end of this time the supernatant was transferred to a new microcentrifuge tube without the pellet to be disturbed. 0.5 ml of ethanol was added to the cleared lysate and was mixed immediately by pipetting. The sample was transferred, including any possible precipitation that may have formed, to an RNeasy spin column which was also placed in a 2 ml collection tube, provided by the manufacturer, and centrifuged for 15 sec at >10,000 rpm in a bench microcentrifuge. When the flow-through was discarded, 700 µl of buffer RW1 (Qiagen) was added to the RNeasy spin column. Another quick centrifugation step was applied as previously for 15 seconds at >10,000 rpm. The flow-through was discarded again and 500 µl of buffer RPE (Qiagen) was added to the RNeasy spin column. After centrifugation for 15 sec at >10,000 rpm the flow-through was discarded and this step was repeated one more time. Finally, the RNeasy spin column was placed in a new 2 ml collection tube, and 30 µl RNase-

free (Qiagen) water was added directly to the spin column. After centrifugation for 1 min at >10,000 rpm, the RNeasy spin column was discarded and the tube was placed carefully on ice, ready for RNA measurement.

After RNA extraction, there followed a DNaseI treatment using DNA free kit (Ambion). For a 30 µl of reaction, in a 1.5 ml microcentrifuge tube was added; 5 µl DNase buffer, 1 µl rDNase (Ambion), and 24 µl RNA sample. After careful mixing the tube has been placed in water bath at 37°C for 30 min. Then was added 5.5 µl of DNase inactivation reagent and the microcentrifuge tube was incubated for 2 min at RT with occasional mixing. Finally, after centrifugation at 3,000 rpm for 1 min, the supernatant was transferred to a new 1.5 ml microcentrifuge tube.

.5.2.3 Polymerase chain reaction

The polymerase chain reaction (PCR) is the *in vitro* enzymatic, amplification of a specific DNA sequence using oligonucleotide primers, DNA polymerase, nucleotides and a DNA template. The two primers flank the region of interest and anneal opposing strands. It is a cyclic reaction sequence that involves three steps: template denaturation, primer annealing to the template, and 5' to 3' extension of the primers by the DNA polymerase. Each event occurs at a specific temperature.

Conditions and reagent concentrations used for the PCR amplification of DNA varied depending on the primers, the nature of the template, and the size of the expected product. Primers were included in reactions at concentrations of 1 µM each. Each 2'-Deoxyribonucleoside 5'-triphosphate (dNTP) was included in reactions at concentrations of 0.4 mM. *Arabidopsis* genomic DNA templates were added at concentrations of 10-15 ng per 50 µl reaction. The different DNA polymerases were used following the guidelines provided by the manufacturers. Amplifications were usually carried out for 30-40 cycles as follows: i) denaturation for 30 s at 92°C; ii) primer annealing for 30 s at temperatures between 55°C and 60°C, depending on the primers; and iii) elongation at 68°C or 72°C for 1-3 min depending upon the length of the expected product. Amplifications were generally followed by a 5 min extension step at 72°C, and finally denaturation followed at 10°C.

5.2.4 Reverse transcriptase-PCR

First strand cDNA, complementary to the RNA previously extracted, was synthesised in a two part reaction. A 12 μ l reaction, containing 5 μ g of total RNA, 5 μ l of 100 μ M CDS-5' primer, 1 μ l of 10 mM dNTPs, and sterile diH₂O, was incubated at 65°C for 5 minutes; this led to denaturation of RNA secondary structures. The reaction mixture was then incubated on ice for 2 minutes. This was followed by the addition of 4 μ l of 5 \times buffer, 2 μ l of 0.1 mM dithiothreitol (DTT), and 1 μ l of 40 u/ μ l RNase inhibitor (Promega). After a 2 minute incubation at 42°C, 1 μ l of Superscript II Reverse Transcriptase (Invitrogen) was added. This 20 μ l reaction was incubated at 42°C in a water bath for an additional 60 minutes, followed by a reverse transcriptase inactivation step at 70°C for 15 minutes. One microlitre of cDNA synthesis reaction was then used as template in each 25 μ l PCR reaction.

5.2.5. Total protein extraction from *Arabidopsis thaliana* plants.

Total protein was prepared for sodium dodecyl sulphate polyacrylamide gel electrophoresis (SDS-PAGE) from ~0.15 g plant tissue that had been collected in liquid N₂ and stored at -80°C. Fresh PEB (1 ml) was prepared from a stock (100 mM Tris-HCl, pH 6.8, 10 % (v/v) glycerol, 0.5 % (w/v) SDS, 0.1 % (v/v) Triton X-100, 5 mM ethylene-diamin-tetraacetic-acid (EDTA) by the addition of 10 mM DTT and 5 μ l protease inhibitors (Sigma) and kept on ice. Care was taken to keep the samples cold during the primary grinding step to prevent proteolysis. Tissue samples were supplemented with liquid N₂ and ground to a fine powder in a 1.5 ml microcentrifuge tube using a pestle of the appropriate size. After addition of 200 μ l of cold protein extraction buffer (PEB), samples were thoroughly homogenized by further grinding on ice. Each sample was taken individually until this point and stored on ice until all other samples were ready to proceed to the next stage. Samples were centrifuged in a bench centrifuge at 13,800 rpm for 10 min at 4°C to remove insoluble material and finally 150 μ l of supernatant was transferred to a fresh tube.

5.2.6 Quantification of protein.

The Bio-Rad protein assay was used to estimate the protein concentration of samples prepared as in 2.2.5. One microlitre of each protein sample was diluted in diH₂O to a final volume of 0.8 ml. At the same time, 0, 1, 2, 4, 6, 8, and 10 μ g quantification standards were prepared by adding the required volume a 1 mg/ml stock solution of bovine serum albumin (BSA), 1 μ l of PEB and diH₂O to a final volume of 0.8 ml. The assay was conducted by

adding 0.2 ml of dye reagent concentrate (Bio-Rad) to each quantification sample and mixing by inversion. After 5 minutes at room temperature, the samples were transferred to 1 ml plastic cuvettes and the absorbance of the samples at 595 nm was determined by spectrophotometry. The 0 μ g quantification standard was used as a blank, and the absorbance of all the other samples was determined sequentially in the same order as the dye reagent was added. If the assay was successful, a near-linear standard curve could be plotted using the values obtained from the BSA standards. The formula defining the curve was derived and this formula was used to determine the concentration of each protein sample.

5.2.7 TAP tagging purification

For a small-scale TAP tagging experiment, the ideal starting amount of chloroplast protein was ~ 2 mg (~ 40×10^6 chloroplasts). A chloroplast pellet of 2 mg was resuspended in 1 ml of 1 \times SB (1 M Tris-HCl, pH 8.0; 3 M NaCl; 0.5 M EDTA plus 1% DDM detergent and protease inhibitors), and then transferred into a 2 ml microcentrifuge tube containing another 1 ml of 1 \times SB. Then the sample was mixed thoroughly. Chloroplasts were left to solubilise by rotating in a rotate wheel for 30 min in 4°C.

While the chloroplasts were solubilising, the Micro Bio-Spin chromatography columns (Bio-Rad) were prepared as follows. First, 160 μ l of IgG beads (homemade, Pfanner lab protocol) was added into the column and centrifuged for 1 min at 4°C at 900 rpm in a pre-cooled bench microcentrifuge; the columns were placed in a 2 ml microcentrifuge tube for each centrifugation step, and these tubes were discarded afterwards.

The IgG beads were washed as follows: 2 times with TBS (10 mM Tris-HCl pH 7.5 and 150 mM NaCl), 3 times with acetate buffer (1.43 ml glacial acetic acid added to 48.57 ml of diH₂O; pH 3.4 adjusted with 0.5 M NH₄Ac), 1 time with TBS, 1 time with acetate buffer and finally 4 times with 2 \times SB. To ensure that the pH has reached the level between 7.5 and 8, pH test paper (Fisher) was used at the end of the procedure. At the end, the foot (end) of the column was closed.

The microcentrifuge tubes were removed from the cold room, and a centrifugation step was performed for 20 min, at 14,000 rpm in a cold microcentrifuge (4°C). After centrifugation, a small pellet was visible, and the supernatant was transferred into a fresh 2 ml tube. From there, an aliquot of 100 μ l sample was taken (TS sample = total solubilised lysate; equivalent to 0.05% of starting material).

From the 1.9 ml left into the 2 ml tube, 400 μ l of sample was carefully pipetted back into the column to resuspend the beads and transfer them into the 2 ml Eppendorf tube. The tip was kept because it was necessary to repeat this step again and wash well the tip from the remained beads which were stuck in it. After 5 min the beads were settled down into the 2 ml Eppendorf tube, and the step was repeated by pipetting this time \sim 450 μ l of sample into the column to transfer any remaining beads back into the 2 ml Eppendorf tube. The tube was sealed and left rotating for 2.5 h in a 4°C cold room.

At the end of the rotation step, the 2 ml Eppendorf tube was centrifuged at 2,500 rpm for 2 min in a cold microcentrifuge. 100 μ l of sample (**PBS** sample = post binding lysate; equivalent to 0.05% of starting material) was removed for later analysis. Most of the remaining supernatant was discarded leaving a final volume of 700 μ l sample. Care was taken while discarding the supernatant for the beads not be disturbed.

The beads were resuspended in the remaining 700 μ l supernatant and transferred back to the column (always with a cut tip). The column foot was left open and the undesired sample drained by gravity. It was necessary to add 500 μ l of fresh wash buffer (+0.3% detergent and protease inhibitors) back to the 2 ml tube, to pipette the remaining beads and transfer them into the column and following the same procedure as previously, it was let to drained by gravity.

The column was placed in a 2 ml eppendorf tube for the washes step. Then the column was transferred in a cold microcentrifuge 4°C and washed 7 times with 500 μ l of wash buffer (0.3% detergent and protease inhibitors), at 900 rpm for 1 minute.

The foot of the column was closed and was added 207 μ l of wash buffer plus 0.3% detergent and protease inhibitors was added together with 3 μ l of TEV (His-TEV) and 90 μ l of 0.5 M EDTA (final conc. 150 mM). The lid of the column was closed well; a Whatman sealing film was used to avoid any loss of the sample, and then an overnight incubation was conducted in the rotating wheel at 4°C.

The next day, Ni-NTA (Qiagen) beads was prepared with 60 μ l of slurry placed in a microcentrifuge tube. After centrifugation of 1 min at 10,000 rpm in a bench microcentrifuge, the supernatant was discarded, and 150 μ l of wash buffer was added (no protease inhibitors). This step was repeated again, the supernatant was discarded, and 40 μ l of wash buffer was

added to the beads. Finally, all of the equilibrated Ni-NTA slurry (prepared as described above) was placed into the TEV column and the rotation was continued for another 1 hour.

When both the foot and the lid of the column had been opened a centrifuge was performed in a cold microcentrifuge at 1,500 rpm for 2 minutes. The sample of the flow-through was collected and kept on ice (~340 µl sample TEV n1).

The foot and the lid of the column were closed. Then to the column was added: 150 µl of wash buffer plus 0.3% detergent but no protease inhibitors, and 150 µl of 0.5 M EDTA (final conc. 250 mM). The column was placed back to the rotate wheel and was left rotating for 1 hour at 4°C.

At the end of the previous step, the foot and the lid of column were opened, and the column was centrifuged again at 1,500 rpm in a cold microcentrifuge (4°C). The sample was collected (~300 µl TEV n2) and both elutions (sample n1 and sample n2) after the TEV incubation were added together in one tube, a total of 600 µl in a 1.5 ml microcentrifuge tube and kept on ice (TEV elution final sample).

To improve the results in the Silver stained gels Protein A Sepharose 4 Fast Flow (GE Healthcare) beads was prepared. More specifically, IgG from most species binds Protein A Sepharose at neutral pH. The binding capacity of Protein A Sepharose depends on the source of the particular immunoglobulin. For the preparation of the Protein A Sepharose 4 Fast Flow beads, 25 mg Protein A Sepharose was added in 80 µl distilled water. It was left to swell well in room temperature for 1 min. Afterwards the beads were washed with 1 ml of distilled water, centrifuged at 1,500 rpm in room temperature in a microcentrifuge, and the supernatant was discarded. The same step was repeated one more time and at the end the supernatant was discarded again. Into the microcentrifuge tube contains the Protein A Sepharose beads 1 ml of wash buffer (no detergent or protease inhibitors) was added. The microcentrifugation step was repeated, the supernatant was discarded, and finally 100 µl of wash buffer (no detergent or protease inhibitors) it was added.

All of the 100 µl of Protease A Sepharose beads was added into the TEV final elution sample and then left to rotate in the cold room at 4°C for 1 h. After centrifugation at 3,000 rpm in a pre-cooled microcentrifuge at 4°C of the TEV final elution sample and without disturbing the beads, the supernatant was transferred slowly into the Microcon centrifugal filter device (Millipore) microcentrifuge tube to proceed with the concentration of the sample(s),

according to the manufacturer's guidelines. The concentrated sample was transferred to a 1.5 ml Eppendorf tube and 2× loading buffer (same amount as the TEV sample) was added (**TEV** sample).

Into the column was added 100 µl of 1× SDS loading buffer; elution was performed by spinning down in a cold microcentrifuge for 1 min at 1,200 rpm. The eluted sample was collected and 5 µl of 1 M DTT was added (**SDS** sample, 0.05% final conc.).

Before placing the samples to boil, 2× loading buffer was added to the TS and PBS samples. After that, the samples were boiled in water bath for 5 min. Afterwards they were cooled on the bench at room temperature for 2 min, and then the samples were ready to proceed to SDS-PAGE and Westerns blotting.

5.3 Electrophoresis techniques

5.3.1 Agarose gels

Agarose gels were employed to resolve DNA and RNA fragments, to determine the concentration of DNA fragments, using Lambda standards, and to assess the quality of RNA samples. Loading buffer [10× = 0.5% (w/v) Orange G, 50% (v/v) glycerol] was added to the samples to a final concentration of 1× prior to loading and electrophoresis. Gels generally contained between 0.8 and 1.5% (w/v) agarose (depending upon the sizes of fragments to be resolved) and 15 µg/ml SYBR Safe DNA gel stain (Invitrogen) in 0.5×TBE (45 mM Tris, 45 mM boric acid, 1 mM EDTA). Agarose was melted and the solution was cooled to ~50°C before SYBR Safe DNA was added. For general analyses, small 10 cm × 15 cm gels (Wide Mini-Sub Cell; Bio-Rad) were employed. Molecular mass markers were used to determine the size of the DNA fragments. Approximately 0.05-0.1 µg of 1 kb + DNA ladder (Invitrogen) was added per mm width of V/cm. Gels were run in electrophoresis tanks (Bio-Rad) containing 0.5 x TBE usually at ~ 10 V/cm.

5.3.2 SDS-PAGE and Western blotting

Separation and identification of protein samples was carried out using sodium dodecyl sulphate-polyacrylamide gel electrophoresis (SDS-PAGE). Gels were cast and run in a Protean III apparatus (Bio-Rad). Glass plates were cleaned with industrial methylated spirits (IMS) prior to assembly. Protein gels consisted of two phases, the top stacking gel [0.5 M Tris-HCl pH 6.8; 0.4% (w/v) SDS] that concentrates the protein to a fine point, and the lower

separating gel [1.5 M Tris-HCl, pH 8.8; 0.4% (w/v) SDS] that separates the proteins according to their size (Laemmli, 1970). When the gel casting apparatus was assembled 4.5 ml of resolving gel [10 ml of 10% gel: 4 ml diH₂O, 2.5 ml of 1.5 M Tris-HCl pH 8.8; 0.1 ml of 10% SDS; 3.3 ml of 30% (w/v) acrylamide; 0.1 ml of 10% ammonium persulphate (APS); 4 μ l *N,N,N,N'*- Tetramethylethylenediamine (TEMED)] was immediately poured and overlaid with 1 ml diH₂O. After solidification of the separating gel, the overlying solution was discarded and 1.5 ml of stacking gel [2.1 ml diH₂O; 0.38 ml of 1 M Tris-HCl, pH 6.8; 30 μ l of 10% SDS; 0.5 ml of 30% (w/v) acrylamide; 30 μ l of 10% APS; 3 μ l TEMED] overlaid. Immediately an appropriate comb was inserted into the stacking gel. The gel was then allowed to set for at least 15 min at room temperature. Protein samples were prepared in 2 \times sample buffer [60 mM Tris-HCl, pH 6.8; 25% (v/v) glycerol; 2% (w/v) SDS; 14 mM 2-mercaptoethanol; 0.1% (w/v) bromophenol blue (Laemmli, 1970) and heated to 100°C for 3 min before loading into the wells of the gel. Gels were usually run at 150V until the dye front reached the bottom of the gel (~1 h). The following antibodies were either made in Jarvis laboratory or were bought; Dr Sybille Kubis made the atToc90, Dr Jocelyn Bédard (atToc33, atTic40, and atTic110), Feijie Wu (atToc75-III, atToc120) and Flores-Perez (atToc132) for preparing antigens for immunization. The atToc34 antibody was bought from Agrisera (www.antibodies-online.com/agrisera).

5.3.3 Coomassie stained gels

Gels were stained for at least 30 minutes with Coomassie stain [1 g Coomassie Brilliant Blue 250 (Fischer); 450 ml methanol; 450 ml diH₂O; and 100 ml glacial acetic acid], and subsequently destained (100 ml methanol; 100 ml glacial acetic acid; and 800 ml H₂O) for several hours or overnight, until the bands were clearly visible, and the surrounding gel was clear.

5.3.4 Silver stain gels

After electrophoresis the gel was removed from the cassette and placed into a tray containing 150 ml of fixing solution [150 ml of 50% (v/v) ethanol; and 5% (v/v) glacial acetic acid]. The gel was soaked in the appropriate solution for 2 h at room temperature or better overnight to improve sensitivity of the staining and avoid any background. Fixation was to restrict protein movement from the gel matrix and remove interfering ions and detergent from the gel. The next day the fixative solution was discarded and the gel was washed twice with diH₂O for 10 min, while the sensitizing solution was made fresh together with the silver nitrate reaction

solution. After the washes with diH₂O, the gel was immersed in 150 ml of sensitizing solution for 45 sec and then washed again briefly with diH₂O before being submerged in 150 ml of silver staining solution and shaken for 1h to allow the silver ions to bind to the proteins. Special care was taken not to pour the staining solution directly to the gel as this may result in unequal background. Just before the staining step was completed the developing solution was made fresh. The gel was rinsed briefly with diH₂O to remove the excess of unbound silver ions. The fresh developing solution was poured (150 ml) in continuously shaking. If the developing solution was turned yellow, then the solution was discarded and a new fresh volume was added. The reaction has been stopped when the desired intensity of the bands was reached. 150 ml of stopping solution was poured into the tray directly onto the gel, and then gently was shaken for 5-10 min. Moist gels can be kept in 12% acetic acid at 4°C for a week time.

5.4 Chloroplast isolation

For one chloroplast isolation (Kubis et al., 2008) (one genotype) were necessary 25-40 petri plates of 14-day-old plants, each containing ~150-200 seedlings were necessary. Plants were grown in a plant tissue culture chamber (Model CU-36L5, Percival Scientific) set at 20°C, providing 100 µmol/m²/s white light with a long day cycle (16-h-light/8-h-dark).

Before the plates were removed from the Percival, a Percoll gradient was prepared for use. To make 26 ml of final volume was added: 13 ml of Percoll (Amersham Biosciences), 13 ml of 2×CIB (0.3 M sorbitol; 5 mM MgCl₂; 5 mM EDTA; 10 mM EGTA; 20 mM HEPES-KOH pH 8.0; and 10 mM NaHCO₃), and 2 mg glutathione. The components were mixed in a 30 ml Nalgene tube and were centrifuged in a SS-34 rotor, Sorvall for 30 min at 19,000 rpm with acceleration set to 7 and de-acceleration set to 2.

Meanwhile, the plates were taken out of the Percival and the seedlings were removed from the medium by gently scraping them with a gloved wet finger, avoiding carry over of medium (medium interferes with the isolation). The removed seedlings were placed into 100 ml of CIB in one 1 lt beaker and kept always on ice. During homogenization, a total of ~250 ml of 1×CIB was used per genotype; this was used in 10 consecutive rounds of homogenization, each one using 20 ml 1×CIB. The 20 ml of 1×CIB were placed each time under the rotor of polytron (PT 10-35), and homogenized for 1-3 seconds, with the speed set to 4.

The homogenized material was filtered through two layers of Miracloth (Calbiochem). The Miracloth filter was gently squeezed and the desired filtered homogenized material was released in another 1 lt beaker also placed on ice. This setp was repeated until the plant material was all homogenized and filtered. Then the desired material was transferred into a 250 ml Nalgene tube and centrifuged in a SLA-1500 rotor, Sorvall, at 3,000 rpm for 5 min at 4°C, with both acceleration and de-accelaration set at 7.

Most of the supernatant was poured off and the pellet that had formed was resuspended in about 500 µl supernatant by rotating the tube gently on ice. A cut 1 ml Gilson pipette tip was used to transfer the homogenized material very slowly into the preformed Percoll gradient taking care not to disturb the gradient. To separate the intact chloroplasts from broken chloroplasts and any other debris, the Percoll gradient with the homogenized material was centrifuged at 7,000 rpm for 10 minutes with acceleration set to 7 and de-acceleration set to 2, in a HB-6 Sorvall RC6 centrifuge rotor. After centrifugation, the tube was removed carefully and placed on ice. The lower green band in the gradient contained intact chloroplasts and the upper band contained the broken chloroplasts. The broken chloroplasts were removed by pipetting and then discarded while the intact chloroplasts were removed using a cut 1 ml Gilson pipette tip and placed into a clean pre-cooled 30 ml Nalgene tube. About 25 ml of 1×HMS buffer (50 mM HEPES-NaOH pH 8.0; 3 mM MgSO₂; and 0.3 M sorbitol) was added to the intact chloroplasts and mixed thoroughly by inverting the tube carefully 2-3 times to wash off the Percoll. The chloroplasts were centrifuged at 2,000 rpm for 5 min at 4°C in the same rotor as previously but with the acceleration and de-acceleration set to 7. After centrifugation, the supernatant was gently poured off and then the formed pellet of chloroplast was resuspended in 150-250 µl of fresh HMS by rotating the tube gently on ice.

5.5 Establishing the yield of the intact chloroplasts

The following procedure was used to assess the amount of the intact chloroplasts. First, 5 µl of isolated chloroplasts were added to 495 µl of 1×HMS buffer in a 1.5 ml microcentrifuge tube to obtain 1:100 dilution. The tube was mixed gently. To determine chloroplast concentration was used a hemocytometer, since it was originally designed to perform blood cell types. The device was used to determine the number of chloroplasts per unit volume of a suspension was called counting chamber. The counting chamber was prepared by cleaning the surface carefully with lens paper. After placing a cover glass on the top of the counting

chamber of the hemocytometer, approximately ~80 μl of the diluted suspension was pipetted onto the counting chamber. The number of chloroplasts was counted in ten different $1/400 \text{ mm}^2$ with the help of a phase contrast microscope with a $16\times$ objectives.

The concentration (number of chloroplasts per ml), was calculated as follows: n (the average number of chloroplasts per $1/400 \text{ mm}^2$) $\times 25$ (the total number of squares in the grid) $\times 100$ (the dilution factor employed) $\times 10^4$ (scaling factor needed to express the data per ml. After calculating the amount of the intact chloroplasts, the chloroplasts were ready for further analysis.

Chapter 6

General Discussion

6.1 Genetic analyses

The atToc90 protein is the fourth member of the Toc159 family of chloroplast protein import receptors. While the other family members have well established roles in the import of photosynthesis related preproteins (atToc159) or non-photosynthetic housekeeping preproteins (atToc132 and atToc120), the function of atToc90 is poorly defined (Jarvis, 2008). The detailed genetic studies of Kubis et al. (2004) and Ivanova et al. (2004) did not detect a significant role for the atToc90 isoform of the *Arabidopsis* family of Toc159 protein import receptors. In the work of Kubis et al. (2004), *toc90* knockout mutants were indistinguishable from the wild-type in relation to phenotypic appearance, growth and development, and chlorophyll accumulation. In addition, no obvious effect of the *toc90* mutation in the *toc132*, *toc120* and *toc159* backgrounds was reported, and so it was concluded that atToc90 does not share significant functional redundancy with these components. However, Hiltbrunner et al. (2004) reported that atToc90 interacts with core TOC components atToc75 and atToc33 physically, and with atToc159 (which is the main isoform of the Toc159 family, involved in the import of photosynthetic proteins) genetically. More recently, Infanger et al. (2011) suggested the ability of atToc90 to support the import of atToc159 client proteins. To shed light on the role of this protein, I also characterized atToc90 knockout mutants as well as an atToc90 overexpression line, but, consistent with the previous reports, I could not detect any differences between them and the wild type under normal growth conditions.

In an attempt to understand the functional relationship between atToc90 and other components of the TOC complex, I identified and studied a large number of *toc90* double and triple mutants. Overall, most of the double *toc90* mutants that I analyzed led to confirmation of previous findings (*i.e.* no genetic interaction was detected). However, my experiments revealed clear evidence of functional redundancy between atToc90 and atToc159, the main import receptor for photosynthetic preproteins, as a *toc90 toc159* double knockout mutant was even sicker than the albino *toc159 (ppi2)* single mutant. This result was consistent with the observations of Hiltbrunner et al. (2004). Moreover, I confirmed and extended this result by studying the triple mutant, *toc90 toc159 toc120*, which showed an even more severe albino phenotype, indicating functional overlap between atToc90, atToc159 and atToc120. An additional significant observation to come out of my genetic studies was that *toc90 toc132 toc120* triple mutants are smaller and paler than *toc132 toc120* double mutants (which are chlorotic due to a defect in the import of housekeeping preproteins). This result, together with

the other results, suggested that atToc90 might play a minor or supporting role in both of the major import pathways, working alongside atToc159 in relation to photosynthetic protein import, and alongside atToc132/atToc120 in relation to non-photosynthetic, housekeeping protein import.

The results of my studies on the double and triple *toc90* mutants were supported by data from a complementation study using an overexpression vector based on the full length *atTOC90* cDNA (H4C12), which was first reported by Hiltbrunner et al. (2004). Kubis et al. (2004) reported that the overexpression of atToc90 was inactive in their *toc159* complementation studies, but their construct was based on a slightly truncated *atTOC90* cDNA clone such that the encoded protein lacked 14 N-terminal residues (as the N-terminal region of atToc159 is not essential for the protein's function, this very small deletion was not considered to be important at the time). In my studies, there was clear evidence of partial complementation of *toc159* by full length 35S-*atTOC90*, but not at all by the truncated construct of Kubis et al. (2004). In my work, the expression of *atTOC90* was at essentially the same level in the lines of Kubis et al. (2004) and in the new lines with the full length construct, so differences in expression could not account for the different results. A likely explanation for the different results is the importance of the usage of the full length *atTOC90* cDNA, and the missing residues in the protein encoded by the shorter construct. An alternative explanation was offered by Infanger et al. (2011), who suggested that the success in their *toc159* complementation studies was due to the fact that they used the Wassilewskija ecotype instead of the Columbia ecotype that Kubis et al. (2004) used. Infanger et al. (2011) also showed that the overexpression of *atTOC90* can partially complement the albino *toc159* knockout and partially restore photoautotrophic growth, in agreement with the results that I have presented here.

It is surprising that my complementation studies using full length 35S-*atTOC90* in the *toc132 toc120* background did not produce a positive result (*i.e.* no partial complementation was found), as the analysis of the *toc90 toc132 toc120* triple mutant clearly suggested a functional relationship between the components. A possible explanation for this is that the phenotypic additivity seen in the *toc90 toc132 toc120* triple mutant was not due to redundancy between the relevant proteins as such, but rather due to the disruption of more than one import pathways (*i.e.* for photosynthetic and non-photosynthetic preproteins) leading to a deficiency in a much broader range of chloroplast proteins. This discrepancy between the double/triple

mutant results and the complementation results illustrates how caution is needed when interpreting the results of genetic experiments.

Hiltbrunner et al. (2004) showed that synthetic atToc90 was bound to chloroplast membranes under protein import assay conditions and that a small portion of the protein specifically co-immunoprecipitated with atToc75-III, suggesting that atToc90 functions as a component of the core TOC complex. My analysis of the respective double mutant, *toc90 toc75-III-3*, did not reveal any different phenotypes from the single mutant, *toc75-III-3*, which is a hypomorphic allele and has a pale phenotype (Stanga et al., 2009). It is possible that a genetic interaction would be observed if a stronger *atTOC75-III* mutant allele was used, but no such allele is available at present, as the complete knockout of this gene causes embryo lethality (Baldwin et al., 2005).

The *toc90 toc33* double mutant was phenotypically the same as in the single *toc33 (ppi1)* mutant, suggesting no significant functional interaction. However, when I analyzed the *toc90 toc33 toc34* triple mutant, I observed a significant effect of the *toc90* mutation, in that the triple mutant was sicker than the *toc33 toc34* double mutant. This result suggested functional redundancy between atToc90 and atToc33/atToc34. Like the other genetic results, these findings suggest that atToc90 cooperates with components that mediate the import of the most highly-abundant photosynthetic preproteins (*i.e.* atToc159 and atToc33) as well as with proteins like atToc132, atToc120 and atToc34, which have specificity for low abundance non-photosynthetic preproteins. However, when I compared the *toc90 toc159 toc33* triple mutant with the *toc159 toc33* double mutant, or the *toc90 toc159 toc34* triple mutant with the *toc159 toc34* double mutant, I could detect no phenotypic differences (data not shown). Further work will be required in order to explain these unexpected genetic results.

Overall, my genetic results demonstrated that all four Toc159 homologues in *Arabidopsis*, including atToc90, play an important role in chloroplast biogenesis. In contrast with other Toc159 family members, a distinct function for the atToc90 protein remains unclear. In fact, some of my genetic data suggest that atToc90 acts in both main import pathways. Ivanova et al. (2004) showed that the four *Arabidopsis* Toc159 homologues differ in the length of their N-terminal acidic domains, and recent evidence from Inoue et al. (2010) suggested the involvement of this domain in the specialization and specificity of the different receptor isoforms. The lack of an A-domain in atToc90 may allow it to act with less specificity in more than one import pathway.

6.2 Purification and analysis of TOC complexes

To biochemically investigate the role of atToc90, I conducted experiments to purify TOC complexes from isolated *Arabidopsis* chloroplasts using the tandem affinity purification (TAP) method. By performing immunoblot analyses on the purified complexes, I showed that atToc159, atToc75-III and atToc90 could be co-purified with TAP-tagged atToc33 (atToc33-NTAPi). These findings were also confirmed by mass spectrometric analysis of the purified fractions. Because atToc33 was not proposed previously to interact with atToc132 and atToc120 (Ivanova et al., 2004) (instead, atToc34 was reported to interact with these two proteins), it is interesting that my mass spectrometry results showed that both atToc132 and atToc120 were co-purified with atToc33-NTAPi. I also purified TOC complexes using TAP-tagged atToc34 (atToc34-NTAPi), and immunoblot analysis of these revealed the presence of atToc132, atToc120, atToc75-III and atToc90. Mass spectrometric analysis confirmed these findings. The presence of the first three proteins (atToc132, atToc120 and atToc75-III) is as expected, as these are the reported partners of atToc34. Most interestingly from the point of view of my project was the finding that atToc90 is also in these complexes. Finally, it was noteworthy that atToc159 was unexpectedly detected in the atToc34 complexes by mass spectrometry.

My results indicate that the substrate specific import pathways model that was presented in Chapter 1 may not be completely accurate. One possible explanation for my unexpected observations (*i.e.* that atToc132 and atToc120 are in atToc33 complexes, and that atToc159 is in atToc34 complexes) is as follows: While the different receptor isoforms may indeed have distinct client specificities, and cooperate preferentially with each other as has been published, they perhaps are nonetheless associated together in large mixed TOC complexes. Another possible explanation is that the use of the strong, constitutive 35S promoter to drive expression of the TAP fusions in my work led to association of the fusion proteins with TOC components that they would not normally associate with in the wild type. Having said that, great care was taken when generating the TAP lines to select only those transformants that express the fusions at levels close to the native level. Indeed, my own data (not shown) suggested that the fusion proteins are not strongly overexpressed.

Interestingly, in both the atToc33- and atToc34-containing TOC complexes, I could detect small quantities of the Tic110 and Tic40 components of the inner membrane TIC complex. After repeating the experiment several times with similar results, I concluded this result to be

reliable and not due to contamination. However, my mass spectrometric results did not identify either TIC protein (or any of the stromal chaperones that they are known to associate with) in the purified complexes; Tic110 is known to recruit the chaperones Hsp93 and Cpn60 with the help of Tic40 (Kovacheva et al., 2007; Kessler and Schnell, 2006), and so one might therefore expect them to be present in purified complexes containing those TIC proteins. Nonetheless, my immunoblot results do suggest that I was able to purify at least some TOC-TIC supercomplexes, as was reported previously (Nielsen, 1997; Kouranov et al., 1998).

My mass spectrometry analyses also revealed the presence of a small amount of actin in the eluted atToc33-NTAPi complexes, but not in the atToc34-NTAPi complexes. Unfortunately, I was unable to confirm these mass spectrometric results by immunoblotting because I did not have access to a suitable actin antibody. Nonetheless, this result is probably reliable as a link between TOC proteins and actin was reported previously. The results of Jouhet and Gray (2009) showed that there is an interaction between Toc159 and actin. Also, many other TOC-TIC components were identified after co-immunoprecipitation with actin antibodies. The significance of this is uncertain but it may play a role in directing preproteins to the chloroplast surface from the cytosol.

From the point of view of my project, by far the most significant result from this TAP work was the observation that atToc90 is associated with both atToc33- and atToc34-containing complexes. This is consistent with the genetic data presented in Chapter 2, and discussed earlier, which suggested a role for atToc90 in photosynthetic and non-photosynthetic protein import pathways. Comparing the immunoblot results suggested that atToc90 may be relatively more abundant in the atToc33 complexes. However, as my immunoblots were conducted on different occasions, the results are not strictly comparable and so this conclusion is not reliable. Thus, it will be interesting to repeat the experiments simultaneously in the future, to rigorously assess whether atToc90 is more abundant in atToc33 complexes than in atToc34 complexes. If confirmed, this would be consistent with the proposal that atToc90 is primarily (if not exclusively) involved in the import of photosynthetic preproteins (Hiltbrunner et al., 2004; Infanger et al., 2010).

6.3 Physiological analysis of the atToc90 knockout and overexpression lines

Analysis of publicly available microarray data using the Genevestigator tool online (Zimmerman et al., 2004) suggested that atToc90 may have a role in senescence. To investigate this possibility, I compared atToc90 knockout mutants and an atToc90 overexpression line with the wild type, under various conditions that are related to senescence. Germinating plants on medium containing jasmonic acid produced a severely senescent phenotype in all genotypes, but unfortunately no difference could be observed between the wild type and the various mutant and overexpressor lines. This treatment may have been too harsh, and so thereafter I used dark treatment to induce premature senescence in attached leaves. These studies were more successful, providing clear evidence that atToc90 plays a role in senescence. In contrast with wild type leaves which turned yellow, the leaves of the *toc90* mutants and of the atToc90 overexpression line remained green after dark treatment, like those of the well studied *psh* “stay green” mutant, which lacks an enzyme of chlorophyll breakdown called pheophytinase (Schelbert et al., 2009). Moreover, my analyses of gene expression changes in the dark treated leaves provided further support for the proposed role of atToc90 during senescence.

The exact nature of this putative role of atToc90 will need to be examined in future studies, but one possibility is that it is responsible for importing into chloroplasts the many enzymes (*e.g.* chlorophyll breakdown enzymes, proteases and nucleases) that are induced during senescence. It will be interesting to conduct import assays with such preproteins using chloroplasts isolated from *toc90* mutants (Aronsson and Jarvis, 2002). Another interesting approach to take would be assess the levels of senescence-related chloroplast proteins in the *toc90* mutants, to see if their levels are reduced. This could be done using quantitative proteomics or immunoblotting, for example, as was done during the characterisation of the atToc33 knockout mutant, *ppi1* (Kubis et al., 2003). Both of these approaches would be interesting avenues of research to pursue, alongside the above mentioned import experiments.

High light stress treatments also revealed a significant difference between the atToc90 mutants and wild type. However, in contrast with the dark induced senescence work discussed above (where an attenuation of the chlorophyll reduction seen in the wild type was observed in the *toc90* mutants), here, the reduction of chlorophyll was even more pronounced in the mutants than in the wild type. More work is needed to shed light on the basis for this difference, but it is conceivable that atToc90 is necessary for the efficient chloroplast import

of proteins that enable the organelle to deal with reactive oxygen species and other stresses that are created under high light conditions (for example, enzymes responsible for the biosynthesis of antioxidant compounds) (Szymanska and Kruk, 2010).

Taking into account the all the above finding I had come with a modification of the working model proposed by Jarvis, 2008 (see Introduction), where atToc90 interacts with both atToc33 and atToc34 for the targeting of photosynthetic and non-photosynthetic preproteins, and has a possible role in high light stress

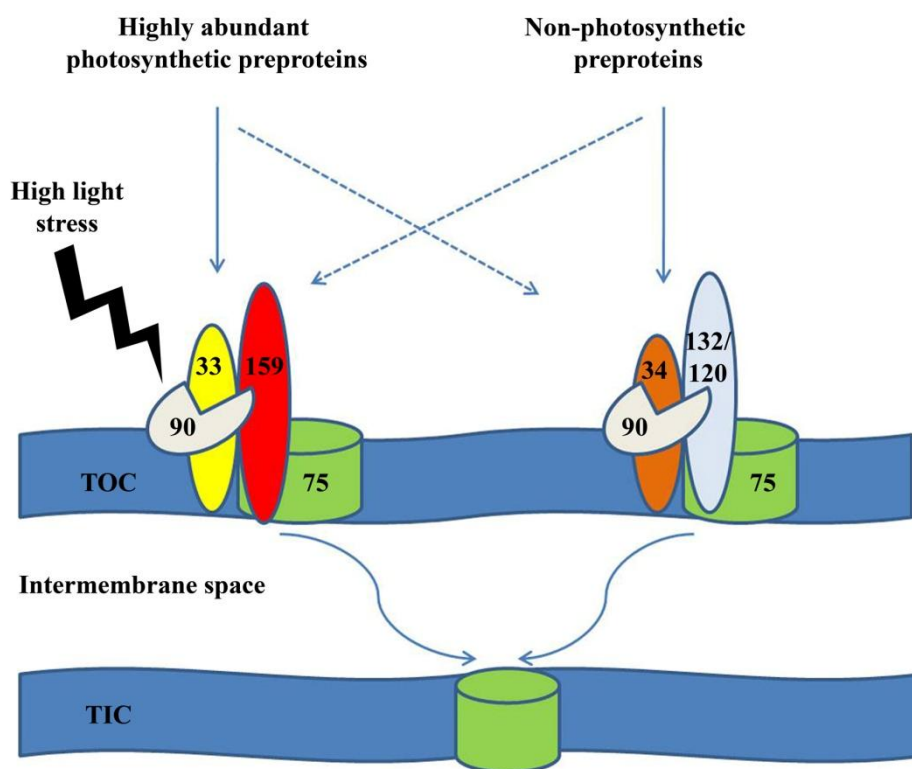


Figure 2: Model of substrate-specific protein import pathways. After careful analysis of my results, atToc90 associated with both atToc33 and atToc159, as well as with atToc34 and atToc132 and/or atToc120. Furthermore, was suggested from the results an involvement of atToc90 in leaf senescence which is due to light stress treatments

References

- Abeliovich, H., and Klionsky, D.J. (2001). Autophagy in yeast: mechanistic insights and physiological function. *Microbiol. Mol. Biol. Rev.* 65, 463-479.
- Agne, B., and Kessler, F. (2009). Protein transport in organelles: The Toc complex way of preprotein import. *FEBS J.* 276, 1156-1165.
- Akita, M., Nielsen, E., and Keegstra, K. (1997). Identification of protein transport complexes in the chloroplastic envelope membranes via chemical cross-linking. *J. Cell Biol.* 136, 983-994.
- Aronsson, H., and Jarvis, P. (2002). A simple method for isolating import-competent *Arabidopsis* chloroplasts. *FEBS Lett.* 529, 215-220.
- Aronsson, H., Boij, P., Patel, R., Wardle, A., Töpel, M., and Jarvis, P. (2007). Toc64/OEP64 is not essential for the efficient import of proteins into chloroplasts in *Arabidopsis thaliana*. *Plant J.* 52, 53-68.
- Aubry, S., Mani, J., and Hortensteiner, S. (2008). Stay-green protein, defective in Mendel's green cotyledon mutant, acts independent and upstream of pheophorbide a oxygenase in the chlorophyll catabolic pathway. *Plant Mol. Biol.* 67, 243-256.
- Baldwin, A., Wardle, A., Patel, R., Dudley, P., Park, S.K., Twell, D., Inoue, K., and Jarvis, P. (2005). A molecular-genetic study of the *Arabidopsis* Toc75 gene family. *Plant Physiol.* 138, 715-733.
- Baldwin, A.J., and Inoue, K. (2006). The most C-terminal tri-glycine segment within the polyglycine stretch of the pea Toc75 transit peptide plays a critical role for targeting the protein to the chloroplast outer envelope membrane. *FEBS J.* 273, 1547-1555.
- Balsera, M., Soll, J., and Bolter, B. (2009a). Protein import machineries in endosymbiotic organelles. *Cell Mol Life Sci* 66, 1903-1923.
- Balsera, M., Goetze, T.A., Kovacs-Bogdan, E., Schurmann, P., Wagner, R., Buchanan, B.B., Soll, J., and Bolter, B. (2009b). Characterization of Tic110, a channel-forming protein at the inner envelope membrane of chloroplasts, unveils a response to Ca(2+) and a stromal regulatory disulfide bridge. *J. Biol. Chem.* 284, 2603-2616.
- Bartsch, S., Monnet, J., Selbach, K., Quigley, F., Gray, J., von Wettstein, D., Reinbothe, S., and Reinbothe, C. (2008). Three thioredoxin targets in the inner envelope membrane of chloroplasts function in protein import and chlorophyll metabolism. *Proc. Natl. Acad. Sci. U S A* 105, 4933-4938.
- Bassham, D.C., Laporte, M., Marty, F., Moriyasu, Y., Ohsumi, Y., Olsen, L.J., and Yoshimoto, K. (2006). Autophagy in development and stress responses of plants. *Autophagy* 2, 2-11.
- Bauer, J., Chen, K., Hiltbunner, A., Wehrli, E., Eugster, M., Schnell, D., and Kessler, F. (2000). The major protein import receptor of plastids is essential for chloroplast biogenesis. *Nature* 403, 203-207.
- Bauer, J., Hiltbrunner, A., Weibel, P., Vidi, P.A., Alvarez-Huerta, M., Smith, M.D., Schnell, D.J., and Kessler, F. (2002). Essential role of the G-domain in targeting of the protein import receptor atToc159 to the chloroplast outer membrane. *J. Cell Biol.* 159, 845-854.
- Becker, T., Jelic, M., Vojta, A., Radunz, A., Soll, J., and Schleiff, E. (2004a). Preprotein recognition by the Toc complex. *EMBO J.* 23, 520-530.
- Becker, T., Hritz, J., Vogel, M., Caliebe, A., Bukau, B., Soll, J., and Schleiff, E. (2004b). Toc12, a novel subunit of the intermembrane space preprotein translocon of chloroplasts. *Mol. Biol. Cell* 15, 5130-5144.
- Bédard, J., Kubis, S., Bimanadham, S., and Jarvis, P. (2007). Functional similarity between the chloroplast translocon component, Tic40, and the human co-chaperone, Hsp70-interacting protein (Hip). *J. Biol. Chem.* 282, 21404-21414.
- Beers, E.P., and McDowell, J.M. (2001). Regulation and execution of programmed cell death in response to pathogens, stress and developmental cues. *Curr. Opin. Plant Biol.* 4, 561-567.
- Bleecker, A.B., and Patterson, S.E. (1997). Last exit: senescence, abscission, and meristem arrest in *Arabidopsis*. *Plant Cell* 9, 1169-1179.

- Boij, P., Patel, R., Garcia, C., Jarvis, P., and Aronsson, H. (2009). In vivo studies on the roles of Tic55-related proteins in chloroplast protein import in *Arabidopsis thaliana*. *Mol. Plant* 2, 1397-1409.
- Borgese, N., Colombo, S., and Pedrazzini, E. (2003). The tale of tail-anchored proteins: coming from the cytosol and looking for a membrane. *J. Cell Biol.* 161, 1013-1019.
- Bourne, H.R., Sanders, D.A., and McCormick, F. (1991). The GTPase superfamily: conserved structure and molecular mechanism. *Nature* 349, 117-127.
- Brautigam, A., and Weber, A.P. (2009). Proteomic analysis of the proplastid envelope membrane provides novel insights into small molecule and protein transport across proplastid membranes. *Mol. Plant* 2, 1247-1261.
- Buchanan-Wollaston, V., Earl, S., Harrison, E., Mathas, E., Navabpour, S., Page, T., and Pink, D. (2003a). The molecular analysis of leaf senescence--a genomics approach. *Plant Biotechnology J.* 1, 3-22.
- Buchanan-Wollaston, V., Earl, S., Harrison, E., Mathas, E., Navabpour, S., Page, T., and Pink, D. (2003b). The molecular analysis of leaf senescence--a genomics approach. *Plant Biotechnol J* 1, 3-22.
- Buchanan-Wollaston, V., Page, T., Harrison, E., Breeze, E., Lim, P.O., Nam, H.G., Lin, J.F., Wu, S.H., Swidzinski, J., Ishizaki, K., and Leaver, C.J. (2005). Comparative transcriptome analysis reveals significant differences in gene expression and signalling pathways between developmental and dark/starvation-induced senescence in *Arabidopsis*. *Plant J.* 42, 567-585.
- Caliebe, A., Grimm, R., Kaiser, G., Lubeck, J., Soll, J., and Heins, L. (1997). The chloroplastic protein import machinery contains a Rieske-type iron- sulfur cluster and a mononuclear iron-binding protein. *Embo J* 16, 7342-7350.
- Canut, H., Alibert, G., and Boudet, A.M. (1985). Hydrolysis of Intracellular Proteins in Vacuoles Isolated from *Acer pseudoplatanus* L. Cells. *Plant Physiol.* 79, 1090-1093.
- Canut, H., Alibert, G., Carrasco, A., and Boudet, A.M. (1986). Rapid Degradation of Abnormal Proteins in Vacuoles from *Acer pseudoplatanus* L. Cells. *Plant Physiol.* 81, 460-463.
- Carrera, A.C. (2004). TOR signaling in mammals. *J. Cell Sci.* 117, 4615-4616.
- Chen, K.Y., and Li, H.M. (2007). Precursor binding to an 880-kDa Toc complex as an early step during active import of protein into chloroplasts. *Plant J.* 49, 149-158.
- Chen, X., Smith, M.D., Fitzpatrick, L., and Schnell, D.J. (2002). In vivo analysis of the role of atTic20 in protein import into chloroplasts. *Plant Cell* 14, 641-654.
- Chew, O., Lister, R., Qbadou, S., Heazlewood, J.L., Soll, J., Schleiff, E., Millar, A.H., and Whelan, J. (2004). A plant outer mitochondrial membrane protein with high amino acid sequence identity to a chloroplast protein import receptor. *FEBS Lett.* 557, 109-114.
- Chigri, F., Hörmann, F., Stamp, A., Stammers, D.K., Bölter, B., Soll, J., and Vothknecht, U.C. (2006). Calcium regulation of chloroplast protein translocation is mediated by calmodulin binding to Tic32. *Proc. Natl. Acad. Sci. USA* 103, 16051-16056.
- Chou, M.L., Chu, C.C., Chen, L.J., Akita, M., and Li, H.M. (2006). Stimulation of transit-peptide release and ATP hydrolysis by a cochaperone during protein import into chloroplasts. *J. Cell Biol.* 175, 893-900.
- Chou, M.L., Fitzpatrick, L.M., Tu, S.L., Budziszewski, G., Potter-Lewis, S., Akita, M., Levin, J.Z., Keegstra, K., and Li, H.M. (2003). Tic40, a membrane-anchored co-chaperone homolog in the chloroplast protein translocon. *EMBO J.* 22, 2970-2980.
- Clark, S.L., Jr. (1957). Cellular differentiation in the kidneys of newborn mice studies with the electron microscope. *J. Biophys. Biochem. Cytol.* 3, 349-362.
- Constan, D., Patel, R., Keegstra, K., and Jarvis, P. (2004). An outer envelope membrane component of the plastid protein import apparatus plays an essential role in *Arabidopsis*. *Plant J.* 38, 93-106.

- Deprost, D., Yao, L., Sormani, R., Moreau, M., Leterreux, G., Nicolai, M., Bedu, M., Robaglia, C., and Meyer, C. (2007). The Arabidopsis TOR kinase links plant growth, yield, stress resistance and mRNA translation. *EMBO Rep.* 8, 864-870.
- Diaz-Troya, S., Perez-Perez, M.E., Florencio, F.J., and Crespo, J.L. (2008). The role of TOR in autophagy regulation from yeast to plants and mammals. *Autophagy* 4, 851-865.
- Doelling, J.H., Walker, J.M., Friedman, E.M., Thompson, A.R., and Vierstra, R.D. (2002). The APG8/12-activating enzyme APG7 is required for proper nutrient recycling and senescence in Arabidopsis thaliana. *J. Biol. Chem.* 277, 33105-33114.
- Doyle, S.M., and Wickner, S. (2009). Hsp104 and ClpB: protein disaggregating machines. *Trends Biochem. Sci.* 34, 40-48.
- Dufour, E., and Larsson, N.G. (2004). Understanding aging: revealing order out of chaos. *Biochim. Biophys. Acta* 1658, 122-132.
- Duy, D., Wanner, G., Meda, A.R., von Wiren, N., Soll, J., and Philippar, K. (2007). PIC1, an ancient permease in Arabidopsis chloroplasts, mediates iron transport. *Plant Cell* 19, 986-1006.
- Eckart, K., Eichacker, L., Sohrt, K., Schleiff, E., Heins, L., and Soll, J. (2002). A Toc75-like protein import channel is abundant in chloroplasts. *EMBO Rep.* 3, 557-562.
- Ertel, F., Mirus, O., Bredemeier, R., Moslavac, S., Becker, T., and Schleiff, E. (2005). The evolutionarily related beta-barrel polypeptide transporters from Pisum sativum and Nostoc PCC7120 contain two distinct functional domains. *J. Biol. Chem.* 280, 28281-28289.
- Eulgem, T., and Somssich, I.E. (2007). Networks of WRKY transcription factors in defense signaling. *Curr. Opin. Plant Biol.* 10, 366-371.
- Firlej-Kwoka, E., Strittmatter, P., Soll, J., and Bolter, B. (2008). Import of preproteins into the chloroplast inner envelope membrane. *Plant Mol. Biol.* 68, 505-519.
- Folly, P., and Engel, N. (1999). Chlorophyll b to chlorophyll a conversion precedes chlorophyll degradation in Hordeum vulgare L. *J. Biol. Chem.* 274, 21811-21816.
- Fujiki, Y., Yoshimoto, K., and Ohsumi, Y. (2007). An Arabidopsis homolog of yeast ATG6/VPS30 is essential for pollen germination. *Plant Physiol.* 143, 1132-1139.
- Fulda, M., Shockey, J., Werber, M., Wolter, F.P., and Heinz, E. (2002). Two long-chain acyl-CoA synthetases from Arabidopsis thaliana involved in peroxisomal fatty acid beta-oxidation. *Plant J.* 32, 93-103.
- Gan, S., and Amasino, R.M. (1995). Inhibition of leaf senescence by autoregulated production of cytokinin. *Science* 270, 1986-1988.
- Geissler, A., Krimmer, T., Bomer, U., Guiard, B., Rassow, J., and Pfanner, N. (2000). Membrane potential-driven protein import into mitochondria. The sorting sequence of cytochrome b(2) modulates the deltapsi-dependence of translocation of the matrix-targeting sequence. *Mol. Biol. Cell* 11, 3977-3991.
- Gentle, I.E., Burri, L., and Lithgow, T. (2005). Molecular architecture and function of the Omp85 family of proteins. *Mol. Microbiol.* 58, 1216-1225.
- Gray, J., Close, P.S., Briggs, S.P., and Johal, G.S. (1997). A novel suppressor of cell death in plants encoded by the Lls1 gene of maize. *Cell* 89, 25-31.
- Gray, J., Wardzala, E., Yang, M., Reinbothe, S., Haller, S., and Pauli, F. (2004). A small family of LLS1-related non-heme oxygenases in plants with an origin amongst oxygenic photosynthesizers. *Plant Mol. Biol.* 54, 39-54.
- Green, D.R., and Reed, J.C. (1998). Mitochondria and apoptosis. *Science* 281, 1309-1312.
- Gregersen, P.L., Holm, P.B., and Krupinska, K. (2008). Leaf senescence and nutrient remobilisation in barley and wheat. *Plant Biol (Stuttg)* 10 Suppl. 1, 37-49.
- Gutensohn, M., Schulz, B., Nicolay, P., and Flügge, U.I. (2000). Functional analysis of the two Arabidopsis homologues of Toc34, a component of the chloroplast protein import apparatus. *Plant J.* 23, 771-783.

- Hanaoka, H., Noda, T., Shirano, Y., Kato, T., Hayashi, H., Shibata, D., Tabata, S., and Ohsumi, Y. (2002). Leaf senescence and starvation-induced chlorosis are accelerated by the disruption of an *Arabidopsis* autophagy gene. *Plant Physiol.* 129, 1181-1193.
- He, Y., Fukushige, H., Hildebrand, D.F., and Gan, S. (2002). Evidence supporting a role of jasmonic acid in *Arabidopsis* leaf senescence. *Plant Physiol* 128, 876-884.
- He, Y., Tang, W., Swain, J.D., Green, A.L., Jack, T.P., and Gan, S. (2001). Networking senescence-regulating pathways by using *Arabidopsis* enhancer trap lines. *Plant Physiol.* 126, 707-716.
- Heins, L., Mehrle, A., Hemmler, R., Wagner, R., K uchler, M., H ormann, F., Sveshnikov, D., and Soll, J. (2002). The preprotein conducting channel at the inner envelope membrane of plastids. *EMBO J.* 21, 2616-2625.
- Hiltbrunner, A., Bauer, J., Alvarez-Huerta, M., and Kessler, F. (2001a). Protein translocon at the *Arabidopsis* outer chloroplast membrane. *Biochem. Cell Biol.* 79, 629-635.
- Hiltbrunner, A., Bauer, J., Vidi, P.A., Infanger, S., Weibel, P., Hohwy, M., and Kessler, F. (2001b). Targeting of an abundant cytosolic form of the protein import receptor at Toc159 to the outer chloroplast membrane. *J. Cell Biol.* 154, 309-316.
- Hinnah, S.C., Hill, K., Wagner, R., Schlicher, T., and Soll, J. (1997). Reconstitution of a chloroplast protein import channel. *EMBO J.* 16, 7351-7360.
- Hinnah, S.C., Wagner, R., Sveshnikova, N., Harrer, R., and Soll, J. (2002). The chloroplast protein import channel Toc75: pore properties and interaction with transit peptides. *Biophys. J.* 83, 899-911.
- Hirayama, T., and Shinozaki, K. (2007). Perception and transduction of abscisic acid signals: keys to the function of the versatile plant hormone ABA. *Trends Plant Sci.* 12, 343-351.
- Hirsch, S., Muckel, E., Heemeyer, F., von Heijne, G., and Soll, J. (1994). A receptor component of the chloroplast protein translocation machinery. *Science* 266, 1989-1992.
- Horie, Y., Ito, H., Kusaba, M., Tanaka, R., and Tanaka, A. (2009). Participation of chlorophyll b reductase in the initial step of the degradation of light-harvesting chlorophyll a/b-protein complexes in *Arabidopsis*. *J. Biol. Chem.* 284, 17449-17556.
- H ormann, F., K uchler, M., Sveshnikov, D., Oppermann, U., Li, Y., and Soll, J. (2004). Tic32, an essential component in chloroplast biogenesis. *J. Biol. Chem.* 279, 34756-34762.
- Hortensteiner, S. (2004). The loss of green color during chlorophyll degradation--a prerequisite to prevent cell death? *Planta* 219, 191-194.
- Hortensteiner, S. (2006). Chlorophyll degradation during senescence. *Annu Rev. Plant Biol.* 57, 55-77.
- Hortensteiner, S., and Feller, U. (2002). Nitrogen metabolism and remobilization during senescence. *J. Exp. Botany* 53, 927-937.
- Hortensteiner, S., Martinoia, E., and Amrhein, N. (1994). Factors affecting the re-formation of vacuoles in evacuated protoplasts and the expression of the two vacuolar proton pumps. *Planta* 192, 395-403.
- Hortensteiner, S., Wuthrich, K.L., Matile, P., Ongania, K.H., and Krautler, B. (1998). The key step in chlorophyll breakdown in higher plants. Cleavage of pheophorbide a macrocycle by a monooxygenase. *J. Biol. Chem.* 273, 15335-15339.
- Hu, G., Yalpani, N., Briggs, S.P., and Johal, G.S. (1998). A porphyrin pathway impairment is responsible for the phenotype of a dominant disease lesion mimic mutant of maize. *Plant Cell* 10, 1095-1105.
- Hust, B., and Gutensohn, M. (2006). Deletion of core components of the plastid protein import machinery causes differential arrest of embryo development in *Arabidopsis thaliana*. *Plant Biol. (Stuttg)* 8, 18-30.
- Inaba, T., Li, M., Alvarez-Huerta, M., Kessler, F., and Schnell, D.J. (2003). atTic110 functions as a scaffold for coordinating the stromal events of protein import into chloroplasts. *J. Biol. Chem.* 278, 38617-38627.

- Inaba, T., Alvarez-Huerta, M., Li, M., Bauer, J., Ewers, C., Kessler, F., and Schnell, D.J. (2005). *Arabidopsis* Tic110 is essential for the assembly and function of the protein import machinery of plastids. *Plant Cell* 17, 1482-1496.
- Infanger, S., Bischof, S., Hiltbrunner, A., Agne, B., Baginsky, S., and Kessler, F. (2011). The chloroplast import receptor Toc90 partially restores the accumulation of Toc159 client proteins in the *Arabidopsis thaliana* *ppi2* mutant. *Mol. Plant* 4, 252-263.
- Inoue, K., and Keegstra, K. (2003). A polyglycine stretch is necessary for proper targeting of the protein translocation channel precursor to the outer envelope membrane of chloroplasts. *Plant J.* 34, 661-669.
- Inoue, Y., Suzuki, T., Hattori, M., Yoshimoto, K., Ohsumi, Y., and Moriyasu, Y. (2006). AtATG genes, homologs of yeast autophagy genes, are involved in constitutive autophagy in *Arabidopsis* root tip cells. *Plant Cell Physiol.* 47, 1641-1652.
- Inoue, H., Rounds, C., and Schnell, D. J. (2010). The molecular basis for distinct pathways for protein import into *Arabidopsis* chloroplasts. *Plant Cell* 22, 1947-1960.
- Ishikawa, A., Okamoto, H., Iwasaki, Y., and Asahi, T. (2001). A deficiency of coproporphyrinogen III oxidase causes lesion formation in *Arabidopsis*. *Plant J.* 27, 89-99.
- Ivanova, Y., Smith, M.D., Chen, K., and Schnell, D.J. (2004). Members of the Toc159 import receptor family represent distinct pathways for protein targeting to plastids. *Mol. Biol. Cell* 15, 3379-3392.
- Ivey, R.A., 3rd, Subramanian, C., and Bruce, B.D. (2000). Identification of a Hsp70 recognition domain within the rubisco small subunit transit peptide. *Plant Physiol.* 122, 1289-1299.
- Jackson-Constan, D., and Keegstra, K. (2001). *Arabidopsis* genes encoding components of the chloroplastic protein import apparatus. *Plant Physiology* 125, 1567-1576.
- Jackson, D.T., Froehlich, J.E., and Keegstra, K. (1998). The hydrophilic domain of Tic110, an inner envelope membrane component of the chloroplastic protein translocation apparatus, faces the stromal compartment. *J. Biol. Chem.* 273, 16583-16588.
- Jarvis, P. (2003). Intracellular signalling: the language of the chloroplast. *Curr. Biol.* 13, R314-R316.
- Jarvis, P. (2008). Targeting of nucleus-encoded proteins to chloroplasts in plants. *New Phytol* 179, 257-285.
- Jarvis, P., and Robinson, C. (2004). Mechanisms of protein import and routing in chloroplasts. *Curr. Biol.* 14, R1064-R1077.
- Jarvis, P., Chen, L.J., Li, H., Peto, C.A., Fankhauser, C., and Chory, J. (1998). An *Arabidopsis* mutant defective in the plastid general protein import apparatus. *Science* 282, 100-103.
- Jelic, M., Soll, J., and Schleiff, E. (2003). Two Toc34 homologues with different properties. *Biochemistry* 42, 5906-5916.
- Jimenez, A., Hernandez, J.A., Pastori, G., del Rio, L.A., and Sevilla, F. (1998). Role of the ascorbate-glutathione cycle of mitochondria and peroxisomes in the senescence of pea leaves. *Plant Physiol.* 118, 1327-1335.
- Jing, H.C., Sturre, M.J., Hille, J., and Dijkwel, P.P. (2002). *Arabidopsis* onset of leaf death mutants identify a regulatory pathway controlling leaf senescence. *Plant J.* 32, 51-63.
- Jing, H.C., Schippers, J.H., Hille, J., and Dijkwel, P.P. (2005). Ethylene-induced leaf senescence depends on age-related changes and OLD genes in *Arabidopsis*. *J. Exp. Bot.* 56, 2915-2923.
- Jongebloed, U., Szederkenyi, J., Hartig, K., Schobert, C., and Komor, E. (2004). Sequence of morphological and physiological events during natural ageing and senescence of a castor bean leaf: sieve tube occlusion and carbohydrate back-up precede chlorophyll degradation. *Physiol. Plant* 120, 338-346.
- Jouhet, J., and Gray, J.C. (2009). Interaction of actin and the chloroplast protein import apparatus. *J. Biol. Chem.* 284, 19132-19141.
- Kakizaki, T., Matsumura, H., Nakayama, K., Che, F.S., Terauchi, R., and Inaba, T. (2009). Coordination of plastid protein import and nuclear gene expression by plastid-to-nucleus retrograde signaling. *Plant Physiol.* 151, 1339-1353.

- Kalanon, M., and McFadden, G.I. (2008). The chloroplast protein translocation complexes of *Chlamydomonas reinhardtii*: a bioinformatic comparison of Toc and Tic components in plants, green algae and red algae. *Genetics* 179, 95-112.
- Kamada, Y., Funakoshi, T., Shintani, T., Nagano, K., Ohsumi, M., and Ohsumi, Y. (2000). Tor-mediated induction of autophagy via an Apg1 protein kinase complex. *J. Cell Biol.* 150, 1507-1513.
- Kato, T., Morita, M.T., Fukaki, H., Yamauchi, Y., Uehara, M., Niihama, M., and Tasaka, M. (2002). SGR2, a phospholipase-like protein, and ZIG/SGR4, a SNARE, are involved in the shoot gravitropism of *Arabidopsis*. *Plant Cell* 14, 33-46.
- Kaup, M.T., Froese, C.D., and Thompson, J.E. (2002). A role for diacylglycerol acyltransferase during leaf senescence. *Plant Physiol.* 129, 1616-1626.
- Keegstra, K., and Cline, K. (1999). Protein import and routing systems of chloroplasts. *Plant Cell* 11, 557-570.
- Kessler, F., and Blobel, G. (1996). Interaction of the protein import and folding machineries of the chloroplast. *Proc. Natl. Acad. Sci. USA* 93, 7684-7689.
- Kessler, F., and Schnell, D.J. (2004). Chloroplast protein import: solve the GTPase riddle for entry. *Trends Cell Biol.* 14, 334-338.
- Kessler, F., Blobel, G., Patel, H.A., and Schnell, D.J. (1994). Identification of two GTP-binding proteins in the chloroplast protein import machinery. *Science* 266, 1035-1039.
- Kikuchi, S., Hirohashi, T., and Nakai, M. (2006). Characterization of the preprotein translocon at the outer envelope membrane of chloroplasts by blue native PAGE. *Plant Cell Physiol.* 47, 363-371.
- Kikuchi, S., Oishi, M., Hirabayashi, Y., Lee, D.W., Hwang, I., and Nakai, M. (2009). A 1-megadalton translocation complex containing Tic20 and Tic21 mediates chloroplast protein import at the inner envelope membrane. *Plant Cell* 21, 1781-1797.
- Kleffmann, T., Russenberger, D., von Zychlinski, A., Christopher, W., Sjolander, K., Grisse, W., and Baginsky, S. (2004). The *Arabidopsis thaliana* chloroplast proteome reveals pathway abundance and novel protein functions. *Curr. Biol.* 14, 354-362.
- Kouranov, A., and Schnell, D.J. (1997). Analysis of the interactions of preproteins with the import machinery over the course of protein import into chloroplasts. *J. Cell Biol.* 139, 1677-1685.
- Kouranov, A., Chen, X., Fuks, B., and Schnell, D.J. (1998). Tic20 and Tic22 are new components of the protein import apparatus at the chloroplast inner envelope membrane. *J. Cell Biol.* 143, 991-1002.
- Kovacheva, S., Bédard, J., Wardle, A., Patel, R., and Jarvis, P. (2007). Further *in vivo* studies on the role of the molecular chaperone, Hsp93, in plastid protein import. *Plant J.* 50, 364-379.
- Kovacheva, S., Bédard, J., Patel, R., Dudley, P., Twell, D., Ríos, G., Koncz, C., and Jarvis, P. (2005). *In vivo* studies on the roles of Tic110, Tic40 and Hsp93 during chloroplast protein import. *Plant J.* 41, 412-428.
- Krishna, P., and Gloor, G. (2001). The Hsp90 family of proteins in *Arabidopsis thaliana*. *Cell Stress Chaperones* 6, 238-246.
- Kubis, S., Baldwin, A., Patel, R., Razzaq, A., Dupree, P., Lilley, K., Kurth, J., Leister, D., and Jarvis, P. (2003). The *Arabidopsis ppi1* mutant is specifically defective in the expression, chloroplast import, and accumulation of photosynthetic proteins. *Plant Cell* 15, 1859-1871.
- Kubis, S., Patel, R., Combe, J., Bédard, J., Kovacheva, S., Lilley, K., Biehl, A., Leister, D., Ríos, G., Koncz, C., and Jarvis, P. (2004). Functional specialization amongst the *Arabidopsis* Toc159 family of chloroplast protein import receptors. *Plant Cell* 16, 2059-2077.
- Küchler, M., Decker, S., Hörmann, F., Soll, J., and Heins, L. (2002). Protein import into chloroplasts involves redox-regulated proteins. *EMBO J.* 21, 6136-6145.
- Kuriyama, H., and Fukuda, H. (2002). Developmental programmed cell death in plants. *Curr. Opin. Plant Biol.* 5, 568-753.

- Kusaba, M., Ito, H., Morita, R., Iida, S., Sato, Y., Fujimoto, M., Kawasaki, S., Tanaka, R., Hirochika, H., Nishimura, M., and Tanaka, A. (2007). Rice NON-YELLOW COLORING1 is involved in light-harvesting complex II and grana degradation during leaf senescence. *Plant Cell* 19, 1362-1375.
- Lee, J., Wang, F., and Schnell, D.J. (2009). Toc receptor dimerization participates in the initiation of membrane translocation during protein import into chloroplasts. *J. Biol. Chem.* 284, 31130-31141.
- Lee, K.H., Kim, S.J., Lee, Y.J., Jin, J.B., and Hwang, I. (2003). The M domain of atToc159 plays an essential role in the import of proteins into chloroplasts and chloroplast biogenesis. *J. Biol. Chem.* 278, 36794-36805.
- Li, H.M., and Chiu, C.C. (2010). Protein transport into chloroplasts. *Annu. Rev. Plant Biol.* 61, 157-180.
- Li, M., and Schnell, D.J. (2006). Reconstitution of protein targeting to the inner envelope membrane of chloroplasts. *J. Cell Biol.* 175, 249-259.
- Lim, P.O., Woo, H.R., and Nam, H.G. (2003). Molecular genetics of leaf senescence in *Arabidopsis*. *Trends Plant Sci.* 8, 272-278.
- Lim, P.O., Kim, H.J., and Nam, H.G. (2007). Leaf senescence. *Annu. Rev. Plant Biol.* 58, 115-136.
- Lin, J.F., and Wu, S.H. (2001). Molecular events in senescing *Arabidopsis* leaves. *Plant J.* 39, 612-628.
- Liu, Y., Schiff, M., Czymmek, K., Talloczy, Z., Levine, B., and Dinesh-Kumar, S.P. (2005). Autophagy regulates programmed cell death during the plant innate immune response. *Cell* 121, 567-577.
- López-Juez, E., and Pyke, K.A. (2005). Plastids unleashed: their development and their integration in plant development. *Int. J. Dev. Biol.* 49, 557-577.
- Lopez, M.A., Bannenberg, G., and Castresana, C. (2008). Controlling hormone signaling is a plant and pathogen challenge for growth and survival. *Curr. Opin. Plant Biol.* 11, 420-427.
- Lorrain, S., Vaillau, F., Balague, C., and Roby, D. (2003). Lesion mimic mutants: keys for deciphering cell death and defense pathways in plants? *Trends Plant Sci.* 8, 263-271.
- Lübeck, J., Heins, L., and Soll, J. (1997). A nuclear-coded chloroplastic inner envelope membrane protein uses a soluble sorting intermediate upon import into the organelle. *J. Cell Biol.* 137, 1279-1286.
- Ma, Y., Kouranov, A., LaSala, S.E., and Schnell, D.J. (1996). Two components of the chloroplast protein import apparatus, IAP86 and IAP75, interact with the transit sequence during the recognition and translocation of precursor proteins at the outer envelope. *J. Cell Biol.* 134, 315-327.
- Majeran, W., Zybailov, B., Ytterberg, A.J., Dunsmore, J., Sun, Q., and van Wijk, K.J. (2008). Consequences of C4 differentiation for chloroplast membrane proteomes in maize mesophyll and bundle sheath cells. *Mol. Cell Proteomics* 7, 1609-16038.
- Maple, J., Vojta, L., Soll, J., and Møller, S.G. (2007). ARC3 is a stromal Z-ring accessory protein essential for plastid division. *EMBO Rep.* 8, 293-299.
- Martin, T., Sharma, R., Sippel, C., Waegemann, K., Soll, J., and Vothknecht, U.C. (2006). A protein kinase family in *Arabidopsis* phosphorylates chloroplast precursor proteins. *J. Biol. Chem.* 281, 40216-40223.
- Martinez, D.E., Bartoli, C.G., Grbic, V., and Guamet, J.J. (2007). Vacuolar cysteine proteases of wheat (*Triticum aestivum* L.) are common to leaf senescence induced by different factors. *J. Exp. Bot.* 58, 1099-1107.
- Matile, P., Hortensteiner, S., Thomas, H., and Krautler, B. (1996). Chlorophyll Breakdown in Senescent Leaves. *Plant Physiol.* 112, 1403-1409.
- May, T., and Soll, J. (2000). 14-3-3 proteins form a guidance complex with chloroplast precursor proteins in plants. *Plant Cell* 12, 53-64.

- Mayer, M.P. (2005). Recruitment of Hsp70 chaperones: a crucial part of viral survival strategies. *Rev. Physiol. Biochem. Pharmacol.* 153, 1-46.
- McCabe, M.S., Garratt, L.C., Schepers, F., Jordi, W.J., Stoopen, G.M., Davelaar, E., van Rhijn, J.H., Power, J.B., and Davey, M.R. (2001). Effects of P(SAG12)-IPT gene expression on development and senescence in transgenic lettuce. *Plant Physiol.* 127, 505-516.
- Melendez, A., Tallozy, Z., Seaman, M., Eskelinen, E.L., Hall, D.H., and Levine, B. (2003). Autophagy genes are essential for dauer development and life-span extension in *C. elegans*. *Science* 301, 1387-1391.
- Miyagishima, S.Y., Froehlich, J.E., and Osteryoung, K.W. (2006). PDV1 and PDV2 mediate recruitment of the dynamin-related protein ARC5 to the plastid division site. *Plant Cell* 18, 2517-2530.
- Morris, K., MacKerness, S.A., Page, T., John, C.F., Murphy, A.M., Carr, J.P., and Buchanan-Wollaston, V. (2000). Salicylic acid has a role in regulating gene expression during leaf senescence. *Plant J.* 23, 677-685.
- Nakatogawa, H., Ichimura, Y., and Ohsumi, Y. (2007). Atg8, a ubiquitin-like protein required for autophagosome formation, mediates membrane tethering and hemifusion. *Cell* 130, 165-178.
- Neupert, W., and Brunner, M. (2002). The protein import motor of mitochondria. *Nat. Rev. Mol. Cell Biol.* 3, 555-565.
- Nielsen, E., Akita, M., Davila-Aponte, J., and Keegstra, K. (1997). Stable association of chloroplastic precursors with protein translocation complexes that contain proteins from both envelope membranes and a stromal Hsp100 molecular chaperone. *EMBO J.* 16, 935-946.
- Niwa, Y., Kato, T., Tabata, S., Seki, M., Kobayashi, M., Shinozaki, K., and Moriyasu, Y. (2004). Disposal of chloroplasts with abnormal function into the vacuole in *Arabidopsis thaliana* cotyledon cells. *Protoplasma* 223, 229-232.
- Nooden, L.D., and Penney, J.P. (2001). Correlative controls of senescence and plant death in *Arabidopsis thaliana* (Brassicaceae). *J. Exp. Bot.* 52, 2151-2159.
- Obara, K., Noda, T., Niimi, K., and Ohsumi, Y. (2008). Transport of phosphatidylinositol 3-phosphate into the vacuole via autophagic membranes in *Saccharomyces cerevisiae*. *Genes Cells* 13, 537-547.
- Oberhuber, M., and Krautler, B. (2002). Breakdown of chlorophyll: electrochemical bilin reduction provides synthetic access to fluorescent chlorophyll catabolites. *Chembiochem* 3, 104-107.
- Oguro, T., Yagawa, K., Momose, T., Sato, T., Yamano, K., and Endo, T. (2009). Structural stabilities of different regions of the titin I27 domain contribute differently to unfolding upon mitochondrial protein import. *J. Mol. Biol.* 385, 811-819.
- Oh, S.A., Park, J.H., Lee, G.I., Paek, K.H., Park, S.K., and Nam, H.G. (1997). Identification of three genetic loci controlling leaf senescence in *Arabidopsis thaliana*. *Plant J.* 12, 527-535.
- Okazaki, K., Kabeya, Y., Suzuki, K., Mori, T., Ichikawa, T., Matsui, M., Nakanishi, H., and Miyagishima, S.Y. (2009). The PLASTID DIVISION1 and 2 components of the chloroplast division machinery determine the rate of chloroplast division in land plant cell differentiation. *Plant Cell* 21, 1769-1780.
- Olsen, L.J., and Keegstra, K. (1992). The binding of precursor proteins to chloroplasts requires nucleoside triphosphates in the intermembrane space. *J. Biol. Chem.* 267, 433-439.
- op den Camp, R.G., Przybyla, D., Ochsenein, C., Laloi, C., Kim, C., Danon, A., Wagner, D., Hideg, E., Gobel, C., Feussner, I., Nater, M., and Apel, K. (2003). Rapid induction of distinct stress responses after the release of singlet oxygen in *Arabidopsis*. *Plant Cell* 15, 2320-2332.
- Ori, N., Juarez, M.T., Jackson, D., Yamaguchi, J., Banowitz, G.M., and Hake, S. (1999). Leaf senescence is delayed in tobacco plants expressing the maize homeobox gene *knotted1* under the control of a senescence-activated promoter. *Plant Cell* 11, 1073-1080.

- Oster, U., Tanaka, R., Tanaka, A., and Rudiger, W. (2000). Cloning and functional expression of the gene encoding the key enzyme for chlorophyll b biosynthesis (CAO) from *Arabidopsis thaliana*. *Plant J.* 21, 305-310.
- Osteryoung, K.W., and McAndrew, R.S. (2001). The Plastid Division Machine. *Annu. Rev. Plant Physiol. Plant Mol. Biol.* 52, 315-333.
- Otegui, M.S., Noh, Y.S., Martinez, D.E., Vila Petroff, M.G., Staehelin, L.A., Amasino, R.M., and Guimnet, J.J. (2005). Senescence-associated vacuoles with intense proteolytic activity develop in leaves of *Arabidopsis* and soybean. *Plant J.* 41, 831-844.
- Park, S.Y., Yu, J.W., Park, J.S., Li, J., Yoo, S.C., Lee, N.Y., Lee, S.K., Jeong, S.W., Seo, H.S., Koh, H.J., Jeon, J.S., Park, Y.I., and Paek, N.C. (2007). The senescence-induced staygreen protein regulates chlorophyll degradation. *Plant Cell* 19, 1649-1664.
- Patel, R., Hsu, S.C., Bedard, J., Inoue, K., and Jarvis, P. (2008). The Omp85-related chloroplast outer envelope protein OEP80 is essential for viability in *Arabidopsis*. *Plant Physiol* 148, 235-245.
- Peltier, J.B., Ripoll, D.R., Friso, G., Rudella, A., Cai, Y., Ytterberg, J., Giacomelli, L., Pillardy, J., and van Wijk, K.J. (2004). Clp protease complexes from photosynthetic and non-photosynthetic plastids and mitochondria of plants, their predicted three-dimensional structures, and functional implications. *J. Biol. Chem.* 279, 4768-4781.
- Perry, S.E., and Keegstra, K. (1994). Envelope membrane proteins that interact with chloroplastic precursor proteins. *Plant Cell* 6, 93-105.
- Pic, E., de La Serve, B.T., Tardieu, F., and Turc, O. (2002). Leaf senescence induced by mild water deficit follows the same sequence of macroscopic, biochemical, and molecular events as monocarpic senescence in pea. *Plant Physiol.* 128, 236-246.
- Pourtau, N., Jennings, R., Pelzer, E., Pallas, J., and Wingler, A. (2006). Effect of sugar-induced senescence on gene expression and implications for the regulation of senescence in *Arabidopsis*. *Planta* 224, 556-568.
- Pourtau, N., Mares, M., Purdy, S., Quentin, N., Ruel, A., and Wingler, A. (2004). Interactions of abscisic acid and sugar signalling in the regulation of leaf senescence. *Planta* 219, 765-772.
- Pruzinska, A., Tanner, G., Anders, I., Roca, M., and Hortensteiner, S. (2003). Chlorophyll breakdown: pheophorbide a oxygenase is a Rieske-type iron-sulfur protein, encoded by the accelerated cell death 1 gene. *Proc. Natl. Acad. Sci. U S A* 100, 15259-15264.
- Pruzinska, A., Anders, I., Aubry, S., Schenk, N., Tapernoux-Luthi, E., Muller, T., Krautler, B., and Hortensteiner, S. (2007). In vivo participation of red chlorophyll catabolite reductase in chlorophyll breakdown. *Plant Cell* 19, 369-387.
- Pruzinska, A., Tanner, G., Aubry, S., Anders, I., Moser, S., Muller, T., Ongania, K.H., Krautler, B., Youn, J.Y., Liljgren, S.J., and Hortensteiner, S. (2005). Chlorophyll breakdown in senescent *Arabidopsis* leaves. Characterization of chlorophyll catabolites and of chlorophyll catabolic enzymes involved in the degreening reaction. *Plant Physiol.* 139, 52-63.
- Pyke, K.A. (1999). Plastid division and development. *Plant Cell* 11, 549-556.
- Qbadou, S., Becker, T., Mirus, O., Tews, I., Soll, J., and Schleiff, E. (2006). The molecular chaperone Hsp90 delivers precursor proteins to the chloroplast import receptor Toc64. *EMBO J.* 25, 1836-1847.
- Qbadou, S., Becker, T., Bionda, T., Reger, K., Ruprecht, M., Soll, J., and Schleiff, E. (2007). Toc64 - a preprotein-receptor at the outer membrane with bipartite function. *J. Mol. Biol.* 367, 1330-1346.
- Ren, G., An, K., Liao, Y., Zhou, X., Cao, Y., Zhao, H., Ge, X., and Kuai, B. (2007). Identification of a novel chloroplast protein AtNYE1 regulating chlorophyll degradation during leaf senescence in *Arabidopsis*. *Plant Physiol.* 144, 1429-1441.
- Reumann, S., and Keegstra, K. (1999). The endosymbiotic origin of the protein import machinery of chloroplastic envelope membranes. *Trends Plant Sci.* 4, 302-307.

- Reumann, S., Davila-Aponte, J., and Keegstra, K. (1999). The evolutionary origin of the protein-translocating channel of chloroplastic envelope membranes: identification of a cyanobacterial homolog. *Proc. Natl. Acad. Sci. USA* 96, 784-789.
- Reumann, S., Inoue, K., and Keegstra, K. (2005). Evolution of the general protein import pathway of plastids. *Mol. Membr. Biol.* 22, 73-86.
- Rial, D.V., Arakaki, A.K., and Ceccarelli, E.A. (2000). Interaction of the targeting sequence of chloroplast precursors with Hsp70 molecular chaperones. *Eur. J. Biochem.* 267, 6239-6248.
- Riefler, M., Novak, O., Strnad, M., and Schmulling, T. (2006). Arabidopsis cytokinin receptor mutants reveal functions in shoot growth, leaf senescence, seed size, germination, root development, and cytokinin metabolism. *Plant Cell* 18, 40-54.
- Robatzek, S., and Somssich, I.E. (2002). Targets of AtWRKY6 regulation during plant senescence and pathogen defense. *Genes Dev.* 16, 1139-1149.
- Robinson, C., and Bolhuis, A. (2001). Protein targeting by the twin-arginine translocation pathway. *Nat Rev Mol Cell Biol* 2, 350-356.
- Roca, M., James, C., Pruzinska, A., Hortensteiner, S., Thomas, H., and Ougham, H. (2004). Analysis of the chlorophyll catabolism pathway in leaves of an introgression senescence mutant of *Lolium temulentum*. *Phytochemistry* 65, 1231-1238.
- Rodoni, S., Vicentini, F., Schellenberg, M., Matile, P., and Hortensteiner, S. (1997). Partial Purification and Characterization of Red Chlorophyll Catabolite Reductase, a Stroma Protein Involved in Chlorophyll Breakdown. *Plant Physiol.* 115, 677-682.
- Rudiger, W. (2002). Biosynthesis of chlorophyll b and the chlorophyll cycle. *Photosynth Res.* 74, 187-193.
- Ruprecht, M., Bionda, T., Sato, T., Sommer, M.S., Endo, T., and Schleiff, E. (2010). On the impact of precursor unfolding during protein import into chloroplasts. *Mol. Plant* 3, 499-508.
- Sánchez-Pulido, L., Devos, D., Genevrois, S., Vicente, M., and Valencia, A. (2003). POTRA: a conserved domain in the FtsQ family and a class of beta-barrel outer membrane proteins. *Trends Biochem. Sci.* 28, 523-526.
- Sangster, T.A., Bahrami, A., Wilczek, A., Watanabe, E., Schellenberg, K., McLellan, C., Kelley, A., Kong, S.W., Queitsch, C., and Lindquist, S. (2007). Phenotypic diversity and altered environmental plasticity in *Arabidopsis thaliana* with reduced Hsp90 levels. *PLoS One* 2, e648.
- Sato, T., Esaki, M., Fernandez, J.M., and Endo, T. (2005). Comparison of the protein-unfolding pathways between mitochondrial protein import and atomic-force microscopy measurements. *Proc. Natl. Acad. Sci. U S A* 102, 17999-18004.
- Sato, Y., Morita, R., Nishimura, M., Yamaguchi, H., and Kusaba, M. (2007). Mendel's green cotyledon gene encodes a positive regulator of the chlorophyll-degrading pathway. *Proc. Natl. Acad. Sci. U S A* 104, 14169-14174.
- Sato, Y., Morita, R., Katsuma, S., Nishimura, M., Tanaka, A., and Kusaba, M. (2009). Two short-chain dehydrogenase/reductases, NON-YELLOW COLORING 1 and NYC1-LIKE, are required for chlorophyll b and light-harvesting complex II degradation during senescence in rice. *Plant J* 57, 120-131.
- Schelbert, S., Aubry, S., Burla, B., Agne, B., Kessler, F., Krupinska, K., and Hortensteiner, S. (2009). Pheophytin pheophorbide hydrolase (pheophytinase) is involved in chlorophyll breakdown during leaf senescence in *Arabidopsis*. *Plant Cell* 21, 767-785.
- Scheumann, V.V., Schoch, S., and Rudiger, W. (1999). Chlorophyll b reduction during senescence of barley seedlings. *Planta* 209, 364-370.
- Schlegel, T., Mirus, O., von Haeseler, A., and Schleiff, E. (2007). The tetratricopeptide repeats of receptors involved in protein translocation across membranes. *Mol. Biol. Evol.* 24, 2763-2774.
- Schleiff, E., Jelic, M., and Soll, J. (2003a). A GTP-driven motor moves proteins across the outer envelope of chloroplasts. *Proc. Natl. Acad. Sci. USA* 100, 4604-4609.

- Schleiff, E., Eichacker, L.A., Eckart, K., Becker, T., Mirus, O., Stahl, T., and Soll, J. (2003b). Prediction of the plant beta-barrel proteome: a case study of the chloroplast outer envelope. *Protein Sci.* 12, 748-759.
- Schnell, D.J., and Hebert, D.N. (2003). Protein translocons: multifunctional mediators of protein translocation across membranes. *Cell* 112, 491-505.
- Schnell, D.J., Kessler, F., and Blobel, G. (1994). Isolation of components of the chloroplast protein import machinery. *Science* 266, 1007-1012.
- Schnell, D.J., Blobel, G., Keegstra, K., Kessler, F., Ko, K., and Soll, J. (1997). A consensus nomenclature for the protein-import components of the chloroplast envelope. *Trends Cell Biol* 7, 303-304.
- Scott, S.V., Hefner-Gravink, A., Morano, K.A., Noda, T., Ohsumi, Y., and Klionsky, D.J. (1996). Cytoplasm-to-vacuole targeting and autophagy employ the same machinery to deliver proteins to the yeast vacuole. *Proc. Natl. Acad. Sci. U S A* 93, 12304-12308.
- Seay, M.D., and Dinesh-Kumar, S.P. (2005). Life after death: are autophagy genes involved in cell death and survival during plant innate immune responses? *Autophagy* 1, 185-186.
- Seedorf, M., Waegemann, K., and Soll, J. (1995). A constituent of the chloroplast import complex represents a new type of GTP-binding protein. *Plant J.* 7, 401-411.
- Slavikova, S., Shy, G., Yao, Y., Glozman, R., Levanony, H., Pietrokovski, S., Elazar, Z., and Galili, G. (2005). The autophagy-associated Atg8 gene family operates both under favourable growth conditions and under starvation stresses in Arabidopsis plants. *J. Exp. Bot.* 56, 2839-2849.
- Smalle, J., and Vierstra, R.D. (2004). The ubiquitin 26S proteasome proteolytic pathway. *Annu. Rev. Plant Biol.* 55, 555-590.
- Smith, M.D., Hiltbrunner, A., Kessler, F., and Schnell, D.J. (2002). The targeting of the atToc159 preprotein receptor to the chloroplast outer membrane is mediated by its GTPase domain and is regulated by GTP. *J. Cell Biology* 159, 833-843.
- Sohrt, K., and Soll, J. (2000). Toc64, a new component of the protein translocon of chloroplasts. *J. Cell Biol.* 148, 1213-1221.
- Stahl, T., Glockmann, C., Soll, J., and Heins, L. (1999). Tic40, a new "old" subunit of the chloroplast protein import translocon. *J. Biol. Chem.* 274, 37467-37472.
- Stanga, J.P., Boonsirichai, K., Sedbrook, J.C., Otegui, M.S., and Masson, P.H. (2009). A role for the TOC complex in Arabidopsis root gravitropism. *Plant Physiol.* 149, 1896-1905.
- Stengel, A., Benz, P., Balsera, M., Soll, J., and Böltner, B. (2008). Tic62 - redox-regulated translocon composition and dynamics. *J. Biol. Chem.*, Epub ahead of print, PMID: 18180301.
- Su, P.H., and Li, H.M. (2010). Stromal Hsp70 is important for protein translocation into pea and Arabidopsis chloroplasts. *Plant Cell* 22, 1516-1531.
- Sun, Y.J., Forouhar, F., Li Hm, H.M., Tu, S.L., Yeh, Y.H., Kao, S., Shr, H.L., Chou, C.C., Chen, C., and Hsiao, C.D. (2002). Crystal structure of pea Toc34, a novel GTPase of the chloroplast protein translocon. *Nat. Struct. Biol.* 9, 95-100.
- Sveshnikova, N., Soll, J., and Schleiff, E. (2000a). Toc34 is a preprotein receptor regulated by GTP and phosphorylation. *Proc. Natl. Acad. Sci. USA* 97, 4973-4978.
- Sveshnikova, N., Grimm, R., Soll, J., and Schleiff, E. (2000b). Topology studies of the chloroplast protein import channel Toc75. *Biol Chem* 381, 687-693.
- Tamura, K., Yamada, K., Shimada, T., and Hara-Nishimura, I. (2004). Endoplasmic reticulum-resident proteins are constitutively transported to vacuoles for degradation. *Plant J.* 39, 393-402.
- Tanaka, A., Ito, H., Tanaka, R., Tanaka, N.K., Yoshida, K., and Okada, K. (1998). Chlorophyll a oxygenase (CAO) is involved in chlorophyll b formation from chlorophyll a. *Proc. Natl. Acad. Sci. U S A* 95, 12719-12723.

- Teng, Y.S., Su, Y.S., Chen, L.J., Lee, Y.J., Hwang, I., and Li, H.M. (2006). Tic21 is an essential translocon component for protein translocation across the chloroplast inner envelope membrane. *Plant Cell* 18, 2247-2257.
- Theg, S.M., Bauerle, C., Olsen, L.J., Selman, B.R., and Keegstra, K. (1989). Internal ATP is the only energy requirement for the translocation of precursor proteins across chloroplastic membranes. *J. Biol. Chem.* 264, 6730-6736.
- Thomas, H., and Howarth, C.J. (2000). Five ways to stay green. *J. Exp. Bot.* 51 Spec No, 329-337.
- Thomas, H., Ougham, H.J., Wagstaff, C., and Stead, A.D. (2003). Defining senescence and death. *J. Exp. Bot.* 54, 1127-1132.
- Thompson, A.R., and Vierstra, R.D. (2005). Autophagic recycling: lessons from yeast help define the process in plants. *Current Opinion Plant Biology* 8, 165-173.
- Thompson, J., Taylor, C., and Wang, T.W. (2000). Altered membrane lipase expression delays leaf senescence. *Biochem. Soc. Trans.* 28, 775-777.
- Thompson, J.E., Froese, C.D., Madey, E., Smith, M.D., and Hong, Y. (1998). Lipid metabolism during plant senescence. *Prog. Lipid Res.* 37, 119-141.
- Tranel, P.J., Froehlich, J., Goyal, A., and Keegstra, K. (1995). A component of the chloroplastic protein import apparatus is targeted to the outer envelope membrane via a novel pathway. *EMBO J.* 14, 2436-2446.
- Tripp, J., Inoue, K., Keegstra, K., and Froehlich, J.E. (2007). A novel serine/proline-rich domain in combination with a transmembrane domain is required for the insertion of AtTic40 into the inner envelope membrane of chloroplasts. *Plant J.* 52, 824-838.
- Tu, S.L., Chen, H.C., and Ku, L.W. (2008). Mechanistic studies of the phytylchromobilin synthase HY2 from *Arabidopsis*. *J. Biol. Chem.* 283, 27555-27564.
- Ueda, J., and Kato, J. (1980). Isolation and Identification of a Senescence-promoting Substance from Wormwood (*Artemisia absinthium* L.). *Plant Physiol.* 66, 246-249.
- Ulker, B., Shahid Mukhtar, M., and Somssich, I.E. (2007). The WRKY70 transcription factor of *Arabidopsis* influences both the plant senescence and defense signaling pathways. *Planta* 226, 125-137.
- van der Graaff, E., Schwacke, R., Schneider, A., Desimone, M., Flugge, U.I., and Kunze, R. (2006). Transcription analysis of *Arabidopsis* membrane transporters and hormone pathways during developmental and induced leaf senescence. *Plant Physiol.* 141, 776-792.
- van Dooren, G.G., Tomova, C., Agrawal, S., Humbel, B.M., and Striepen, B. (2008). *Toxoplasma gondii* Tic20 is essential for apicoplast protein import. *Proc. Natl. Acad. Sci. U S A* 105, 13574-13579.
- Vernoud, V., Horton, A.C., Yang, Z., and Nielsen, E. (2003). Analysis of the small GTPase gene superfamily of *Arabidopsis*. *Plant Physiol.* 131, 1191-1208.
- Viana, A.A., Li, M., and Schnell, D.J. (2010). Determinants for stop-transfer and post-import pathways for protein targeting to the chloroplast inner envelope membrane. *J. Biol. Chem.* 285, 12948-12960.
- Vojta, A., Alavi, M., Becker, T., Hörmann, F., Kuchler, M., Soll, J., Thomson, R., and Schleiff, E. (2004). The protein translocon of the plastid envelopes. *J. Biol. Chem.* 279, 21401-21405.
- Vojta, L., Soll, J., and Bölter, B. (2007). Requirements for a conservative protein translocation pathway in chloroplasts. *FEBS Lett.* 581, 2621-2624.
- Waagemann, K., and Soll, J. (1991). Characterization of the protein import apparatus in isolated outer envelopes of chloroplasts. *Plant J.* 1, 149-158.
- Wagner, D., Przybyla, D., Op den Camp, R., Kim, C., Landgraf, F., Lee, K.P., Wursch, M., Laloi, C., Nater, M., Hideg, E., and Apel, K. (2004). The genetic basis of singlet oxygen-induced stress responses of *Arabidopsis thaliana*. *Science* 306, 1183-1185.
- Wallas, T.R., Smith, M.D., Sanchez-Nieto, S., and Schnell, D.J. (2003). The roles of Toc34 and Toc75 in targeting the Toc159 preprotein receptor to chloroplasts. *J. Biol. Chem.* 278, 44289-44297.

- Wandinger, S.K., Richter, K., and Buchner, J. (2008). The Hsp90 chaperone machinery. *J. Biol. Chem.* 283, 18473-18477.
- Weaver, L.M., Gan, S., Quirino, B., and Amasino, R.M. (1998). A comparison of the expression patterns of several senescence-associated genes in response to stress and hormone treatment. *Plant Mol. Biol.* 37, 455-469.
- Weber, P., Fulgosi, H., Piven, I., Muller, L., Krupinska, K., Duong, V.H., Herrmann, R.G., and Sokolenko, A. (2006). TCP34, a nuclear-encoded response regulator-like TPR protein of higher plant chloroplasts. *J. Mol. Biol.* 357, 535-549.
- Weibel, P., Hiltbrunner, A., Brand, L., and Kessler, F. (2003). Dimerization of Toc-GTPases at the chloroplast protein import machinery. *J. Biol. Chem.* 278, 37321-37329.
- Wingler, A., Masclaux-Daubresse, C., and Fischer, A.M. (2004). Sugars, senescence, and ageing in plants and heterotrophic organisms. *J. Exp. Bot.* 60, 1063-1066.
- Wingler, A., Purdy, S., MacLean, J.A., and Pourtau, N. (2006). The role of sugars in integrating environmental signals during the regulation of leaf senescence. *J. Exp. Bot.* 57, 391-399.
- Woo, H.R., Chung, K.M., Park, J.H., Oh, S.A., Ahn, T., Hong, S.H., Jang, S.K., and Nam, H.G. (2001). ORE9, an F-box protein that regulates leaf senescence in *Arabidopsis*. *Plant Cell* 13, 1779-1790.
- Wuthrich, K.L., Bovet, L., Hunziker, P.E., Donnison, I.S., and Hortensteiner, S. (2000). Molecular cloning, functional expression and characterisation of RCC reductase involved in chlorophyll catabolism. *Plant J.* 21, 189-198.
- Xie, Z., and Klionsky, D.J. (2007). Autophagosome formation: core machinery and adaptations. *Nat. Cell Biol.* 9, 1102-1109.
- Xiong, Y., Contento, A.L., and Bassham, D.C. (2005). AtATG18a is required for the formation of autophagosomes during nutrient stress and senescence in *Arabidopsis thaliana*. *Plant J.* 42, 535-546.
- Yang, M., Wardzala, E., Johal, G.S., and Gray, J. (2004). The wound-inducible Lls1 gene from maize is an orthologue of the *Arabidopsis* Acd1 gene, and the LLS1 protein is present in non-photosynthetic tissues. *Plant Mol. Biol.* 54, 175-191.
- Yang, S.H., Berberich, T., Sano, H., and Kusano, T. (2001). Specific association of transcripts of *tbzF* and *tbz17*, tobacco genes encoding basic region leucine zipper-type transcriptional activators, with guard cells of senescing leaves and/or flowers. *Plant Physiol.* 127, 23-32.
- Yang, Y., Glynn, J.M., Olson, B.J., Schmitz, A.J., and Osteryoung, K.W. (2008). Plastid division: across time and space. *Curr. Opin. Plant Biol.* 11, 577-584.
- Yeh, Y.H., Kesavulu, M.M., Li, H.M., Wu, S.Z., Sun, Y.J., Konozy, E.H., and Hsiao, C.D. (2007). Dimerization is important for the GTPase activity of chloroplast translocon components atToc33 and psToc159. *J. Biol. Chem.* 282, 13845-13853.
- Yen, H.C., Lee, S., Tanksley, S.D., Lanahan, M.B., Klee, H.J., and Giovannoni, J.J. (1995). The tomato Never-ripe locus regulates ethylene-inducible gene expression and is linked to a homolog of the *Arabidopsis* ETR1 gene. *Plant Physiol.* 107, 1343-1353.
- Yoon, H.K., Kim, S.G., Kim, S.Y., and Park, C.M. (2008). Regulation of leaf senescence by NTL9-mediated osmotic stress signaling in *Arabidopsis*. *Mol. Cells* 25, 438-445.
- Yorimitsu, T., and Klionsky, D.J. (2005). Autophagy: molecular machinery for self-eating. *Cell Death Differ.* 12 Suppl 2, 1542-1552.
- Yoshimoto, K., Hanaoka, H., Sato, S., Kato, T., Tabata, S., Noda, T., and Ohsumi, Y. (2004). Processing of ATG8s, ubiquitin-like proteins, and their deconjugation by ATG4s are essential for plant autophagy. *Plant Cell* 16, 2967-2983.
- Yu, S.M. (1999). Cellular and genetic responses of plants to sugar starvation. *Plant Physiol.* 121, 687-693.
- Yu, T.S., and Li, H. (2001). Chloroplast protein translocon components atToc159 and atToc33 are not essential for chloroplast biogenesis in guard cells and root cells. *Plant Physiol.* 127, 90-96.

- Zentgraf, U., Jobst, J., Kolb, D., and Rentsch, D. (2004). Senescence-related gene expression profiles of rosette leaves of *Arabidopsis thaliana*: leaf age versus plant age. *Plant Biol (Stuttg)* 6, 178-183.
- Zhang, X.P., and Glaser, E. (2002). Interaction of plant mitochondrial and chloroplast signal peptides with the Hsp70 molecular chaperone. *Trends Plant Sci.* 7, 14-21.

APPENDIX

Table 1: Genetic analysis of *Arabidopsis* Toc90 double homozygous knockout mutants. All the double mutants have been PCR tested and a comprehensive phenotypic analysis was carried out with the appropriate controls.

Genotype	Zygoty	PCR genotype	Appropriate controls for phenotypic comparison
<i>toc90-1 toc33 (ppi1)</i>	hom/hom	yes	<i>ppi1, toc90-1, Col-0</i>
<i>toc90-1 toc34-2 (ppi3-2)</i>	hom/hom	yes	<i>ppi3-2, toc90-1, Col-0</i>
<i>toc90-1 toc120-2</i>	hom/hom	yes	<i>toc120-2, toc90-1, Col-0</i>
<i>toc90-1 toc132-2</i>	hom/hom	yes	<i>toc132-2, toc90-1, Col-0</i>
<i>toc90-1 toc159 (ppi2)</i>	hom/seg	yes	<i>toc159</i> (albino plants)
<i>toc90-1 toc75III-3</i>	hom/hom	yes	<i>toc75-III-3, toc90-1, Col-0</i>
<i>toc90-1 toc75IV-1</i>	hom/hom	yes	<i>toc75-IV-1, toc90-1, Col-0</i>

Abbreviations in the table are defined as follows: hom, homozygous; het, heterozygous; seg, segregating; Col-0, Columbia

Table 2: Genetic analysis of *Arabidopsis* Toc90 triple mutants. All the triple mutants have been PCR tested and a comprehensive phenotypic analysis was carried out with the appropriate controls

Genotype	Zygoty	PCR genotype	Appropriate controls for phenotypic comparison
<i>toc90-1 toc132-2 toc120-2</i>	hom/hom/hom (bleached)	yes	<i>toc132-2 toc120-2</i> bleached
<i>toc90-1 toc132-2 toc120-2</i>	hom/hom/het (pale)	yes	<i>toc132-2 toc120-2</i> pale
<i>toc90-1 toc159 toc120-2</i>	hom/seg/hom	yes	<i>toc90-1 toc159, toc159, toc159 toc120-2</i>
<i>toc90-1 toc33 toc34-2</i>	hom/hom/het	yes	<i>toc33 toc34-2</i>
<i>toc90-1 toc159 toc33</i>	hom/seg/hom	yes	<i>toc159, toc33 toc159</i>
<i>toc90-1 toc159 toc34-2</i>	hom/seg/hom	yes	<i>toc159, toc34-2 toc159</i>
<i>toc90-1 toc33 toc132-2</i>	hom/hom/hom	yes	<i>toc33 toc132-2, Col-0</i>

Abbreviations in the table are defined as follows: hom, homozygous; het, heterozygous; seg, segregating; Col-0, Columbia

Table 3: The T-DNA and gene specific primers used for genotyping

Gene	Primers
<i>toc90-1</i>	5'-TAGCATCTGAATTCATAACCAATCTCGATACAC-3' LB3 (left border) 5'-TTCCGTGACCCTCATCAAGAAC-3' forward 5'-GAGAAATCACTGTATCGCATGTTCG-3' reverse
<i>toc90-2</i>	5'-TGGTTCACGTAGTGGGCCATCG-3' LBa1 (left border) 5'-GAGAAATCACTGTATCGCATGTTCG-3' reverse 5'-TTCCGTGACCCTCATCAAGAAC-3' forward
<i>toc90-3</i>	5'-TGGTTCACGTAGTGGGCCATCG-3' LBa1 (left border) 5'-CAGCGCATGGATGTGGTTCAA-3' forward 5'-CTCCCGCCGTTTGCTGTTT-3' reverse
<i>toc34-2</i>	5'-TGGTTCACGTAGTGGGCCATCG-3' LBa1 (left border) 5'-TAATTTGATACGAGGTCAGCGAATCCGGC-3' forward 5'-TGATCTGGTTTGACTACACAATCGCACCC-3' reverse
<i>toc33</i>	5'-ATAACGCTGCGGACATCTAC-3' LB/CGN3 5'-GGTCTCTCGTTCGTGAATGG-3' 127 Ex2 forward 5'-CTGAGCGCCTATGATAAGAG-3' 127 Ex7 reverse
<i>toc132-2</i>	5'-CCCATTTGGACGTGAATGTAGACAC-3' LB Gabi kat (left border) 5'-GATGGGACTGAGTTTGTGGTTAGGTC-3' forward 5'-TCCTCCAACAATTGGTCTCTTGCTACCAG-3' reverse
<i>toc75-III-3</i>	5'-GCAAATCACAGGTGGACCAG-3' dCAPS forward 5'-TGCCCATGGAGGACTAGAAC-3' dCAPS reverse
<i>toc75-IV-1</i>	5'-GGTGCAGCAAAACCCACACTTTTACTTC-3' dspm11 5'-CTATCATCTTCTACTCCGAGTCTCCG-3' forward 5'-GCTGAATGAACTTGTTAATGATAGT-3' reverse
<i>toc120-2</i>	5'-CAGTCATAGCCGAATAGCCTCTCCA-3' FISH2 5'-CTCCCAGAAAGCTGGATACTGTCAATGTG-3' forward 5'-AATTGGTTCGCAGGAGGGTC-3' forward 5'-CTTTCAGTCTCTCCCTTCTC-3' reverse
<i>toc159</i>	5'-GATGCAATCGATATCAGCCAATTTTAGAC-3' LB102A 5'-CAGTAGCAAAGCGGAAATGGACTCAAAG-3' forward 5'-GCACGTGGAGCTGCTGCAGGCTTCAAGGG-3' reverse

Table 4: *atTOC90* gene specific primers used to make the overexpression for the construct complementation studies

Gene	Primers
<i>Toc90attB1-F</i>	5'-AAAAAGCAGGCTATGAAAGGCTTCAAAGACTG-3'
<i>Toc90attB2-R</i>	5'-AGAAAGCTGGGTTTAGGAAACGAGAAAATTCAC-3'
<i>Toc90 H4C12/F</i>	5'-CATCTGGCATAACCGGAGCTTGA-3'
<i>Toc90 H4C12/R</i>	5'-CTTCGAAACACGGCGGGACTT-3'

Table 5: *atTOC90* and translation initiation factor *eIF4E1* gene specific primers used for RT-PCR

Gene	Primers
<i>eIF4E1-F</i>	5'-AAACAATGGCGGTAGAAGACATCT-3'
<i>eIF4E1-R</i>	5'-AAGATTTGAGAGGTTTCAAGCGGTGTAAG-3'
<i>Toc90 PL/RT-F</i>	5'-CTCCCGCCGTTTGCTGTTT-3'
<i>Toc90 RT-R</i>	5'-TTCCGTGACCCTCATCAAGAAC-3'